THE JOURNAL
OF
CHEMICAL PHYSICS

VOLUME 5 AUGUST, 1937 NUMBER 8

Spectroscopic Studies of the Hydrogen Bond

I. A Photometric Investigation of the Association Equilibrium in the Vapor of Acetic Acid*

RICHARD M. BADGER AND SIMON H. BAUER
Gates and Crellin Laboratories of Chemistry, California Institute of Technology, Pasadena, California
(Received April 2, 1937)

The association equilibrium in the vapor of acetic acid has been studied by photometric measurement of the intensity of a narrow O−H band at λ9750 which appears to be characteristic of the single molecules. The results are in reasonable agreement with vapor density measurements, indicating that the association is at least largely due to hydrogen bond formation and that two hydrogen bonds are formed in the majority of the double molecules. An O−H absorption characteristic of the double molecules could not be observed in the vapor state, due to insufficient path length, but in the liquid and in carbon tetrachloride solutions a broad band was found with maximum around λ10,100. It is suggested that the spectroscopic criterion for the presence of hydrogen bonds is not the disappearance but rather the shift and modification of the O−H absorption.

INTRODUCTION

IT has recently been observed that the comparatively narrow and intense bands which ordinarily are characteristic of the O−H group are absent from the spectra of certain compounds which contain hydroxyl hydrogen but which for various reasons are believed to contain hydrogen bonds in which this hydrogen is involved. The absence of these bands has consequently been proposed as a criterion for the existence of hydrogen bonds.[1] It appeared to the authors to be worthwhile to investigate this criterion in some detail in a clean-cut case. As is well known, in the vapor of formic and acetic acids there is an equilibrium between single and double molecules, which has been carefully studied by vapor density measurements.[2, 3] The association appears to be due to the formation of hydrogen bonds for two reasons. In the first place the heat of association is about what would be expected for two such bonds.[4] In the second place the electron diffraction measurements of Pauling and Brockway[5] establish a structure for the double molecule of formic acid which is at least a strong indication of hydrogen bond formation because of the close approach of oxygen atoms of the two halves of the molecule, though unfortunately the hydrogen atoms could not be located. Presumably the structure of acetic acid is similar. Now if the narrow O−H bands are to be expected only in the case of hydroxyl groups not involved in hydrogen bonds, their intensity should be a

* The investigation here described is a part of a program of research made possible by a Grant-in-Aid of the National Research Council to one of us (R. M. B.) for which it is desired to express appreciation.

[1] Hilbert, Wulf, Hendricks and Liddel, J. Am. Chem. Soc. **58**, 548 (1936).

[2] A. S. Coolidge, J. Am. Chem. Soc. **50**, 2166 (1928).

[3] F. H. MacDougall, J. Am. Chem. Soc. **58**, 2585 (1936).

[4] M. L. Huggins, J. Org. Chem. **1**, 407 (1936).

[5] Pauling and Brockway, Proc. Nat. Acad. Sci. **20**, 336 (1934).

measure of the concentration of single molecules and it should be possible to follow the association equilibrium by photometric means.

Preliminary studies of the vapor of acetic acid indicated that this is the case. At moderate pressures and somewhat elevated temperatures we observed a rather narrow O—H band at λ9750, as shown in Fig. 1 which is a microphotometer tracing of a plate taken with our 21-ft. grating. Even under the high dispersion no fine structure could be resolved and there is apparently an overlapping of the rotation lines. At higher pressures and lower temperatures, which tend to increase the association, the intensity of this band was much weaker. As will be discussed in a later paper it is apparently replaced by a broad O—H absorption band with a flat maximum around λ10,100, which is characteristic of the double molecule. The total O—H absorption does not appear to be greatly decreased on association but is shifted to longer wave-lengths and so broadened that its intensity in any given region is very low. For this reason an inconveniently long path of vapor would be required for its observation and our studies of it have consequently been confined to the liquid and to solutions of the acid in carbon tetrachloride. The broad band of the double molecules may overlap somewhat the narrow one of the single molecules but its intensity is so weak in this region that it could not have interferred in our photometric measurements of the latter.

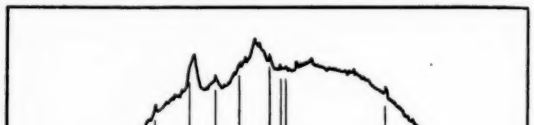

FIG. 1. Microphotometer curves of the O—H absorption band at λ9750 in acetic acid vapor, and of the water vapor band (lower curve) in the same region. Traces of water vapor in the spectrograph are responsible for some minor maxima in the acetic acid spectrum.

EXPERIMENTAL

The experiments here described were performed on acetic acid vapor confined in a cylindrical Pyrex cell provided with plane windows at the ends. The length of the tube was 304.8 cm and its volume was 5776 cc. It was supported in a resistance furnace of somewhat greater length which had glass windows (lenses which were a part of the optical system) placed intermediate between the ends of the furnace and of the cell to prevent circulation of air from the outside. The acetic acid, which had been purified by several recrystallizations, was distilled into the evacuated cell which was then sealed off and not disturbed until a complete series of photographs had been taken. Three fillings of the cell were made, with 5.699, 3.124 and 1.4606 grams of the acid, respectively, and measurements were made on the intensity of the O—H absorption band at λ9750 at numerous temperatures of the furnace in each case. In all of the measurements which we shall report all of the acetic acid was in the vapor state and the total pressure was at most approximately half the saturation pressure and usually considerably less.

In the photometric study of the equilibrium it was convenient to use a large glass spectrograph of dispersion about 70A per mm at λ9000. This would have been inadequate to resolve fine structure, had any been present, but was sufficient to give some idea of the general intensity distribution in the band. Since the shape of the band seemed to be constant under all the conditions of our experiments we decided to use as arbitrary measure of its intensity the absorption at its maximum, or more precisely, the apparent absorption in the maximum of the band as photographed under the moderate dispersion employed.

Eastman 144*Q* plates sensitized with ammonia were used. The ammonia sensitization led to some difficulties in the photometry since it is very difficult to obtain plates which are equally sensitive all over, but without its use the exposure times would have been so long that it would have been difficult to maintain steady conditions. For each condition of temperature and pressure of the acetic acid vapor a set of six exposures was made, side by side on the same plate. One was made without a screen and the remaining five with wire screens of transmissivities 0.788, 0.598, 0.385, 0.275 and 0.165, respectively, which were placed

in the optical path outside the spectrograph. The transmission of the screens had been determined with deep red light under geometrical conditions identical with those employed in the absorption measurements. A photronic cell was used which had been calibrated for red light by means of the inverse square law.

After the spectrograms had been microphotometered each set of six records was treated as follows. The microphotometer deflections were plotted against the transmissivity of the corresponding screen both for the maximum and for the toes of the band, and smooth curves were drawn through the two sets of points so obtained. Now since the sensitivity of the 144Q emulsion does not change appreciably with wave-length across the width of the band the density of the plates at the toes of the band could be taken as a measure of the background at the maximum. Consequently the fraction of light transmitted by the acetic acid vapor at the maximum of the band was given by the ratio of the abscissas (transmissivity) of the two curves at a given ordinate (deflection). Due to errors this was not quite constant and an average value was taken.

Owing to the overlapping of the rotation lines in the band, mentioned above, an effectively continuous absorption is produced and it seemed reasonable to suppose that Beer's law should hold in any small spectral region. However, in using a spectrograph of limited resolving power, so that the intensity varies appreciably in the region subtended by the slit, one should expect to find apparent deviations and it was necessary to make a direct calibration of our arbitrary intensity standard against the concentration of single molecules. Three points on a calibration curve were obtained by plotting the intensity of the O—H band against temperature for each filling of the cell. At high temperatures for each filling the absorption approached a constant value and the slight extrapolation to complete dissociation could be made without great error. By the use of tentative equilibrium constants which could then be obtained the extrapolation was improved on. As will be seen in Fig. 2, the plot of *—log transmission* against *concentration of single molecules* is nearly a straight line, and the deviation is about what would be expected with our limited resolving power.

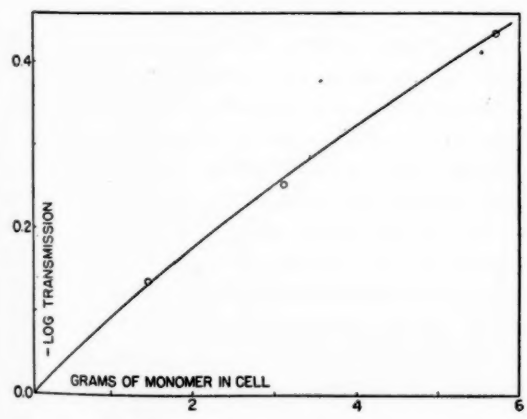

FIG. 2. Calibration curve relating the concentration of acetic acid single molecules to the absorption at the maximum of the O—H band at λ9750.

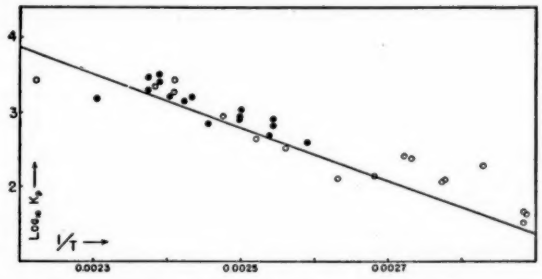

FIG. 3. Plot of the logarithm of the equilibrium constant against the reciprocal of the absolute temperature. The closed and open circles represent measurements made when the cell contained 5.699 and 1.4606 g of acetic acid, respectively. The straight line represents MacDougall's equation expressing the results of his vapor density measurements.

We have considered the question as to whether the absorption may depend not only on the concentration but also on the pressure and temperature. It seems unlikely that the pressure can have an appreciable effect since the absorption is for all practical purposes continuous as the overlapping of rotation lines is quite complete. The temperature might be expected to have some effect in changing the intensity distribution in the band, but this seems to be small in the range in which we worked as we have been unable to observe it.

Assuming that the intensity of the O—H band is a measure of the concentration of single molecules, and that both single and double molecules may be treated as perfect gases, we have calculated equilibrium constants for the dissociation

equilibrium. The constants calculated by the relation

$$K_p = (P_{\text{monomer}})^2/P_{\text{dimer}}$$

are plotted against $1/T$ in Fig. 3. The straight line is an extrapolation of the data of MacDougall,[3] obtained from vapor density measurements of the same equilibrium, made by use of the equation he gives:

$$\log_{10} K_p = 11.789 - (3590/T).$$

On our plot are shown only the points for the first and third fillings of the cell. The measurements with the second filling scattered very badly for some unknown reason, though the average agreed fairly well with the other data.

Conclusion

Owing to the difficulties of photometry when one is obliged to use ammonia sensitized plates our individual determinations cannot claim the accuracy of MacDougall's measurements. Nevertheless, in the region of intermediate temperatures where our accuracy was greatest the best line through our points does not deviate greatly from that representing MacDougall's equation. There are several reasons why the agreement might have been less good. In the first place the vapor density measurements were made at relatively low temperatures and the straight line represents a considerable extrapolation. It is possible that its slope is slightly in error or indeed that it should not be quite straight, since the heat of reaction presumably changes slightly with the temperature. In the second place one may not be measuring quite the same thing in the two types of investigation. The vapor density measurements cannot directly be used to distinguish between associations due to different causes, while our method presumably measures only that due to a specific cause, namely the formation of hydrogen bonds. The agreement between the two shows that the association is indeed due to that cause, for the greater part at least. In the third place it is conceivable that some double molecules of acetic acid are held together by only one hydrogen bond, one pair of oxygen atoms not being so connected. Molecules of this type would be expected to retain half of the ability to absorb in the λ9750 region. If this situation occurred frequently our equilibrium "constants" calculated in the manner described should increase at higher pressures. Actually within experimental error they seem to be independent of pressure and indeed to be truly constants, from which we may conclude that the majority of double molecules are held together by two hydrogen bonds.

The experiments which we have described appear to lend justification to the use of the position and general appearance of the O–H bands as a criterion for the presence or absence of hydrogen bonds. In the strict sense these bands do not disappear on hydrogen bond formation, and in some cases are actually strengthened. But in all of a number of cases which we have studied and will describe later, they are greatly shifted toward longer wave-lengths and are broadened. In some cases at least, this broadening is partly due to a splitting of the band into several components which overlap to a considerable extent. In some cases the O–H bands do disappear for all practical purposes. The shift to long wave-lengths carries them into regions where they overlap with strong C–H bands and are consequently obscured. Furthermore the absorption is so spread out that it is difficult to observe with path lengths which are quite adequate for studying the narrow bands found in the absence of hydrogen bonds.

We suggest some caution in the use of spectroscopic data in the discussion of hydrogen bonds. Since we have found no evidence for any great decrease in integral absorption coefficients on the formation of these bonds, decisions must be based on the shifts and general character of the absorption. This necessitates the use of adequate dispersion, and in case a substance cannot be studied in the two conditions, with the hydrogen bond present and absent, a knowledge of where the O–H absorption should be expected in the absence of such bonds. Even in the absence of hydrogen bond formation, in the ordinary sense, the O–H frequency appears to be somewhat variable due to the presence of various other types of interaction.

The Ultraviolet Absorption Spectrum of Benzene

G. B. KISTIAKOWSKY AND ARTHUR K. SOLOMON
Mallinckrodt Chemical Laboratory, Harvard University, Cambridge, Massachusetts
(Received April 19, 1937)

The variation of the ultraviolet absorption spectrum of benzene with temperature has been studied. From the Boltzmann distribution function two fundamental frequencies of the normal state are deduced. One is best identified with the Raman frequency of 404 cm^{-1}, whereas the other is possibly the 605 cm^{-1} vibration, but may be somewhat lower. The significance of these findings for the interpretation of the ultraviolet spectrum of benzene is discussed.

THE absorption spectrum of benzene consists in the main of several band groups beginning at 37494 cm^{-1} and extending into the violet with a frequently reappearing difference of 920 cm^{-1}. Upon further resolution of these band groups, they are found to consist of two progressions shaded to the red with an identical interval of about 160 cm^{-1} in each. The two progressions have heads *ca.* 80 cm^{-1} apart, the one on the violet side being more intense.

Considerable discussion has been aroused on the question of whether these small intervals are fundamentals in the ground state, or in the excited state, or combinations of both.

In 1931, Shapiro, Gibbs, and Johnson[1] investigated the temperature variation of the absorption of benzene vapor. Their measurements showed that the Boltzmann distribution within the 160 cm^{-1} progressions was satisfied if one assumed that the measured bands came from levels in the ground state 160 cm^{-1} apart. Since that time considerable criticism has been leveled at the concept of either a fundamental or a combination which would produce an interval of 160 cm^{-1}. In particular, the work of Lord and Andrews[2] on the entropy of benzene would be considerably in error should there be a fundamental of so low a frequency. Consequently it was thought advisable to repeat the work of Shapiro *et al.* with modified technique.

EXPERIMENTAL PROCEDURE

The source of ultraviolet radiation was a hydrogen arc lamp operating on a current of one-half of an ampere. The light from the lamp was focused as evenly as possible along the slit of a Hilger E-1 spectroscope, which gave a dispersion of 3.5A/mm in the region of 37000 to 38000 cm^{-1}. The plates were Eastman type 40, developed in Eastman D-7 developer for eight minutes at about 12°C. The normal exposure time was fifteen minutes. Between the lamp and the lens a 40 cm quartz absorption tube with plane parallel windows was placed. Liquid benzene was contained in a reservoir, chilled to 0°C, and the vapor was measured out by means of two small gas pipettes in the line between the reservoir and the absorption tube. The concentration of benzene in the absorption tube was of the order of 10^{-5} moles/cc. At each temperature exposures were taken at three different concentrations in order to cover the greatest range of density on the plate. For the purposes of evacuation the usual connections were made to a two-stage mercury diffusion pump backed by a Cenco Hyvac pump.

Temperatures were controlled by means of a small electrical furnace surrounding the absorption tube. Measurements were made with a mercury thermometer inserted in the furnace above the absorption tube, and were accurate to within five degrees. For the work below freezing a mixture of salt and ice was used to attain temperatures of about −18°C. The furnace was replaced by a galvanized iron box which contained the freezing mixture. The absorption tube within the box was supported on either end by a concentric glass tube, whose open end extended through and beyond the box. The glass tubes were attached to the absorption tube and the box by Gooch tubing. To avoid condensation a drying agent was inserted in the glass tubes, and the open ends were then closed by another pair

[1] Shapiro, Gibbs, and Johnson, Phys. Rev. **38**, 1170 (1931).
[2] Lord and Andrews, J. Phys. Chem. **41**, 149 (1937).

of quartz windows, sealed in with picein. In all, a range of temperature of about 240°C was covered, the highest temperature being almost double the lowest on the absolute scale.

The benzene used was pure thiophene free C. P. commercial benzene. The benzene-d_6 was the remainder of a sample kindly furnished by Professor H. S. Taylor of Princeton University to Cuthbertson and Kistiakowsky and used in their experiments on resonance fluorescence.[3]

In order to get a quantitative measurement of the amount of absorption a rotating sector (*ca.* 3000 r.p.m.) was constructed with five steps, each of which interrupted the light through a different angle. This was placed immediately in front of the slit, and one exposure was made on each plate with no benzene in the absorption tube, while the sector rotated.

Since the angles of the sector were known, the ratios of the illumination intensity of different parts of the slit were calculable. The plates were run through a microdensitometer and thus a relation between light intensity and deflections of the densitometer established. This was used to calculate the $\ln I/I_0$ *versus* frequency curve for benzene absorption, where I/I_0 represents the fraction of light intensity absorbed by benzene. Several points were obtained for each band and the area under the curve calculated by means of graphical integration. Unfortunately the bands within a progression over-lap rather considerably, and the more so the higher the temperature. It was thus necessary either to extrapolate the curve of each band or to limit the integration process to parts not covered by other bands. The second procedure appeared less arbitrary since by the calculational method outlined below any systematic errors that might be so introduced are largely eliminated. Each band was integrated over the same frequency interval at all temperatures.

These individual band areas are, within limitations discussed later, proportional to the transition probabilities integrated over all rotational states of the molecule and hence are suitable for determining the vibrational energy of the molecules responsible for the absorption. We can write for each an expression of the form:

$$A_i = f_i \frac{N g_i e^{-E_i/RT}}{\Sigma_i g_i e^{-E_i/RT}},$$

where A_i is the band area, f_i a proportionality factor including transition probability, N the total number of molecules, g_i the degeneracy of the absorbing state and E_i its energy above the lowest. To eliminate most of the constants in this expression, we form the ratio of the A's for any two neighboring bands and compare these ratios determined at two temperatures. The result is:

$$\frac{(A_i/A_{i+1})_{T_1}}{(A_i/A_{i+1})_{T_2}} = \frac{(f_i/f_{i+1})_{T_1}}{(f_i/f_{i+1})_{T_2}} e^{(E_{i+1}-E_i)(1/T_1-1/T_2)}$$

and hence, if the ratio of the f_i's is independent of temperature, the difference of energies of the molecules responsible for the two bands can be determined.

With a spectrograph of sufficient resolving power one can safely assume that the ratio of the f's is independent of temperature. Unfortunately this is not the case in the present work since the rotational structure of the benzene spectrum is not fully resolvable with a moderately sized spectrograph. Indeed, we have indications that Beer's law is not obeyed, a plot of $\ln A$ for some one band against vapor concentration not giving a straight line. Similarly, the ratio of A's for any two bands at the same temperature but at different vapor concentrations does not remain constant. These effects may easily result in a temperature coefficient of the ratio of the f's and thus lead to erroneous values for the vibrational energy, but their elimination appears impossible at present. This is due mainly to the circumstance that "accidental" errors in determining individual values of the A's are very large on account of uncertainties in extrapolation of the band absorption curves, over-lapping of fainter bands, belonging to other band groups, with those here measured and other measurement errors. There may be deviations from Beer's law whose magnitude at different temperatures cannot be established with any degree of certainty.

All in all, the results to be reported must be regarded as very crude, but we believe that the

[3] Cuthbertson and Kistiakowsky, J. Chem. Phys. **4**, 9 (1936).

order of magnitude of the effects observed is correct, which is all that is needed in order to interpret the absorption spectrum with the aid of other data available.

The Results

The measurements were limited to two band groups, 37494 and 38624 cm^{-1} (denoted in the following as I and II) which are the longest wavelength members of the absorption spectrum. In the band groups situated farther to the violet too much over-lapping from bands not belonging to the two 160 cm^{-1} progressions is apparent to place any reliance on absorption intensity measurements in this region. Within the measured band groups the relative intensity of the constituent bands varies within wide limits and only a few bands at each concentration of benzene vapor are suitable for measurement. Tables I and II give the results of measurements of the ratio of the temperature coefficient of absorption of those pairs of bands on which most reliance can be placed. The tables are incomplete because in many instances one of the bands needed to form the ratio gave either too strong or too weak absorption at some temperatures to make the calculation of the area under its curve at all certain. The successive bands of the stronger progression in each band group are denoted as I_0, I_1, II_0, II_1, etc., the numbering starting from the band on the violet end. The corresponding bands belonging to the weaker progressions are denoted as I_0', etc. The values in the tables give energy differences in cm^{-1}.

Table I. *Energy difference between states responsible for successive bands in a progression.*

Bands: Temp. °C	I_0/I_1	II_0/II_1	I_1/I_2	II_1/II_2	II_2/II_3	I_0'/I_1'	II_1'/II_2'
−15/220	324	340					
−15/102	334	426					
32/220	206			394	391		290
	457						
102/220			223	430		278	360
				554			
Average	340	383	223	445	391	278	325

Final average: 358 cm^{-1}

Table II. *Energy difference between states responsible for primed and unprimed progressions.*

Bands: Temp. °C	I_0/I_0'	II_0/II_0'	II_1/II_1'
−15/220	450	800	
−15/102	398	846	
32/220	800		356
	204		
102/220	534	730	510
	400		468
Average	465	792	444

Final average: 538 cm^{-1}

The large deviations of individual values from the mean may raise the question as to whether one is justified in regarding the energy differences between successive bands in the unprimed and primed progressions (and also in the groups I and II) as identical, thus whether the taking of a mean is a correct procedure. The tables give some instances of measurement of the same band ratio at different concentrations. These values are no more accurate than those given for different band ratios. The extremely regular structure and reproducibility of the four band progressions studied makes the assumption of regular energy differences more than probable and hence justifies the averaging process. It is to be noted that results on the primed progressions are less reliable because this progression is much weaker, so that over-lapping from neighboring bands causes greater uncertainty.

In a recent paper Sklar[4] calls attention to the observation of Henri that with increasing temperature the total intensity of the benzene absorption rapidly rises and interprets this as indicating that the whole absorption is due to vibrating molecules. While it is true, as the discussed measurements show, that the intensity of higher members of the progressions increases with temperature, the same is not true for the bands I_0 and II_0. Table III gives the integrated absorption of the first members of the series I and II at several different temperatures. It is to be noticed that for the first members the in-

[4] Sklar, paper presented at Symposium on Molecular Structure, Princeton, December, 1936.

tensity decreases as the temperature rises, due to a depopulation of these levels to provide the molecules for the higher levels. Most of the errors in Table III can be traced to the fact that the concentrations used may not have been the same at all temperatures, due to allowing insufficient time for the attainment of equilibrium with the benzene reservoir. However, concentration effects should not affect the energies calculated in Tables I and II.

It is clear that the vibrational energy of molecules responsible for the first band (I_0 and II_0) in each band group is quite low if at all different from zero. Since, as will be presently shown, the data of Table I utilize the lowest vibrational frequency of benzene and any other frequency would be entirely incompatible with these data, we must conclude that the first member of each band group is due to nonvibrating molecules.

Absorption spectrum of benzene-d_6 was also photographed, using the same technique. The evaluation of the plates led to very unsatisfactory results, individual values fluctuating even more than those of Tables I and II. A close inspection of the plates showed that superimposed on the benzene-d_6 spectrum was another, with band progression origins at 38679 and 38746 cm^{-1}. On comparing these values with those of Bowman, Benedict, Kirkpatrick and Taylor[5] it was discovered that the first band progression belongs to $C_6D_4H_2$, since they give for the latter the value 38676. In view of the complexity of the spectrum the measurements were abandoned.

Discussion

Sufficient data on the energy difference within each progression are available to make the "accidental" error of the average of Table I so small (some 90 cm^{-1}) that its identification with the hypothetical frequency of 160 cm^{-1} is out of the question. These measurements are therefore

Table III. *Integrated absorption of bands.*

Temp.	I_0	II_0
−15°	2.51	5.66
32°	3.23 5.14	
102°	2.24 4.21	4.72
220°	1.80 2.60	1.40

[5] Unpublished manuscript.

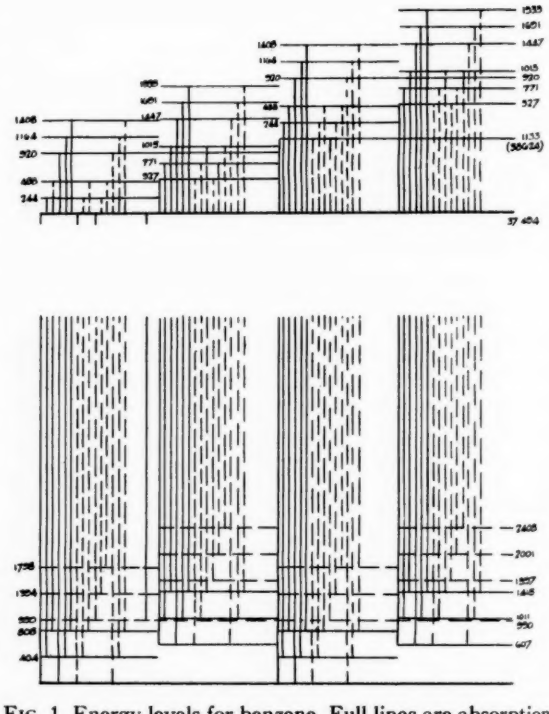

Fig. 1. Energy levels for benzene. Full lines are absorption lines, dotted lines and levels are for fluorescence.

in direct disagreement with the results of Shapiro and co-workers. The fact that the earlier work was done with the measurement of the intensity of the maximum of the band rather than the integrated absorption of nearly the whole band probably accounts for the discrepancy.

The limitation of the integration process to a part of the bands (probably some 95 percent of the total area at the lowest and some 70 percent at the highest temperature) does not introduce systematic errors because at each temperature a ratio of two consecutive band areas is taken for calculation. The same applies to the error due to incomplete resolving of the rotational structure. If not the ratios of two bands but single bands were taken for comparison, this effect would cause too high energy differences to be found. With the method used errors of this kind cannot be important.

It appears therefore on the whole that errors affecting the results are of essentially accidental nature; quite unfortunately they are extremely high.

If the choice for the assignment of the 358 cm^{-1} is limited to 160 cm^{-1} or 404 cm^{-1}, we are forced

to select the latter as the only one compatible with the present data. The difference between 358 and 404 cm^{-1} is within the limits of accidental error. If we interpret the difference as a systematic one, without knowing its cause, and assign it also to the result given in Table II, we find that the energy difference of molecules responsible for corresponding bands in the unprimed and primed progressions is 584 cm^{-1}. This is in good agreement with the Raman frequency 607 cm^{-1}, but of course the uncertainty of the present value is so large that no choice between 607 and a frequency of 538 calculated by Lord and Andrews is possible.

Selecting quite arbitrarily the former, the representation of the band progressions within each band group is as indicated by solid lines on the left side of Fig. 1. Bands due to transitions from vibrational levels with two quanta of the 605 cm^{-1}, aside from being weak, are unobservable because they coincide almost exactly with members of the unprimed progression. The near absence of any but the two progressions suggests that transitions in which the quantum numbers of either vibration change are very weak. However, the more complex structure of band groups situated farther to the violet from those here studied may indicate that when the molecules acquire a large amount of vibrational energy in other degrees of freedom, selection rules governing these transitions break down considerably.[4]

In order to complete the picture of the ultraviolet spectrum of benzene and benzene-d_6 it is necessary to revise somewhat the available results on the absorption spectrum. The chief difficulty in interpreting this work, as well as the detailed measurements of high pressure fluorescence or Tesla luminescence, is that not enough discrimination was applied in giving tables of measured "lines."

On comparing plates of benzene absorption and of high pressure fluorescence available here with published tables, we have become convinced that some of the data in the latter clearly refer to semi-resolved agglomerations of rotational lines within the bands. It is therefore impossible to fit all published measurements into a strictly vibrational pattern and only the more important "lines" or bands can be considered. Another, even if lesser, difficulty is that frequencies given by different authors do not agree to better than 5 or even 10 cm^{-1}. This must be borne in mind when reading the following.

The work of Witte[6] is the first detailed paper on the subject of absorption. Later work was done by Schulz[7] who got results in complete agreement with those of Witte, although they were not quite so extensive. Schulz attempted to break up his spectrum into series and succeeded in representing all of his results, with the exception of three bands, in eleven series. The more recent paper of Henri[8] is also in good agreement with that of Schulz and Witte. He fitted his results into four series, as follows:

$$1,\ 1/\lambda = 37703 + 921.4n - 161p;$$
$$n = 1, 2, \cdots;\ p = 0, 1, 2\cdots;$$
$$2,\ 1/\lambda = 37494 + 921.4n - 161p;$$
$$n = 0, 1\cdots;\ p = 0, 1\cdots;$$
$$3,\ 1/\lambda = 37613 + 921.4n - 161p;$$
$$n = 1, 2\cdots;\ p = 0, 1\cdots;$$
$$4,\ 1/\lambda = 37426 + 921.4n - 166p;$$
$$n = 0, 1\cdots;\ p = 0, 1\cdots.$$

These series leave out rotational fine structure since we are only concerned with vibration. In his later book Henri seems to have changed his interpretation, presumably supported by new experimental results which were not presented. Since the early work is in such good agreement with that of others, we are basing our conclusions on it.

It is significant that Henri did not observe any values in his series 1 and 3, for $n = 0$. Hence these two progressions can be represented thus:

$$1,\ 1/\lambda = 38624 + 921.4n - 161p;$$
$$n = 0, 1\cdots;\ p = 0, 1\cdots;$$
$$3,\ 1/\lambda = 38534 + 921.4n - 161p;$$
$$n = 0, 1\cdots;\ p = 0, 1\cdots.$$

Nine of Schulz's eleven series may be fitted into these four series of Henri. There are left two series, given below, and two bands which Schulz was unable to fit into series. These can be transformed into:

$$5,\ 1/\lambda = 38656 + 920n - 162p;$$
$$n = 0, 1\cdots;\ p = 0, 1\cdots;$$
$$6,\ 1/\lambda = 39649 + 920n;\quad n = 0, 1\cdots,$$

[6] Witte, Zeits. f. wiss. Phot. **14**, 347 (1915).
[7] Schulz, Zeits. f. wiss. Phot. **20**, 1 (1920).
[8] Henri, J. de phys. et rad. [6] **3**, 181 (1922); *Structure des Molecules* (Hermann, Paris, 1925), pp. 108 ff.

supplying a few of the missing members from Witte's data. The complete series will be given in Table IV. The band 37627.9 found by both Witte and Schulz will be accounted for on our scheme, leaving only the band 40123.9 unaccounted for in the complete work of Henri and of Schulz. Because of the many additional lines reported by Witte, probably of smaller intensity, the analysis has not been extended to his work.

It can be seen that the sets 1 and 3, and 2 and 4 are pairs having the characteristic difference of about 80 cm^{-1} between each pair. Consequently they fit very well into the scheme shown in Fig. 1, with one electronic level at 37494 cm^{-1}.

Superimposed on the electronic level are vibrational levels of several frequencies: 244 and 527 cm^{-1}, together with the 404 and 605 of the normal state, give rise to the 160 and 80 cm^{-1} spacings within each group; 920 produces consecutive band groups, while 1133 is responsible for Henri's series 1 and 3. We are inclined to consider this 1133 level as a vibrational one, rather than to assign it to a new electronic state because the other frequencies of the excited molecule (i.e., 244,527,920), when superimposed upon it, remain completely unchanged; this would require more explanation were it a different electronic level. Series 5 and 6 are not included in Fig. 1.

The band at 37628, if real, must be interpreted as representing absorption from a vibrating molecule with 990 cm^{-1} energy to the excited level with one quantum of the 1130 frequency.

To understand the structure of the high pressure fluorescence, as discussed more recently by one of the present authors with collaborators and by Ingold *et al.*,[9] one must make the fundamental assumption—which is contrary to earlier suggestions—that as the result of inelastic collisions with other benzene molecules or with molecules of inert gas the excited benzene molecules retain a considerable amount of vibrational energy which roughly corresponds to a temperature of several hundred degrees Centigrade. This is necessary because the 160 cm^{-1} progressions extend much farther than in absorption and also because the primed progressions almost equal in intensity the unprimed ones (see a microdensitometer record in the Kistiakowsky and Nelles paper[10]). Cuthbertson and Kistiakowsky also report band groups originating in the 38624 level (given there as 38609), while Ingold's data, beside confirming these, give also bands which we interpret readily as originating in states having $920+n244$ and $920+527+n244$ cm^{-1}. vibrational energy. Some of the bands in these rather faint progressions must be due to molecules having altogether some 1500 cm^{-1} or even more vibrational energy, and it is rather puzzling that no better temperature equilibration has taken place, particularly under experimental conditions of Wilson who had a very thorough quenching of the resonance fluorescence by the added gas. Ingold's data confirm these results, and give the following three series for benzene fluorescence:

$$1/\lambda = 37473 - 990.4n - 160.8p; \quad n=0, 1\cdots; p=0, 1\cdots;$$
$$1/\lambda = 38535 - 990.4n - 160.8p; \quad n=0, 1\cdots; p=0, 1\cdots;$$
$$1/\lambda = 38607 - 990.4n - 160.8p; \quad n=0, 1\cdots; p=0, 1\cdots.$$

For benzene-d_6 the following series are given:

$$1/\lambda = 37709 - 942.8n - 141.2p; \quad n=0, 1\cdots; p=0, 1\cdots;$$
$$1/\lambda = 38707 - 942.8n - 141.2p; \quad n=0, 1\cdots; p=0, 1\cdots;$$
$$1/\lambda = 38785 - 942.8n - 141.2p; \quad n=0, 1\cdots; p=0, 1\cdots.$$

Complete tables of frequencies of bands observed are also given, and it is from these tables that the values presented in the fluorescence section of Table IV are taken.

Table IV gives the members of the new series found.

Columns 1 and 2 are obtained from the results of Schulz[7] and Witte.[6] Witte's contributions are marked with a "w." Column 1 gives series 5, observed in absorption,

$$1/\lambda = 38656 + 920n - 162p; \quad n=0, 1, \cdots, p=0, 1\cdots.$$

Column 2 gives series 6;

$$1/\lambda = 39649 + 920n, \quad n=0, 1\cdots.$$

[9] Angus, Bailey, Hale, Ingold, Leckie, Raisin, Thompson, and Wilson, J. Chem. Soc. 912 (1936); Wilson, ibid. 1210 (1936).

[10] Kistiakowsky and Nelles, Phys. Rev. **41**, 595 (1932).

Columns 3 through 5 give series found in fluorescence taken from the results of Ingold, Wilson *et al.*[9] for C_6H_6. Column 3 gives the series,

$$1/\lambda = 37428 - 990n - 160p;$$
$$n = 0, 1\cdots,\ p = 0, 1\cdots,$$

coming from the upper levels $37494 + 527 + 244m$, $m = 0, 1\cdots$. Column 4 gives the series,

$$1/\lambda = 38416 - 990n - 160p;$$
$$n = 0, 1\cdots,\ p = 0, 1\cdots,$$

coming from the upper levels $37494 + 920 + 244m$, $m = 0, 1\cdots$. Column 5 gives the series,

$$1/\lambda = 38344 - 990n - 160p;$$
$$n = 0, 1\cdots,\ p = 0, 1\cdots,$$

coming from the upper levels, $37494 + 920 + 527 + 244m$, $m = 0, 1\cdots$. Columns 6 through 9 give series found in fluorescence taken from the results of Ingold, Wilson *et al.*[9] for C_6D_6. Column 6 gives the series,

$$1/\lambda = 37635 - 942n - 141p;$$
$$n = 0, 1\cdots,\ p = 0, 1\cdots,$$

coming from the upper levels, $37711 + 500 + 196m$, $m = 0, 1\cdots$. Column 7 gives the series,

$$1/\lambda = 38515 - 942n - 141p;$$
$$n = 0, 1\cdots,\ p = 0, 1\cdots,$$

coming from the upper levels, $37711 + 500 + 880 + 196m$, $m = 0, 1\cdots$. Column 8 gives the series,

$$1/\lambda = 38592 - 942n - 141p;$$
$$n = 0, 1\cdots,\ p = 0, 1\cdots,$$

coming from the upper levels, $37711 + 880 + 196m$, $m = 0, 1\cdots$.

TABLE IV.

Absorption		Fluorescence					
		C_6H_6			C_6D_6		
Series 5	Series 6						
38656w	39649	37428	38416	38344	37635	38515	38592
505w		265	258	184	493	374	450
328	40569	108	098	028	352	233	312
		36946	37936	37866	216	093	169
	41492	789	775		073	37956	030
39576					36934		37892
417w	42411w			37357	795		
251		36440	37425	197	656	37578	
		283	265	033	517	439	37650
		123	104	36878	380	296	508
40499		35962	36947		240	155	380
322w		804	785		099		243
172				36364			106
				206	36696	36636	36966
		35447	36429	045	554	497	815
41418		289	275	35885	406	359	
252w		131	119	724	269		
		34973	35958	570	130		36711
42336		810	798	408	35990	35698	572
			635		850	560	428
					710	420	291
		34458		35375		280	149
		298	35445	216		142	010
		140	284	056	35756		35871
		33979	127	34896	614		731
		818		726	473		591
					334		453
					195		314
					052		175
					34914		
							35770
					34811		629
					672		485
							346
							207
							065
							34925

For benzene, the fluorescence is shown in Fig. 1. The series beginning with 38607 and 38535 are to be identified with the 38624 level. Likewise the series at 37473 and the new series at 37428 are to be identified with the 37494 level. The set of new series at 38416 and 38344 originate in states superimposed on the electronic level with vibrational energy of $920 + 244n$ cm^{-1}, and $920 + 527 + 244n$ cm^{-1}.

The Tesla luminescence of benzene has been investigated by McVicker, Marsh and Stewart.[11] Under their conditions of excitation one might expect a considerably more complex spectrum since high speed electrons may impart to benzene not only electronic but also variable amounts of vibrational energy. In fact, however, the spectrum agrees quite well with the high pressure fluorescence data (cf. Ingold and collaborators), only a few weaker bands remaining after the rest has been fitted into the pattern above. It appears thus that in electronic collisions some vibrational energy is transferred but that the amount is rather limited.

Austin and Black[12] in a later paper on Tesla luminescence fit their results in the following six series:

$$a,\quad 1/\lambda = 37485 + 924m - 161n,$$
$$b,\quad 1/\lambda = 37398 + 924m - 161n,$$
$$c,\quad 1/\lambda = 37485 - 986m - 162n,$$
$$d,\quad 1/\lambda = 37425 - 986m - 162n,$$
$$e,\quad 1/\lambda = 36479 - 991m - 162n,$$
$$f,\quad 1/\lambda = 36412 - 991m - 162n,$$

[11] McVicker, Marsh and Stewart, Phil. Mag. **48**, 628 (1924).

[12] Austin and Black, Phys. Rev. **35**. 452 (1930).

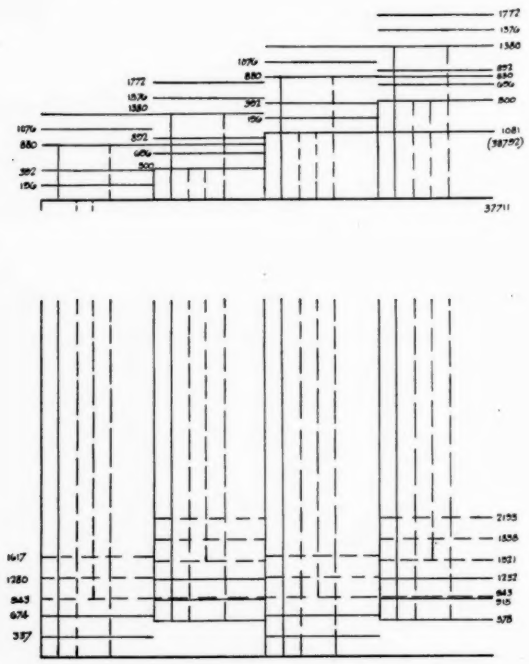

FIG. 2. Energy levels for benzene-d_6. Full lines are absorption lines, dotted lines and levels are for fluorescence.

with $m=0, 1\cdots$ and $n=0, 1\cdots$ for all the series. Their results, though more complete, are in good agreement with those of Marsh and co-workers, so we should expect to fit these six series into our pattern also. Series "*c*" and "*d*" can be identified as coming from fluorescence of molecules on the 37494 level. A series corresponding to series "*a*" has already been mentioned in fluorescence. If one is justified in identifying series "*b*" as coming from the same level as series "*d*," this can be accounted for on the same scheme. From the figures given by Austin and Black it is possible to get a series beginning as

$$1/\lambda = 38624 - 994m - 160n,$$
$$m=0, 1\cdots, n=0, 1\cdots$$

and the first member of series "*e*" can be fitted into this series for $m=2$, $n=1$. Series "*f*" is the other member of this pair. These results agree quite well with those to be expected on the basis of Fig. 1.

A scheme similar in all respects to the one given in Fig. 1 can be set up for benzene-d_6. Bowman *et al.* (reference 5) report levels at 37711 and 38792 which are also found in high pressure fluorescence (see C. and K. and Ingold *et al.*). These correspond to the 37494 and 38624 levels of the ordinary benzene. The whole pattern of the band groups, as discussed before by one of us, remains unchanged and hence a scheme analogous to that given in Fig. 1 is fully justified. This is given in Fig. 2.

It is to be emphasized that the pattern here proposed is only one of many possible ones. No proof can be given at present that it is the uniquely correct one, but, considering that we have succeeded in bringing together such a large fraction of all available evidence concerning the ultraviolet spectrum of benzene, we feel that the true solution cannot be far different.

In conclusion, the authors wish to express their thanks to Dr. E. B. Wilson, Jr. for many valuable discussions, and suggestions incorporated in the paper.

The Vibration-Rotation Energy Levels of Polyatomic Molecules

III. Effect of Centrifugal Distortion

E. Bright Wilson, Jr.
Mallinckrodt Chemical Laboratory, Harvard University, Cambridge, Massachusetts

(Received April 12, 1937)

The effect of the centrifugal distortion on the individual rotational energy levels of semi-rigid asymmetrical rotator molecules is calculated by an approximate quantum-mechanical treatment. A secular equation is obtained which reduces to the Wang equation when the molecule is rigid and which can be factored to the same extent as the Wang equation. It is shown that the numerical coefficients which occur are identical with those which enter the classical treatment of this problem, if the assumption is made that the vibrational wave functions are harmonic oscillator functions.

In Part I of this series[1] it was shown that the matrix for the energy corresponding to a single vibrational state of an asymmetrical rotator molecule could be approximated by the expression (see Eq. (49) of I)

$$\mathfrak{H}=\mathbf{W}_V+\tfrac{1}{2}\sum_{\alpha,\beta}\sigma_{\alpha\beta}\mathbf{P}_\alpha\mathbf{P}_\beta+\tfrac{1}{4}\sum_{\alpha,\beta,\gamma,\delta}\tau_{\alpha\beta\gamma\delta}\mathbf{P}_\alpha\mathbf{P}_\beta\mathbf{P}_\gamma\mathbf{P}_\delta, \quad (1)$$

in which $\mathbf{W}_V$ is a constant diagonal matrix representing the vibrational energy, $\mathbf{P}_\alpha$ is the matrix for the component of the total angular momentum along the α axis (α, β, γ, δ may each represent either x, y, or z), and the sums are over all sets of values of these indices. $\sigma_{\alpha\beta}$ is a numerical coefficient related to the moments of inertia of the molecule and is a fixed number for a definite vibrational state. Likewise the coefficients $\tau_{\alpha\beta\gamma\delta}$ are fixed numbers dependent only on the vibrational state and are associated with the resistance to rotational distortion offered by the molecule.

Since the matrix elements for $\mathbf{P}_x$, $\mathbf{P}_y$, and $\mathbf{P}_z$ are known[2] in terms of a representation in which $\mathbf{P}_z$ and $\mathbf{P}^2=\mathbf{P}_x^2+\mathbf{P}_y^2+\mathbf{P}_z^2$ are diagonal, it is possible to obtain by matrix multiplication the elements of $\mathbf{P}_\alpha\mathbf{P}_\beta$ and $\mathbf{P}_\alpha\mathbf{P}_\beta\mathbf{P}_\gamma\mathbf{P}_\delta$. Using these, together with numerical values of the σ's and τ's obtained as shown below, one can determine numerically the elements of the energy matrix $\mathfrak{H}$ and consequently the secular equation

$$|\mathfrak{H}-W|=0, \quad (2)$$

from which the energy levels W can be computed. The methods of carrying out each of these steps will be shown below.

The Coefficients $\sigma_{\alpha\beta}$

In this paper only molecules with orthorhombic symmetry will be treated in detail since for such molecules the cross product coefficients σ_{xy}, σ_{yz}, and σ_{zx} vanish, leaving only σ_{xx}, σ_{yy} and σ_{zz} to be considered. These are related to the "effective moments of inertia" A_e, B_e and C_e by the relations $\sigma_{xx}=1/A_e$, $\sigma_{yy}=1/B_e$, $\sigma_{zz}=1/C_e$. As pointed out in I, these quantities are not strictly equal to the geometrical moments of inertia because of the vibrational motion. The usual procedure is to determine A_e, B_e and C_e from the observed rotational spectrum.

The Coefficients $\tau_{\alpha\beta\gamma\delta}$

These coefficients are given by Eq. (54) of I as

$$\tau_{\alpha\beta\gamma\delta}=\sum_{V'}{}'(\mu_{\alpha\beta})_{V,V'}(\mu_{\gamma\delta})_{V',V}/h\nu_{V,V'}, \quad (3)$$

in which the sum is over the vibrational states V', excluding the state V under consideration. $h\nu_{VV'}$ is the difference in energy $W_V{}^0-W_{V'}{}^0$. The μ's are related to the moments of inertia as described in I (Eq. (13) of I) while $(\mu_{\alpha\beta})_{V,V'}$ is the matrix element of $\mu_{\alpha\beta}$ in terms of the vibrational wave functions ψ for the states V and V'. In other words, $(\mu_{\alpha\beta})_{V,V'}=\int\psi_V{}^*\mu_{\alpha\beta}\psi_{V'}d\tau$.

[1] J. B. Howard and E. B. Wilson, Jr., J. Chem. Phys. **4**, 260 (1936).
[2] O. Klein, Zeits. f. Physik **58**, 730 (1929).

An important reduction is feasible if the assumption is made that the vibrational wave functions are harmonic oscillator functions. The functions $\mu_{\alpha\beta}$ can be expanded in terms of the normal coordinates Q_k as follows

$$\mu_{\alpha\beta}=\mu_{\alpha\beta}^0+\sum_k \mu_{\alpha\beta}^{(k)}Q_k+\cdots, \tag{4}$$

in which $\mu_{\alpha\beta}^0$ is the equilibrium value and

$$\mu_{\alpha\beta}^{(k)}=(\partial\mu_{\alpha\beta}/\partial Q_k)_0. \tag{5}$$

If powers of Q_k higher than the first in Eq. (4) are neglected, the matrix elements $(\mu_{\alpha\beta})_{VV'}$ will be given by

$$(\mu_{\alpha\beta})_{VV'}=\sum_k \mu_{\alpha\beta}^{(k)}(Q_k)_{VV'}. \quad (V'\neq V). \tag{6}$$

But $(Q_k)_{VV'}$, which is the matrix element of the normal coordinate Q_k in terms of the vibrational wave functions, is zero for harmonic oscillator functions unless V' differs from V only in the single quantum number n_k associated with the normal coordinate Q_k and even then it is zero unless the change in this quantum number is ± 1. For this latter case[3] $(Q_k)_{VV'}$ is

$$\begin{aligned}&[(n_k+1)h/8\pi^2\nu_k^0]^{\frac{1}{2}} \quad \text{for} \quad n_k\rightarrow n_k+1\\ \text{and}\quad &[n_kh/8\pi^2\nu_k^0]^{\frac{1}{2}} \quad \text{for} \quad n_k\rightarrow n_k-1.\end{aligned} \tag{7}$$

Also $h\nu_{VV'}=\mp h\nu_k^0$ for the two cases. When these results are used in Eq. (3), it is found that the only states V' entering into the summation are those differing by one unit in one quantum number n_k. The sum may therefore be written as two sums over k, one involving $\Delta n_k=+1$, the other $\Delta n_k=-1$. Thus

$$\begin{aligned}\tau_{\alpha\beta\gamma\delta}&=\sum_k \mu_{\alpha\beta}^{(k)}\mu_{\gamma\delta}^{(k)}(1/8\pi^2\nu_k^{02})\{-(n_k+1)+n_k\}\\ &=-\tfrac{1}{2}\sum_k \mu_{\alpha\beta}^{(k)}\mu_{\gamma\delta}^{(k)}/\lambda_k,\end{aligned} \tag{8}$$

where $\lambda_k=4\pi^2\nu_k^{02}$. Examination shows that this result holds even when one of the quantum numbers n_k for the state V is zero, for in that case although there is no state for which $\Delta n_k=-1$, corresponding to the second term in the parenthesis above, the formula is correct because $n_k=0$.

The importance of Eq. (8) is seen when the classical treatment of the centrifugal expansion of molecules is examined.[4] For the classical treatment, the energy is given by an equation of the same form as Eq. (1), except that P_x, P_y, P_z are not matrices but the actual components of angular momentum. Furthermore the classical treatment, under similar assumptions, gives an expression for $\tau_{\alpha\beta\gamma\delta}$ identical with Eq. (8) (see Eq. (19) of reference 4). Consequently the methods of calculating these coefficients which have been given in reference 4 for the classical case may equally well be applied in the quantum-mechanical problem.

For orthorhombic molecules, only τ_{xxxx}, τ_{yyyy}, τ_{zzzz}, τ_{xxyy}, τ_{yyzz}, τ_{zzxx}, τ_{xyxy}, τ_{yzyz}, and τ_{zxzx} and related coefficients in which $\gamma\delta$ have been exchanged with $\alpha\beta$ are different from zero. A still greater simplification is possible when triatomic molecules such as water are treated, since in this case only τ_{xxxx}, τ_{yyyy}, τ_{zzzz}, $\tau_{xxyy}=\tau_{yyxx}$, $\tau_{yyzz}=\tau_{zzyy}$, $\tau_{zzxx}=\tau_{xxzz}$, and $\tau_{xyxy}=\tau_{yxyx}=\tau_{xyyx}=\tau_{yxxy}$ are non-vanishing.

The numerical computation of the τ's requires geometrical data concerning the molecule, a knowledge of the normal modes of vibration (or of the force constants) and the values of the fundamental vibration frequencies. For many molecules this information is known with sufficient accuracy to permit useful calculations to be made. Further details of the calculation of these coefficients will be found in reference 4.

The Matrix Elements of $\mathbf{P}_\alpha\mathbf{P}_\beta\mathbf{P}_\gamma\mathbf{P}_\delta$

From Klein's[2] work, or in other ways, it is known that the nonvanishing elements of the matrices for P_x, P_y, P_z are

$$\begin{aligned}(P_x)_{J,K,M;\,J,K\pm1,M}&=\pm i(P_y)_{J,K,M;\,J,K\pm1,M}\\ &=(h/4\pi)[J(J+1)-K(K\pm1)]^{\frac{1}{2}},\end{aligned} \tag{9}$$

$$(P_z)_{J,K,M;\,J,K,M}=K(h/2\pi).$$

J, K, and M are the usual quantum numbers for the symmetrical rotator wave functions. All other elements of these matrices are zero. By using matrix multiplication the matrices for P_x^2, P_y^2, etc., can be obtained. Some of these matrices are given in Eq. (3) of Part II of this series,[5] for

[3] See, for example, Pauling and Wilson, *Introduction to Quantum Mechanics*, p. 82.

[4] E. B. Wilson, Jr., J. Chem. Phys. **4**, 526 (1936).

[5] E. B. Wilson, Jr., J. Chem. Phys. **4**, 313 (1936).

example. From these by further use of matrix multiplication the elements of the matrices for the quartic terms of the type $P_\alpha P_\beta P_\gamma P_\delta$, for example P_x^4, can be calculated. In the treatment of water-type molecules only a few of these terms occur and are given below:

$$
\begin{aligned}
(P_x^4)_{J,K,M;J,K,M} &= (P_y^4)_{J,K,M;J,K,M} = (h^4/128\pi^4)(3f^2-2f-6fK^2+5K^2+3K^4),\\
(P_x^4)_{J,K,M;J,K\pm2,M} &= -(P_y^4)_{J,K,M;J,K\pm2,M} = (h^4/128\pi^4)[2f-K^2-(K\pm2)^2]\\
&\quad\times\{[f-K(K\pm1)][f-(K\pm1)(K\pm2)]\}^{\frac{1}{2}},\\
(P_x^4)_{J,K,M;J,K\pm4,M} &= (P_y^4)_{J,K,M;J,K\pm4,M} = (h^4/256\pi^4)\{[f-K(K\pm1)]\\
&\quad\times[f-(K\pm1)(K\pm2)][f-(K\pm2)(K\pm3)][f-(K\pm3)(K\pm4)]\}^{\frac{1}{2}},\\
(P_z^4)_{J,K,M;J,K,M} &= (h^4/16\pi^4)K^4,\\
(P_x^2P_y^2+P_y^2P_x^2)_{J,K,M;J,K,M} &= (h^4/64\pi^4)\{f^2+2f-2fK^2-5K^2+K^4\},\\
(P_x^2P_y^2+P_y^2P_x^2)_{J,K,M;J,K\pm4,M} &= -2(P_x^4)_{J,K,M;J,K\pm4,M},\\
(P_y^2P_z^2+P_z^2P_y^2)_{J,K,M;J,K,M} &= (P_z^2P_x^2+P_x^2P_z^2)_{J,K,M;J,K,M} = (h^4/16\pi^4)K^2(f-K^2),\\
-(P_y^2P_z^2+P_z^2P_y^2)_{J,K,M;J,K\pm2,M} &= (P_z^2P_x^2+P_x^2P_z^2)_{J,K,M;J,K\pm2,M} = (h^4/64\pi^4)\\
&\quad\times[K^2+(K\pm2)^2]\{[f-K(K\pm1)][f-(K\pm1)(K\pm2)]\}^{\frac{1}{2}},\\
[(P_xP_y+P_yP_x)^2]_{J,K,M;J,K,M} &= (h^4/32\pi^4)(f^2-2f-2fK^2+5K^2+K^4),\\
[(P_xP_y+P_yP_x)^2]_{J,K,M;J,K\pm4,M} &= -4(P_x^4)_{J,K,M;J,K\pm4,M}.
\end{aligned}
\tag{10}
$$

In the above matrices, $f=J(J+1)$. Elements not given above are zero.

The Secular Equation

When the simplifications possible for water are introduced, Eq. (1) reduces to the following expression for the energy matrix expressed in terms of the momentum matrices:

$$
\begin{aligned}
\mathfrak{H} &= \mathbf{W}_V+\tfrac{1}{2}(\mathbf{P}_x^2/A_e+\mathbf{P}_y^2/B_e+\mathbf{P}_z^2/C_e)\\
&+\tfrac{1}{4}\{\tau_{xxxx}\mathbf{P}_x^4+\tau_{yyyy}\mathbf{P}_y^4+\tau_{zzzz}\mathbf{P}_z^4\\
&+\tau_{xxyy}(\mathbf{P}_x^2\mathbf{P}_y^2+\mathbf{P}_y^2\mathbf{P}_x^2)+\tau_{yyzz}(\mathbf{P}_y^2\mathbf{P}_z^2+\mathbf{P}_z^2\mathbf{P}_y^2)\\
&+\tau_{zzxx}(\mathbf{P}_z^2\mathbf{P}_x^2+\mathbf{P}_x^2\mathbf{P}_z^2)\\
&+\tau_{xyxy}(\mathbf{P}_x\mathbf{P}_y+\mathbf{P}_y\mathbf{P}_x)^2\}.
\end{aligned}
\tag{11}
$$

The elements of the matrix for $\mathfrak{H}$ can be obtained explicitly by substituting the expressions of the previous section. If the energy matrix has the elements $\mathfrak{H}_{R,R'}$, R representing J, K, M, then the secular equation leading to the energy levels W is a determinantal equation of which a typical element is

$$\mathfrak{H}_{R,R'}-\delta_{RR'}W. \tag{12}$$

$\delta_{RR'}$ is zero unless $R=R'$, in which case it is unity. This equation has properties similar to the Wang[6] equation for the rigid asymmetrical rotator, to which it reduces if all the τ's vanish. In particular it factors into smaller equations, one for each J, M value, since $\mathfrak{H}_{R,R'}$ is diagonal in both J and M. The elements of the secular equation can thus be denoted by the symbol $(K|K')$, it being assumed that $J'=J$ and $M'=M$. It is convenient to divide all terms by the constant quantity $(h^2/8\pi^2)c'$, where $c'=(1/C_e)-\frac{1}{2}[(1/A_e)+(1/B_e)]$, and to introduce the quantity ϵ defined by the relation

$$W=W_V+(h^2/8\pi^2)\{J(J+1)\tfrac{1}{2}\times[(1/A_e)+(1/B_e)]+c'\epsilon\}. \tag{13}$$

When this has been done, the elements of the secular equation have the following form, for fixed J and M values,

[6] S. C. Wang, Phys. Rev. **34**, 243 (1929).

$$(K|K)=-\epsilon+K^2+(h^2/64\pi^2c')\{(3f^2-2f-6fK^2+5K^2+3K^4)(\tau_{xxxx}+\tau_{yyyy})+8K^4\tau_{zzzz}$$
$$+2(f^2+2f-2fK^2-5K^2+K^4)\tau_{xxyy}+8K^2(f-K^2)(\tau_{xxxz}+\tau_{yyyz})$$
$$+4(f^2-2f-2fK^2+5K^2+K^4)\tau_{xyxy}\}, \quad (14)$$

$$(K|K\pm2)=\tfrac{1}{2}\{[f-K(K\pm1)][f-(K\pm1)(K\pm2)]\}^{\frac{1}{2}}\{b+(h^2/64\pi^2c')[(\tau_{xxxx}-\tau_{yyyy})$$
$$\times2(2f-K^2-(K\pm2)^2)+(\tau_{xxzz}-\tau_{yyzz})4(K^2+(K\pm2)^2)]\}, \quad (15)$$

$$(K|K\pm4)=(h^2/64\pi^2c')\{\tau_{xxxx}+\tau_{yyyy}-2\tau_{xxyy}-4\tau_{xyxy}\}\tfrac{1}{2}\{[f-K(K\pm1)][f-(K\pm1)(K\pm2)]$$
$$\times[f-(K\pm2)(K\pm3)][f-(K\pm3)(K\pm4)]\}^{\frac{1}{2}}, \quad (16)$$

$$(-K|-K')=(K|K')=(K'|K)=(-K'|-K). \quad (17)$$

In the above, $f=J(J+1)$, $b=\frac{1}{2}[(1/A_e)-(1/B_e)]/c'$.

Because of the fact that no nonvanishing elements of the secular equation connect odd and even values of K, the secular equation can be factored into one equation for odd K's and one for even K's. Furthermore, on account of Eq. (17), these equations can be factored once more by using the linear combinations

$$(\tfrac{1}{2})^{\frac{1}{2}}(\psi_K+\psi_{-K}) \text{ and } (\tfrac{1}{2})^{\frac{1}{2}}(\psi_K-\psi_{-K}) \text{ for } K\neq0 \text{ and } \psi_0 \text{ for } K=0. \quad (18)$$

If $[K|K']^{\pm}$ is used to represent the general element of the completely factored secular equation, the plus sign meaning the factor corresponding to the plus sign in Eq. (18), etc., then

$$[K|K']^{+}=(K|K')+(K|-K'), \quad K>0, \quad K'>0,$$
$$[0|K]^{+}=[K|0]^{+}=\sqrt{2}(0|K), \quad (19)$$
$$[K|K']^{-}=(K|K')-(K|-K').$$

The secular equation for the nonrigid rotator therefore factors in exactly the same manner as the Wang equation for the rigid rotator.

Conclusion

The method of applying the above equations to an actual molecule is as follows. By considering the molecule as rigid an approximate set of moments of inertia A_e, B_e, and C_e is obtained from the spectrum. From the geometry of the molecule deduced from these, and from the normal coordinates or force constants obtained from an analysis of the vibrational spectrum, the coefficients τ are calculated. The general secular equation given above is then solved, regarding the τ's as known and A_e, B_e, C_e as parameters to be adjusted to fit the rotational spectra.

This procedure has been applied in the following paper by Professor Cross and Mr. B. L. Crawford to hydrogen sulphide.

The approximations used in the present treatment are doubtless not valid for very high rotational states, in which the centrifugal distortion is too great to be given correctly by Eq. (1). Sixth power terms in P_α could be added but their coefficients would probably depend on the anharmonicity of the potential energy, which is not known.

The general methods described in this paper can be modified to treat symmetrical molecules as well as asymmetrical molecules.

Elements of the Factored Secular Equation for the Semi-Rigid Water Type Rotator, With Application to the Hydrogen Sulfide Band at 10,100A

BRYCE L. CRAWFORD, JR. AND PAUL C. CROSS
Stanford University, Stanford University, California

(Received April 12, 1937)

The necessary numerical coefficients of the molecular constants in the secular equation obtained in the previous paper are tabulated up to $j=12$. A rapid approximate procedure for obtaining the roots of the secular equation is described. The treatment is applied to the hydrogen sulfide band at 10,100A. A slight improvement is obtained over the previous analysis which used the Wang equation classically corrected for centrifugal distortion. New molecular constants and term values are given.

ONE of the most interesting applications of the equation developed in the preceding paper[1] which can be made is to the analysis of the hydrogen sulfide band at 10,100A. The previous analysis of this band[2] included a classical centrifugal distortion correction which was applied to the rigid rotator term values calculated from the Wang equation.[3] Although this treatment allowed many assignments to be made with certainty, numerous discrepancies between calculated and observed values seemed larger than the estimated experimental error. The present work was undertaken with the hope of reducing these discrepancies, and with the purpose of comparing the results of the classically corrected Wang equation with the closer approximation given by the equation derived by Wilson.

The experimental data used were those obtained by Cross.[2] The assignments required by both analyses were found to be identical.

ELEMENTS OF THE SECULAR EQUATION

In reducing the secular equation to numerical form, extensive tables of coefficients applicable to all water type molecules were calculated. Since it seems desirable to have these generally available, they are presented in Table I.

For each value of the rotational quantum number j, the table gives directly the nonvanishing coefficients for the elements of the four factors of the secular equation (see Eqs. (14) to (19) of the preceding paper). It is convenient to introduce the following notations:

$$\begin{aligned}
x&=(h^2/64\pi^2c')(\tau_{xxxx}+\tau_{yyyy}),\\
y&=(h^2/64\pi^2c')\ \tau_{zzzz},\\
z&=(h^2/64\pi^2c')\ \tau_{xxyy},\\
u&=(h^2/64\pi^2c')(\tau_{xxzz}+\tau_{zzyy}),\\
v&=(h^2/64\pi^2c')\ \tau_{zyzy},\\
s&=(h^2/64\pi^2c')(\tau_{xxxx}-\tau_{yyyy}),\\
w&=(h^2/64\pi^2c')(\tau_{xxxx}-\tau_{zzyy}),\\
t&=2x-4z-8v.
\end{aligned} \tag{1}$$

With the use of this notation, and the relation given in Eq. (13) of the preceding paper, the nonvanishing elements of the four factors for a given value of j may be written:

$$\begin{aligned}
[K,K]^{\pm}&=-\epsilon+K^2+Xx+Yy+Zz+Uu\\
&\quad+Vv\pm(Bb+Ss+Ww)\pm(Tt),\\
[K,K+2]^{\pm}&=Bb+Ss+Ww\pm Tt,\\
[K,K+4]^{\pm}&=Tt,
\end{aligned} \tag{2}$$

where X, Y, Z, U, V, B, S, W, T are the coefficients given in Table I. The "even plus" factor, $\mathbf{E}^+$, runs through even values of K from $[0,0]^+$, $[0,2]^+$, $[0,4]^+$, and takes the positive value of all optional signs in Eq. (2). The "even minus" factor, $\mathbf{E}^-$, runs through even values of K from $[2,2]^-$, $[2,4]^-$, $[2,6]^-$, and takes the negative value of the optional signs in Eq. (2). The two odd factors, $\mathbf{O}^+$ and $\mathbf{O}^-$, run through all odd values of K and take positive and negative values, respectively, of the optional signs in Eq. (2).

The authors have found it most convenient to determine the values of ϵ by applying successive approximations to the factors of the secular equation in determinantal form. The complete array of term values up to $j=8$ may be calcu-

[1] E. B. Wilson, Jr., J. Chem. Phys. **5**, 617 (1937).
[2] P. C. Cross, Phys. Rev. **47**, 7 (1935).
[3] S. C. Wang, Phys. Rev. **34**, 247 (1929).

TABLE I.

Elements of the factored secular equation for the water type rotator. Diagonal elements, type $[K, K]\pm$; $[K, K]\pm = -\epsilon + K^2 + Xx + Yy + Zz + Uu + Vv \pm (Bb + Ss + Ww) \pm (Tt)$.

ELEMENT	X	Y	Z	U	V
j=1					
1.1	4	8	0	8	8
		$\pm(b+4s+8w)$			
0.0	8	0	16	0	0
j=2					
1.1	68	8	64	40	72
		$\pm(3b+60s+24w)$			
0.0	96	0	96	0	96
2.2	20	128	−8	64	48
		$\pm 6t$			
j=3					
1.1	344	8	280	88	402
		$\pm(6b+264s+48w)$			
3.3	48	648	−24	216	120
0.0	408	0	336	0	480
2.2	188	128	136	256	240
		$\pm 30t$			
j=4					
1.1	1048	8	792	152	1304
		$\pm(10b+760s+80w)$			
3.3	368	648	232	792	504
0.0	1160	0	880	0	1440
2.2	748	128	552	512	944
		$\pm 90t$			
4.4	88	2048	−48	512	224
j=5					
1.1	2468	8	1792	232	3144
		$\pm(15b+1740s+120w)$			
3.3	1308	648	912	1512	1704
5.5	140	5000	−80	1000	360
0.0	2640	0	1920	0	3360
2.2	1988	128	1432	832	2544
		$\pm 210t$			
4.4	608	2048	352	1792	864
j=6					
1.1	4964	8	3520	328	6408
		$\pm(21b+3444s+168w)$			
3.3	3228	648	2256	2376	4200
5.5	908	5000	496	3400	1320
0.0	5208	0	3696	0	6720
2.2	4268	128	3016	1216	5520
		$\pm 420t$			
4.4	2024	2048	1360	3328	2688
6.6	204	10368	−120	1728	528
j=7					
1.1	8968	8	6264	440	11672
		$\pm(28b+6160s+224w)$			
3.3	6560	648	4552	3384	8568
5.5	2896	5000	1896	6200	3896
7.7	280	19208	−168	2744	728
0.0	9296	0	6496	0	12096
2.2	8020	128	5592	1664	10448

ELEMENT	X	Y	Z	U	V
j=7 (continued)					
		$\pm 756t$			
4.4	4768	2048	3264	5120	6272
6.6	1268	10368	664	5760	1872
j=8					
1.1	14984	8	10360	568	19608
		$\pm(36b+10224s+288w)$			
3.3	11808	648	8136	4536	15480
5.5	6608	5000	4456	9400	8760
7.7	1688	19208	856	9016	2520
0.0	15408	0	10656	0	20160
2.2	13748	128	9496	2176	18000
		$\pm 1260t$			
4.4	9344	2048	6400	7168	12288
6.6	3924	10368	2520	10368	5238
8.8	368	32768	−224	4096	960
j=9					
1.1	23588	8	16192	712	30984
		$\pm(45b+16020s+360w)$			
3.3	19548	648	13392	5832	25704
5.5	12620	5000	8560	13000	16680
7.7	5108	19208	3232	16072	6984
9.9	468	52488	−288	5832	1224
0.0	24120	0	16560	0	31680
2.2	22028	128	15112	2752	28944
		$\pm 1980t$			
4.4	16328	2048	11152	9472	21504
6.6	8748	10368	5832	15552	11664
8.8	2168	32768	1072	13312	3264
j=10					
1.1	35428	8	24192	872	46664
		$\pm(55b+23980s+440w)$			
3.3	30428	648	20752	7272	40104
5.5	21580	5000	14640	17000	28520
7.7	11188	19208	7392	23912	14984
9.9	2708	52488	1312	18792	4104
0.0	36080	0	24640	0	47520
2.2	33508	128	22872	3392	44144
		$\pm 2970t$			
4.4	26368	2048	17952	12032	34784
6.6	16388	10368	11032	21312	21744
8.8	6448	32768	4032	23552	8864
10.10	580	80000	−360	8000	1520
j=11					
1.1	51224	8	34840	1048	67608
		$\pm(66b+34584s+528w)$			
3.3	45168	648	30696	8856	59640
5.5	34208	5000	23176	21400	45240
7.7	20648	19208	13816	32536	27480
9.9	7944	52488	4920	33048	10968
11.11	704	117128	−440	10648	1848
0.0	52008	0	35376	0	68640
2.2	48908	128	33256	4096	64560
		$\pm 4290t$			
4.4	40184	2048	27280	14848	53088
6.6	27564	10368	18600	27648	36528
8.8	13928	32768	9136	34816	18720
10.10	3308	80000	1576	25600	5040

TABLE I, *continued*.

ELEMENT	X	Y	Z	U	V	ELEMENT	X	Y	Z	U	V
j=12											
1.1	71768	8	48664	1240	94872	0.0	72696	0	49296	0	96096
		$\pm(78b+48360s+624w)$				2.2	69020	128	46792	4864	91248
3.3	64560	648	43752	10584	85368			$\pm 6006t$			
5.5	51296	5000	34696	26200	67896	4.4	58568	2048	39664	17920	77472
7.7	34280	19208	23032	41944	45528	6.6	43068	10368	29064	34560	57072
9.9	16968	52488	11064	48600	22872	8.8	25400	32768	16912	47104	33888
11.11	3968	117128	1864	33880	6072	10.10	9596	80000	5896	44800	13296
						12.12	840	165888	−528	13824	2208

Off-diagonal elements, type $[K, K+2]\pm$; $[K, K+2]\pm = Bb+Ss+Ww\pm Tt$.

ELEMENT	B	S	W	ELEMENT	B	S	W
j=2				*j=9*			
0.2	3.464	55.42	55.42	1.3	42.988	14615.90	1719.52
j=3					$\pm 1934.46t$		
1.3	3.873	108.44	154.92	3.5	36.945	10787.90	5024.52
	$\pm 23.24t$			5.7	26.833	5688.60	7942.57
0.2	7.746	309.84	123.94	7.9	12.369	1236.90	6431.88
j=4				0.2	62.928	22150.70	1006.85
1.3	7.937	476.24	317.49	2.4	40.472	12951.00	3237.76
	$\pm 79.37t$			4.6	32.404	8295.42	6740.03
				6.8	20.199	3231.84	8079.60
0.2	13.416	965.95	214.66	*j=10*			
2.4	5.292	211.66	423.32	1.3	52.991	22256.20	2119.64
j=5					$\pm 2914.48t$		
1.3	12.962	1296.15	518.46	3.5	46.957	17468.00	6386.15
	$\pm 194.42t$			5.7	36.878	10768.40	10915.90
3.5	6.708	348.83	912.32	7.9	22.650	4077.00	11778.00
				0.2	77.071	33294.70	1233.14
0.2	20.494	2295.33	327.90	2.4	50.477	20190.80	4038.16
2.4	10.392	831.36	831.36	4.6	42.426	14255.10	8824.61
				6.8	30.299	7271.76	12119.60
j=6				8.10	13.784	1543.81	9042.30
1.3	18.974	2808.10	758.95	*j=11*			
	$\pm 398.45t$			1.3	63.992	32507.90	2559.68
3.5	12.845	1284.52	1746.95		$\pm 4223.47t$		
				3.5	57.965	26663.90	7883.20
0.2	28.983	4637.25	463.72	5.7	47.906	18204.30	14180.20
2.4	16.432	2103.24	1314.53	7.9	33.764	9048.75	17557.30
4.6	8.124	519.94	1689.79	9.11	15.199	1884.68	12280.80
j=7				0.2	92.628	48166.60	1482.05
1.3	25.982	5300.23	1039.26	2.4	61.481	30002.70	4918.48
	$\pm 727.48t$			4.6	53.442	22659.40	11115.90
3.5	19.900	3104.34	2706.34	6.8	41.352	13563.50	16540.80
5.7	9.539	724.99	2823.66	8.10	25.100	5020.00	16465.60
0.2	38.884	8398.99	622.15	*j=12*			
2.4	23.452	4315.17	1876.16	1.3	75.993	45899.80	3039.72
4.6	15.297	1835.64	3181.78		$\pm 5927.49t$		
				3.5	69.971	38903.90	9516.06
j=8				5.7	59.925	28524.30	17737.80
1.3	33.985	9108.03	1359.41	7.9	45.826	16680.70	23829.50
	$\pm 1223.47t$			9.11	27.550	6061.00	22260.40
3.5	27.928	6144.25	3798.26				
5.7	17.748	2484.76	5253.50	0.2	109.599	67512.40	1753.57
				2.4	73.484	42914.60	5878.72
0.2	50.200	14055.89	803.19	4.6	65.452	34035.00	13614.00
2.4	31.464	7803.15	2517.14	6.8	53.385	22635.20	21354.00
4.6	23.367	4299.45	4860.25	8.10	37.229	11019.80	24422.20
6.8	10.954	963.99	4381.76	10.12	16.613	2259.37	16214.30

Off-diagonal elements, type $[K, K+4]\pm$; $[K, K+4]\pm = Tt$.

ELEMENT	T	ELEMENT	T
j=4		*j=10*	
0.4	70.99	1.5	2488.30
		3.7	1731.70
j=5		5.9	835.27
1.5	86.95		
		0.4	3890.38
0.4	212.98	2.6	2141.59
		4.8	1285.45
j=6		6.10	417.64
1.5	243.72		
		j=11	
0.4	476.24	1.5	3709.34
2.6	133.49	3.7	2776.90
		5.9	1617.50
j=7		7.11	513.17
1.5	517.01		
3.7	189.83	0.4	5694.93
		2.6	3285.68
0.4	911.92	4.8	2209.92
2.6	358.75	6.10	1037.93
j=8		*j=12*	
1.5	949.16	1.5	5317.37
3.7	495.68	3.7	4193.03
		5.9	2746.11
0.4	1579.50	7.11	1262.50
2.6	735.21		
4.8	255.97	0.4	8053.87
		2.6	4809.74
j=9		4.8	3494.20
1.5	1588.24	6.10	1987.49
3.7	991.36	8.12	618.49
5.9	331.90		
0.4	2546.86		
2.6	1311.45		
4.8	654.53		

lated in a day's time, after some practice, with the aid of the following procedure.[4]

In the zeroth approximation, the values of ϵ for a particular factor are given by the successive diagonal terms. If, for a specific root, an approximate value of ϵ, ϵ_0, be substituted in all diagonal elements save the one which is itself the zeroth approximation to that root, the determinant is reduced to one with all elements numerical save one, which has the form $(\epsilon'-\epsilon)$. If then all nondiagonal elements are reduced to zero by suitable addition of rows and columns, this element will become $(\epsilon_1-\epsilon)$ where ϵ_1 is the next approximation to ϵ, since $(\epsilon_1-\epsilon)$ must vanish if the determinant is to vanish. The true value of ϵ lies between ϵ_0 and ϵ_1; this relationship facilitates a close estimation of the true value of ϵ. After some practice, a value of ϵ accurate to six significant figures may be obtained in three or four approximations.

Application to the Hydrogen Sulfide Band at 10,100A

For this application, the coefficients were calculated (Eq. (8) of the preceding paper) from the molecular structure deduced from the previous analysis[2] and the vibrational assignments used therein.[5] The constants of Eq. (1), for hydrogen sulfide, were found to be

$$\begin{aligned} x&=7.10\times(10^{-5}), & v&=0.645\times(10^{-5}),\\ y&=0.163, & s&=1.47,\\ z&=-2.16, & w&=-0.0401,\\ u&=0.645, & t&=17.70. \end{aligned} \qquad (3)$$

Table II. *Constants of the H_2S molecule.*

	Normal State	Excited State
$(h/8\pi^2c)(1/A_e)$	10.393 cm^{-1}	9.910 cm^{-1}
$(h/8\pi^2c)(1/B_e)$	9.040	8.379
$(h/8\pi^2c)(1/C_e)$	4.723	4.470
A_e	$2.661\times(10^{-40})$ g cm^2	$2.791\times(10^{-40})$ g cm^2
B_e	3.060	3.301
C_e	5.856	6.188

$\nu_0=9911.03$ cm^{-1}.

The term values were first calculated from the secular equation for the semi-rigid rotator, using the constants of Eq. (3) and the moments of inertia obtained from the classically corrected Wang treatment. The best values of the moments of inertia and the band center were then obtained by a least squares treatment (see Section IX of reference 2). In this treatment the derivatives given by Eq. (7) to (10) of reference 2 were used. These derivatives were found to give changes in the term values accurate to within 0.03 cm^{-1} for changes in the moments of inertia up to 1 percent. The final values of the molecular constants, given in Table II, were obtained from the 33 best lines.[6] The median deviation of the calculated from the observed values runs from 0.06 cm^{-1} for the 24 most reliable lines to 0.11 cm^{-1} for the full set of uniquely assigned lines. This represents a slight improvement over the classically corrected Wang treatment.

It is apparent from the above results that the experimental measurements available at present are not sufficiently precise to demonstrate the superiority of the Wilson treatment to the classically corrected Wang treatment. This is readily accounted for by the extreme difficulty of obtaining photographs suitable for highly accurate measurement.[7, 8]

Term values for rotational levels for which the fourth-order Wilson treatment is probably satisfactory, calculated from the constants of Table II, are given in Table III.

Preliminary attempts to apply this treatment to the rotational analysis of the 9420A band of water vapor have also been made, and have as yet been only partially successful. It appears advisable to delay any report of this work until a more complete analysis has been made.

In conclusion, we wish to thank Professor

[4] This procedure was originally suggested to one of us by Professor R. M. Badger.

[5] The change in the vibrational analysis and valence angle proposed by Sprague and Nielsen [J. Chem. Phys. **5**, 85 (1937)] would have a small effect on the coefficients given here, but would not change the term values appreciably. As we have pointed out elsewhere, however [J. Chem. Phys. **5**, 371 (1937)], this proposed change is incompatible with the intensity pattern observed in the 10,100A band.

[6] Of the 84 lines assigned in reference 2, all but 33 were discarded for the least squares treatment for one or more of the following reasons: (1) more than one calculated transition fell in the immediate vicinity of the observed line; (2) the observed line was extremely weak and the measurement correspondingly unreliable; (3) the assigned transition was between term values for which the fourth-order Wilson treatment was believed to be an insufficiently close approximation.

[7] F. D. Carvin, J. Chem. Phys. **5**, 159 (1937).

[8] P. C. Cross, J. Chem. Phys. **5**, 370 (1937).

TABLE III. *Calculated term values (cm^{-1}) and symmetries.*

LEVEL	SYMMETRY	NORMAL STATE	EXCITED STATE	LEVEL	SYMMETRY	NORMAL STATE	EXCITED STATE	LEVEL	SYMMETRY	NORMAL STATE	EXCITED STATE
0_0	++	0.00	0.00	5_4	−−	297.14	282.14	8_{-2}	−−	568.95	534.54
				5_5	+−	297.72	282.50	8_{-1}	−+	569.10	534.86
1_{-1}	−+	13.76	12.85					8_0	++	610.23	571.61
1_0	−−	15.11	14.38	6_{-6}	++	227.79	215.12	8_1	+−	612.34	575.17
1_1	+−	19.43	18.29	6_{-5}	+−	227.79	215.12	8_2	−−	637.00	595.05
				6_{-4}	−−	281.86	265.47	8_3	−+	648.45	610.11
2_{-2}	++	38.04	35.78	6_{-3}	−+	281.86	265.48	8_4	++	657.20	615.93
2_{-1}	+−	38.32	36.16	6_{-2}	++	325.56	305.92	8_5	+−	682.79	645.31
2_0	−−	51.26	47.86	6_{-1}	+−	325.77	306.30	8_6	−−	684.32	646.18
2_1	−+	55.31	52.46	6_0	−−	357.37	334.49	8_7	−+	719.94	684.54
2_2	++	58.54	55.21	6_1	−+	360.29	338.73	8_8	++	720.08	684.62
				6_2	++	376.49	351.83				
3_{-3}	−+	71.43	67.35	6_3	+−	389.03	367.05	9_{-9}	−+	468.72	442.97
3_{-2}	−−	71.48	67.41	6_4	−−	393.14	369.80	9_{-8}	−−	468.72	442.97
3_{-1}	+−	95.27	89.24	6_5	−+	418.14	397.25	9_{-7}	+−	552.12	520.64
3_0	++	96.58	90.99	6_6	++	418.43	397.41	9_{-6}	++	552.12	520.64
3_1	−+	107.65	100.65					9_{-5}	−+	625.14	588.59
3_2	−−	115.68	109.74	7_{-7}	−+	298.73	282.20	9_{-4}	−−	625.14	588.59
3_3	+−	117.75	111.34	7_{-6}	−−	298.73	282.20	9_{-3}	+−	687.86	646.78
				7_{-5}	+−	362.59	341.67	9_{-2}	++	687.86	646.78
4_{-4}	++	114.15	107.73	7_{-4}	++	362.59	341.67				
4_{-3}	+−	114.15	107.73	7_{-3}	−+	416.18	391.43	10_{-10}	++	567.78	536.65
4_{-2}	−−	148.38	139.46	7_{-2}	−−	416.21	391.51	10_{-9}	+−	567.78	536.65
4_{-1}	−+	148.66	139.90	7_{-1}	+−	459.00	430.66	10_{-8}	−−	660.91	623.40
4_0	++	170.76	159.65	7_0	++	459.74	431.98	10_{-7}	−+	660.91	623.40
4_1	+−	174.39	164.32	7_1	−+	488.46	456.55	10_{-6}	++	743.58	700.32
4_2	−−	183.16	171.51	7_2	−−	494.77	465.28	10_{-5}	+−	743.58	700.32
4_3	−+	196.30	186.29	7_3	+−	507.25	474.38				
4_4	++	197.44	187.08	7_4	++	526.01	496.72	11_{-11}	−+	676.18	639.18
				7_5	−+	528.50	498.22	11_{-10}	−−	676.18	639.18
5_{-5}	−+	166.26	156.98	7_6	−−	559.61	531.45	11_{-9}	+−	779.00	734.95
5_{-4}	−−	166.26	156.98	7_7	+−	559.35	531.73	11_{-8}	++	779.00	734.95
5_{-3}	+−	210.48	198.10								
5_{-2}	++	210.52	198.18	8_{-8}	++	379.05	358.14	12_{-12}	++	793.91	750.54
5_{-1}	−+	243.87	228.70	8_{-7}	+−	379.05	358.14	12_{-11}	+−	793.91	750.54
5_0	−−	244.93	230.31	8_{-6}	−−	452.69	426.73	12_{-10}	−−	906.38	855.32
5_1	+−	264.45	247.06	8_{-5}	−+	452.69	426.73	12_{-9}	−+	906.38	855.32
5_2	++	271.85	256.28	8_{-4}	++	516.03	485.62				
5_3	−+	278.16	261.02	8_{-3}	+−	516.04	485.63				

E. B. Wilson, Jr., for making available to us, before publication, the results of his treatment, together with many of the numerical coefficients used and reported here.

The Molecular Structure of P_4O_6, P_4O_8, P_4O_{10} and As_4O_6 by Electron Diffraction

L. R. MAXWELL, S. B. HENDRICKS AND LOLA S. DEMING
Bureau of Chemistry and Soils, Washington, D. C.

(Received June 14, 1936)

Molecular structures of P_4O_6 and As_4O_6 were determined from electron diffraction data. P_4O_6 was found to have the symmetry of the point group T_d with an angle P−O−P of 128.5±1.5°, and a P−O distance of 1.67±0.03A. In this structure the phosphorus oxygen distances and the phosphorus valence angles were preserved with resulting deformation of the oxygen valence angle. The separation of the arsenic atoms in As_4O_6 was found to be 3.20±0.05A. Because of the predominant scattering of the arsenic atoms it was difficult to determine the oxygen valence angle, As−O−As. Values of 120°, 127.5° and 140° gave approximate agreement between the observed and calculated positions of maxima. Electron diffraction photographs obtained from P_4O_{10} differ considerably from those found for P_4O_6. It was not possible to explain all of the features of the P_4O_{10} diffraction pattern by a model having the symmetry of the point group T_d and it is thought that the structure might be one of lower symmetry. Data were obtained on P_4O_8 which indicated that it has approximately the same electron diffraction pattern as P_4O_{10}.

INTRODUCTION

MOLECULAR structure determinations of phosphorus trioxide, phosphorus pentoxide, and arsenic trioxide by means of electron diffraction were undertaken as part of a general study of these compounds. Under the experimental conditions used the molecular forms of these gases are known to be P_4O_6, P_4O_{10} and As_4O_6. An attempt was also made to study antimony trioxide but the extreme corrosive character of the molten compound caused the work to be abandoned. Arsenic pentoxide could not be studied since it dissociates upon heating to give oxygen and the trioxide. The results obtained for the molecules investigated give further information about the valence angles of oxygen and phosphorus as well as the internuclear distances.

ARSENIC AND PHOSPHORUS TRIOXIDES (As_4O_6 AND P_4O_6)

These molecules are expected to have the symmetry of the point group T_d and their structures are fixed by two parameters. For convenience these are taken as the P−P or As−As distance and the P−O−P or As−O−As valence angle. Cartesian coordinates of the atomic positions are:

As or P; $u\ u\ u$, $\bar{u}\ \bar{u}\ u$, $u\ \bar{u}\ \bar{u}$, $\bar{u}\ u\ \bar{u}$

O; $v\ o\ o$, $o\ v\ o$, $o\ o\ v$, $\bar{v}\ o\ o$, $o\ \bar{v}\ o$, $o\ o\ \bar{v}$.

Intensity of electron scattering $I_1(\theta)$ from this structure is given by

$$I_1(\theta)=4\psi^2_{P,As}\left(1+3\frac{\sin s\cdot(8u^2)^{\frac{1}{2}}}{s\cdot(8u^2)^{\frac{1}{2}}}\right)+24\psi_{P,As}\psi_0\left(\frac{\sin s\cdot[(u-v)^2+2u^2]^{\frac{1}{2}}}{s\cdot[(u-v)^2+2u^2]^{\frac{1}{2}}}+\frac{\sin s\cdot[(u+v)^2+2u^2]^{\frac{1}{2}}}{s\cdot[(u+v)^2+2u^2]^{\frac{1}{2}}}\right)$$
$$+6\psi_0^2\left(1+\frac{\sin s\cdot 2v}{s\cdot 2v}+\frac{4\sin s\cdot(2v^2)^{\frac{1}{2}}}{s\cdot(2v^2)^{\frac{1}{2}}}\right)+I'_{inc}(\theta), \quad (1)$$

where $\psi_{P,As}$ and ψ_0 represent the atomic electron scattering amplitudes, $I'_{inc}(\theta)$ the incoherent electron scattering[1] and $s=4\pi(1/\lambda)\sin\frac{1}{2}\theta$. For the purpose of comparing the theoretical electron scattering with the observed interference pattern it is desirable in certain instances to modify the theoretical scattering formula in such a manner as to provide a direct comparison with the visual measurements. A method followed by other investigators[2] uses a modified scattering formula in which ψ_i is replaced by Z_i and the incoherent scattering is omitted. Theoretical curves obtained in this manner show prominent maxima which are then compared with the ob-

[1] See L. Bewilogua, Physik. Zeits. 33, 688 (1932).

[2] See for instance L. Pauling and L. O. Brockway, J. Chem. Phys. 2, 867 (1934).

served interference maxima as determined visually. Another method[3] for transforming the calculated scattering curves into many real maxima involves only a plot of $I_1(\theta)\cdot s^2$. This procedure is considerably less drastic than the former method and gives correctly the relative atomic scattering probabilities of the different constituents of the molecule. In the present case several models were calculated according to the two different methods and a comparison of the results obtained is shown in Table I where

$$x_{i-i}=s\cdot(8u^2)^{\frac{1}{2}}=4\pi l_{i-i}(1/\lambda)\sin\tfrac{1}{2}\theta \qquad (2)$$

and l_{i-i} is the distance between nearest phosphorus or arsenic atoms. It is noticed that the positions computed from $I_1(\theta)\cdot s^2$ are usually less than those obtained by the approximate method, however the difference is generally not greater than 2 percent. In some cases the relative intensities of the maxima are different. In order to reduce the labor involved the approximate method was used to a considerable extent with a realization of the approximations involved. We have thus shown in Figs. 1, 2, 3 and 4 theoretical curves calculated for P_4O_6 and As_4O_6 using the approximate method.

[3] L. R. Maxwell, S. B. Hendricks and V. M. Mosley, J. Chem. Phys. **3**, 699 (1935).

Electron diffraction photographs were obtained using the electron diffraction camera and boiler previously described.[3, 4] A reproduction of a typical photograph obtained from As_4O_6 is shown in Fig. 5. Positions of the interference maxima as measured visually are shown in Table II and are indicated for comparison with the theoretical curves in Figs. 1, 2, 3 and 4.

Arsenic trioxide (As_4O_6)

Since the arsenic atoms are responsible for a large amount of the electron scattering their positions can be determined but it is difficult to obtain the oxygen valence angle. By a comparison between the experimental and the theoretical positions for the various interference maxima as shown in Fig. 3 and Fig. 4 it is noticed that fair agreement is found for 120°, 127.5° and 140° while all of the other angles considered can definitely be excluded. The model with an oxygen valence angle of 140° appears to give somewhat better agreement than the other possible angles. An As−As distance of 3.20±0.05A is thus obtained from a consideration of the agreement existing for these angles. The good agreement

[4] S. B. Hendricks, L. R. Maxwell, V. M. Mosley and M. E. Jefferson, J. Chem. Phys. **1**, 549 (1933).

TABLE I. *Comparison of methods used for transforming theoretical electron scattering curves into a form possessing real maxima in all cases.*

		Position of Maxima in Terms of x_{i-i}				
	No.	$\psi_i=Z_i$		$I(\theta)\cdot s^2$		% Difference
P_4O_6, P−O−P=130°	1	7.5	(7)*	7.35	(10)	2.0
	2	13.75	(10)	13.5	(7)	1.5
	3	19.1	(1)	absent		—
	4	25.5	(6)	25.1	(3)	1.6
	5	32.5	(1)	32.0	(1)	1.6
	6	38.0	(3)	37.6	(1)	1.1
As_4O_6, As−O−As=130°	1	7.5	(10)	7.5	(10)	0
	2	13.8	(9.3)	13.75	(8.5)	.4
	3	20.0	(2.5)	19.75	(1.5)	1.3
	4	26.0	(5.5)	25.5	(3.5)	2.0
	5	32.7	(1.5)	32.3	(.8)	1.2
	6	38.5	(2.5)	37.75	(.5)	2.0
P_4O_{10} Model No. 1	1	8.0	(3)	7.7	(5)	3.9
	2	13.5	(10)	13.3	(10)	1.5
	3	22.25	(4)	21.75	(3)	2.3
	4	26.8	(3)	26.70	(1.5)	0.4
	5	33.9	(5)	33.7	(1.5)	0.6
	6	39.2	(2)	39.0	(.5)	0.5
P_4O_{10} Model No. 5	1	8.5	(4)	8.0	(2.5)	6.2
	2	14.0	(10)	13.70	(10)	2.2

* Numbers in parenthesis represent an estimated relative intensity.

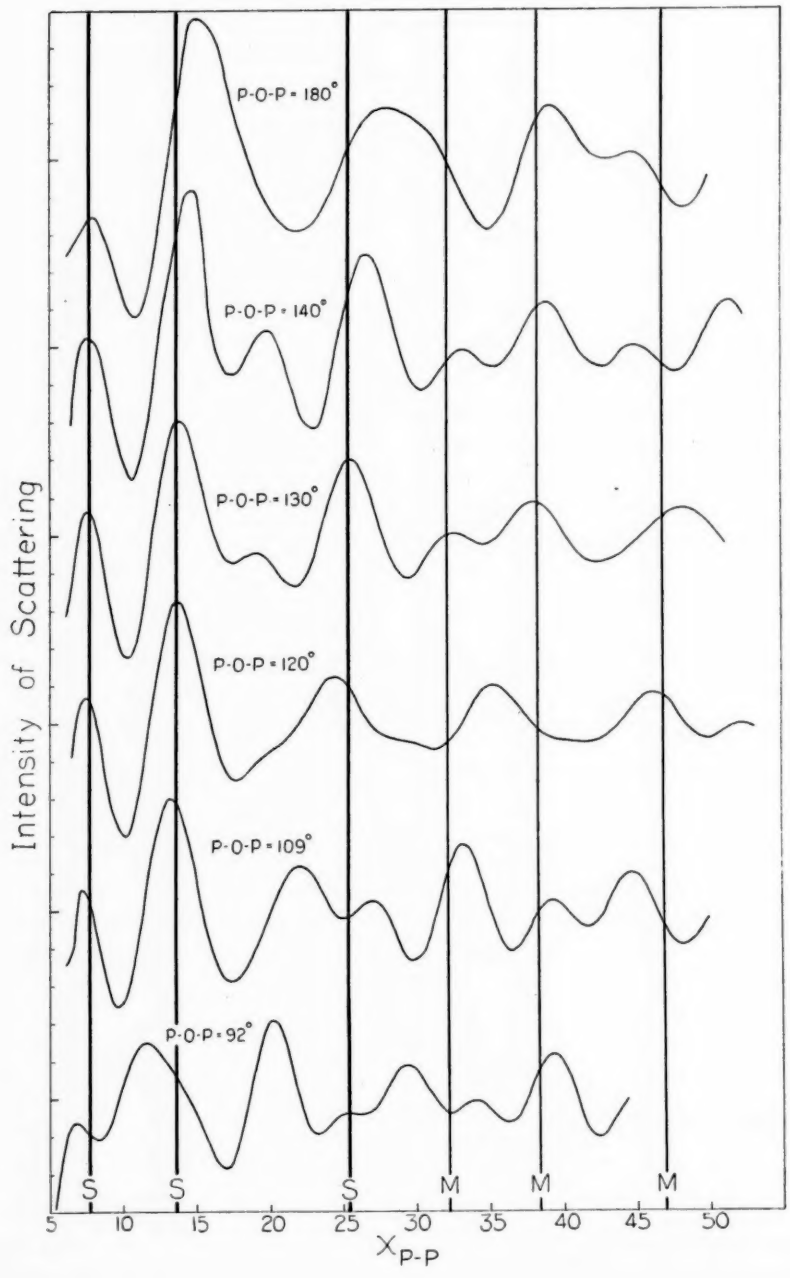

FIG. 1. Electron scattering curves for P_4O_6 where ψ_i is replaced by Z_i calculated for various P−O−P valence angles. Vertical lines give the position of the experimental maxima where $l_{p-p}=3.00$A. The incoherent scattering has been omitted.

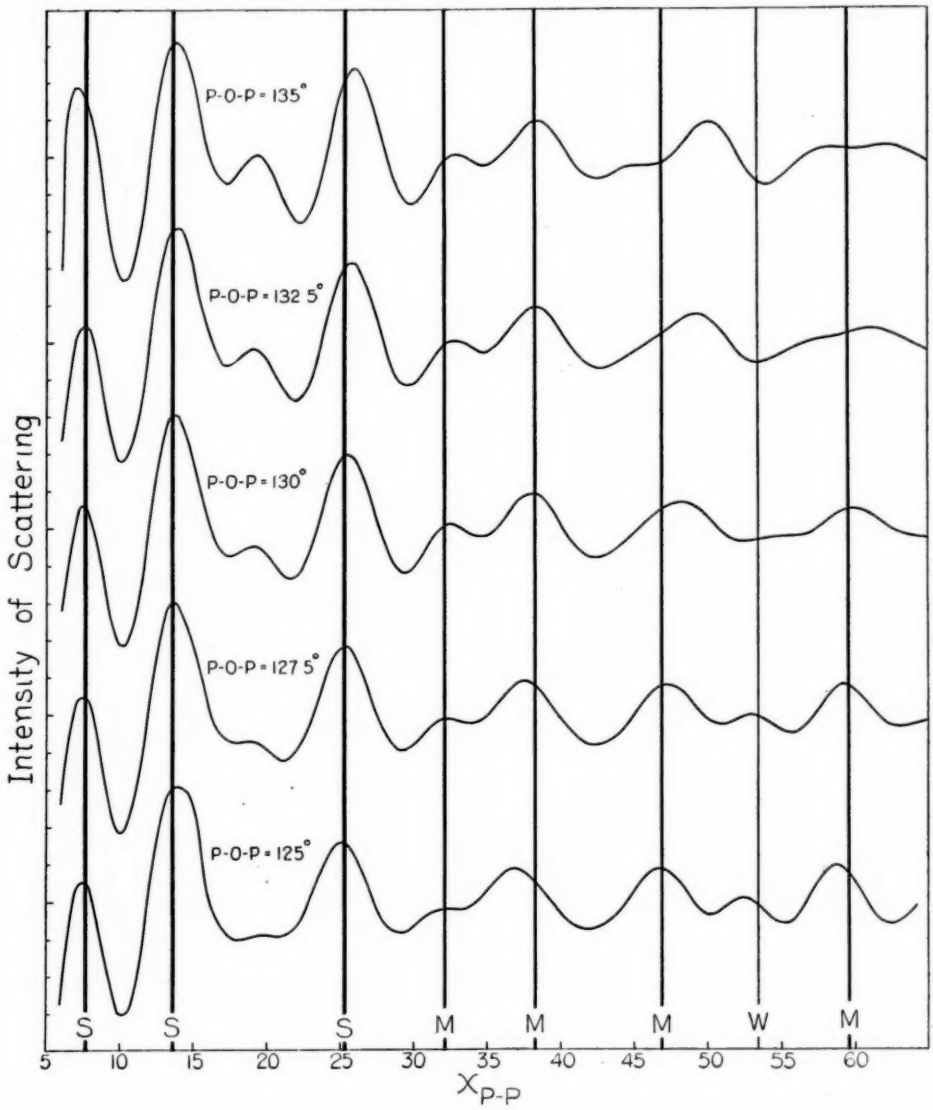

FIG. 2. Electron scattering curves for P_4O_6 where ψ_i is replaced by Z_i calculated for P−O−P valence angles near 130°. Vertical lines give the position of the experimental maxima where l_{p-p} =3.00A. The incoherent scattering has been omitted.

between experiment and theory shows that the arsenic atoms have a regular tetrahedral arrangement and that the symmetry of the molecules is probably that of the point group T_d.

Phosphorus trioxide (P_4O_6)

A value of $l_{p-p}=3.00$A was found to give the best agreement with the position of the theoretical maxima, as illustrated in Figs. 1 and 2. Although the model for P−O−P=130° shows quite good agreement it is noticed that the weak seventh maximum does not appear for this model. For an angle of 127.5° the seventh maximum is present, however, the fourth ring has weakened considerably. Therefore the valence angle probably lies between these two values since all other angles considered are excluded. Thus we arrive at 128.5±1.5° as the final value for the oxygen valence angle. This leads to the following complete structure for

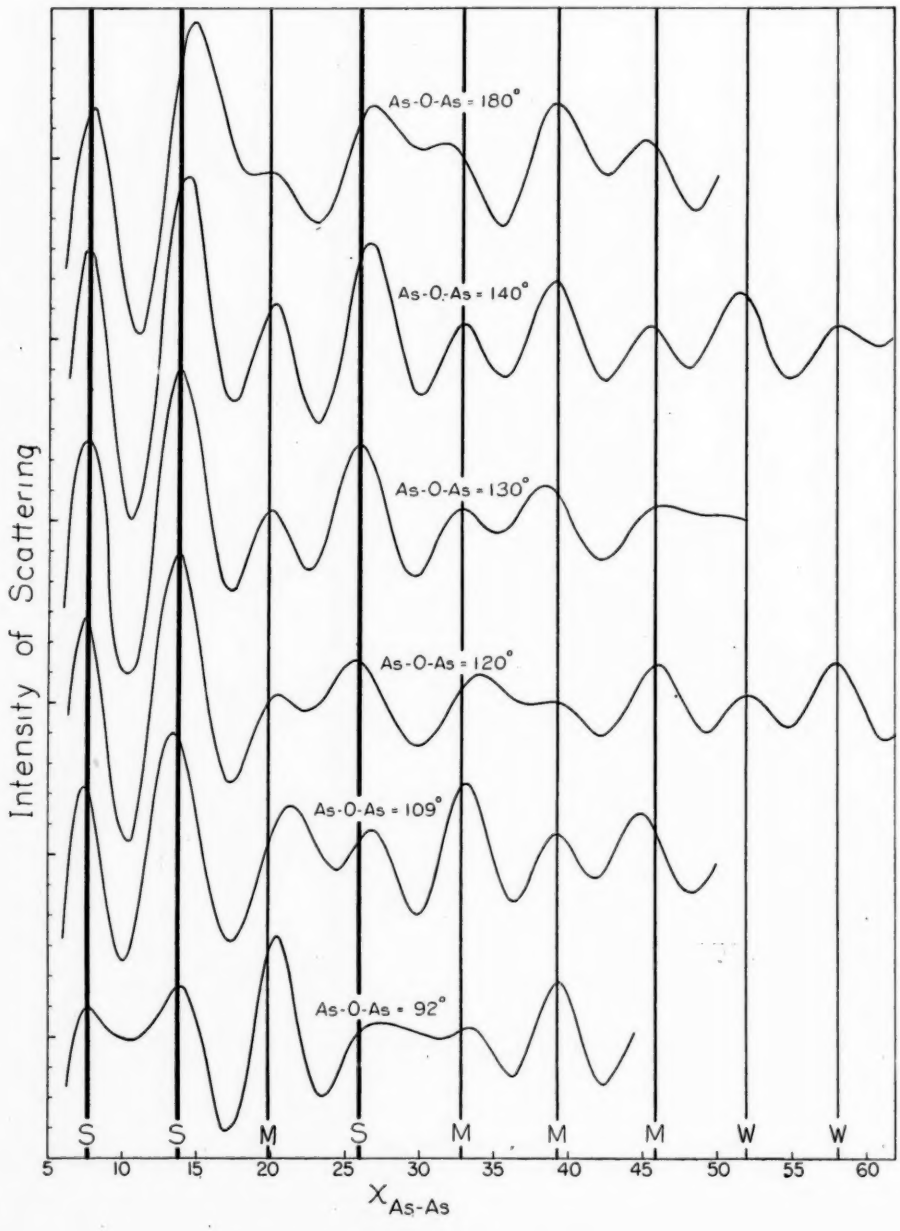
As-O-As = 180°
As-O-As = 140°
As-O-As = 130°
As-O-As = 120°
As-O-As = 109°
As-O-As = 92°
Intensity of Scattering
S S M S M M M W W
5 10 15 20 25 30 35 40 45 50 55 60
X As-As

FIG. 3. Electron scattering curves for As_4O_6 where ψ_i is replaced by Z_i calculated for various As−O−As valence angles. Vertical lines give the position of the experimental maxima where $l_{As-As}=3.20$A. The incoherent scattering has been omitted.

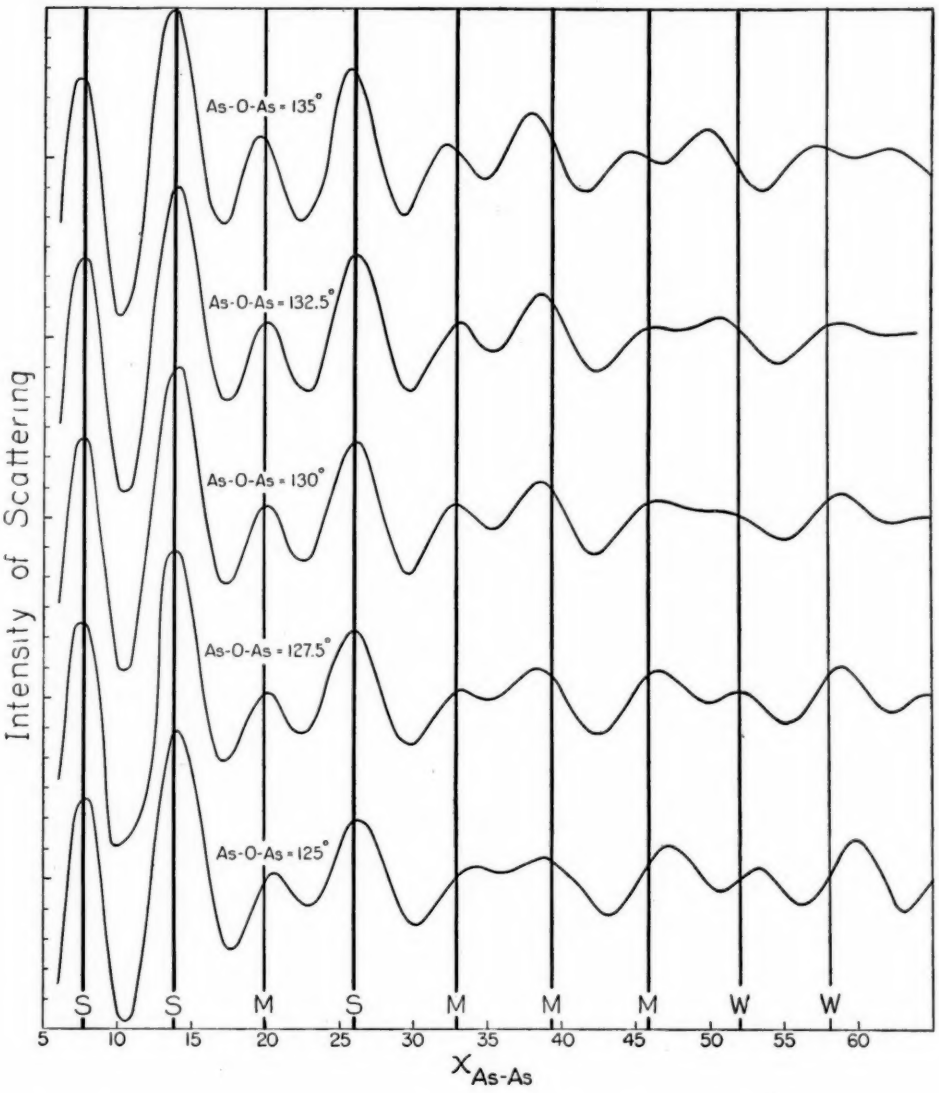
As-O-As = 135°
As-O-As = 132.5°
As-O-As = 130°
As-O-As = 127.5°
As-O-As = 125°
Intensity of Scattering
S S M S M M M W W
5 10 15 20 25 30 35 40 45 50 55 60
X_{As-As}

FIG. 4. Electron scattering curves for As_4O_6 where ψ_i is replaced by Z_i calculated for As−O−As valence angles near 130°. Vertical lines give the position of the experimental maxima where l_{As-As} =3.20A. The incoherent scattering has been omitted.

P_4O_6.

$$P-O-P=128.5\pm1.5°,$$
$$P-P=3.00\ \pm0.05A,$$
$$P-O=1.67\ \pm0.03A.$$

There are some features of the visual measurements from P_4O_6 which support the theoretical data computed by using $I_1(\theta)\cdot s^2$ as compared to the approximate method. For example the weak third theoretical maximum noticed in Figs. 1 or 2 for an oxygen valence angle of 130° is not observed experimentally in accordance with the calculations made using $I_1(\theta)\cdot s^2$ as shown in Table I. Also the fourth and fifth experimental maxima which correspond to the fifth and sixth theoretical maxima listed in Table I appear from visual measurements to be of approximately equal intensity. This observed intensity relationship is in considerably better agreement with the $I_1(\theta)\cdot s^2$ computations in contrast to the approximate method. These additional theoretical confirmations of the visual measurements

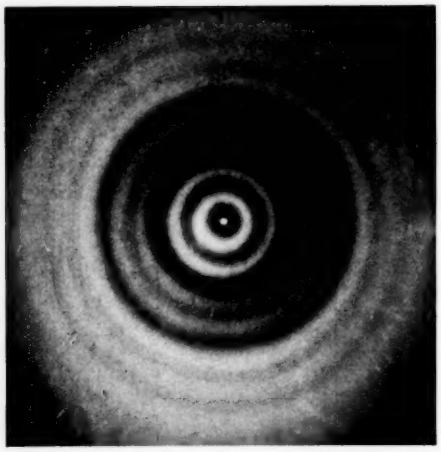

FIG. 5. Reproduction of electron diffraction photograph obtained from As_4O_6.

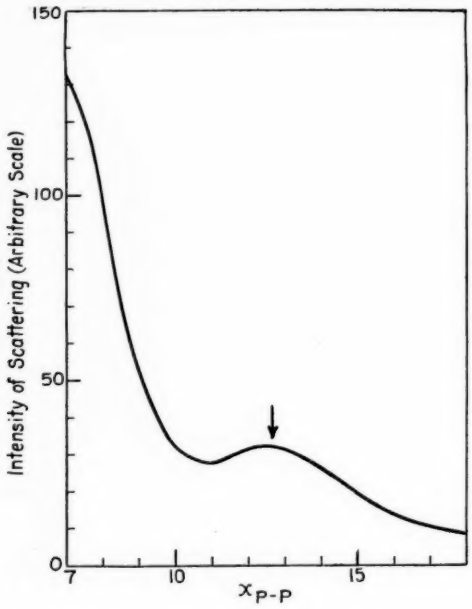

FIG. 6. Electron scattering curve for P_4O_6 using the complete scattering formula for an oxygen valence angle of 130°.

further support the correctness of the chosen model.

The complete scattering curve in the region of the second maximum for an oxygen valence angle of 130° was computed according to Eq. (1). A real maximum was obtained at $x_{p-p}=12.7$ as illustrated in Fig. 6. Fig. 7 illustrates a typical densitometer record of the second maximum whose position occurs at $(1/\lambda)\sin\frac{1}{2}\theta=0.342$. From Eq. (2) we thus obtained a $l_{p-p}=2.95$A from the densitometer measurements. This provides a confirmation of the P−P separation rather than the oxygen valence angle since the position of the second maximum is a relatively insensitive function of this angle.

Phosphorus pentoxide (P_4O_{10})

In the first instance it is assumed that P_4O_{10} has the molecular symmetry of the point group *Td* and that the atomic positions are given by the parameters used for P_4O_6 with additional oxygen atoms at www, $\bar{w}\bar{w}w$, $\bar{w}w\bar{w}$, and $w\bar{w}\bar{w}$. The general formula for the intensity of electron scattering $I_2(\theta)$ becomes

TABLE II. *Visual measurements of* $(1/\lambda)\sin\frac{1}{2}\theta$ *for the electron interference maxima obtained from* P_4O_6, P_4O_{10} *and* As_4O_6.

No.	P_4O_6	P_4O_{10}	As_4O_6
1	0.205±.001 (2)* s.	0.163±.004 (4) sharp, w.	0.1916±.0004 (3) s.
2	0.361±.001 (2) s.	0.388±.001 (5) v. s.	0.3436±.001 (3) s.
3	0.672±.006 (5) s.	0.498±.003 (6) barely resolved	0.4935±.002 (5) m.
4	0.852±.005 (3) m.	0.66 approx. (diffuse band)	0.6457±.004 (7) s.
5	1.016±.014 (3) m.	1.020±.003 (6) medium	0.8181±.003 (7) m.
6	1.244±.006 (6) m.	1.275±.004 (6) medium	0.9756±.004 (7) m.
7	1.418 (1) w.	1.618±.006 (3) v. w.	1.138 ±.003 (10) m.
8	1.580±.006 (4) m.	—	1.293 ±.005 (6) w.
9	—	—	1.445 ±.004 (5) w.
		Two very prominent minima occur at 0.315±0.003 and 0.561 ±0.005, respectively.	

* Number in parenthesis gives number of photographs taken. Variations shown are the average deviations obtained between measurements taken on different photographs.

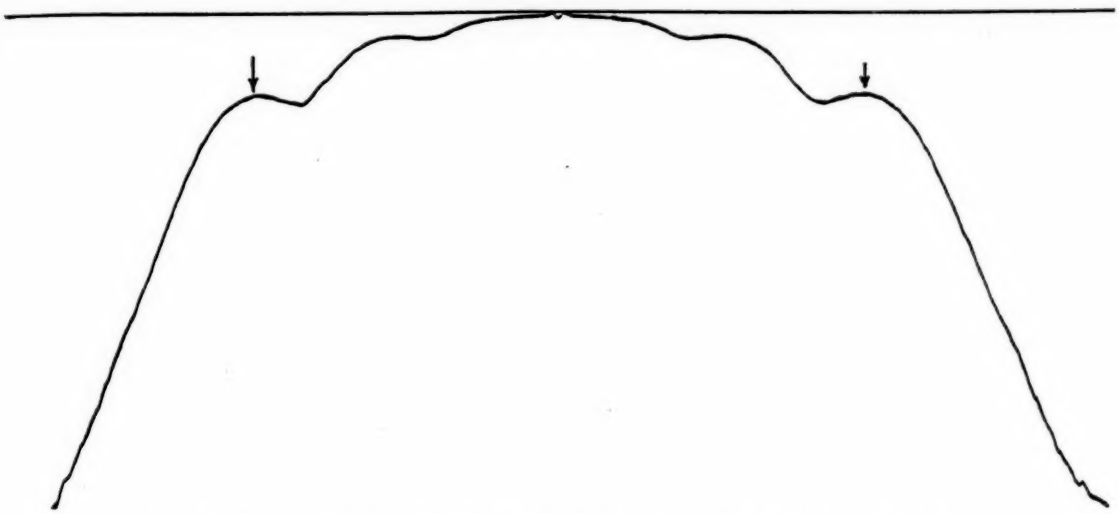

FIG. 7. Densitometer record taken of P_4O_6 showing the presence of a real second maximum.

$$I_2(\theta)=I_1(\theta)+8\psi_P\psi_O\left(\frac{\sin s\cdot[3(w-u)^2]^{\frac{1}{2}}}{s\cdot[(3(w-u)^2]^{\frac{1}{2}}}+\frac{3\sin s\cdot[2(w+u)^2+(w-u)^2]^{\frac{1}{2}}}{s\cdot[2(w+u)^2+(w-u)^2]^{\frac{1}{2}}}\right)$$
$$+4\psi_O^2\left(1+\frac{6\sin s\cdot[(w-v)^2+2w^2]^{\frac{1}{2}}}{s\cdot[(w-v)^2+2w^2]^{\frac{1}{2}}}+\frac{6\sin s\cdot[(w+v)^2+2w^2]^{\frac{1}{2}}}{s\cdot[(w+v)^2+2w^2]^{\frac{1}{2}}}+\frac{3\sin s\cdot(8w^2)^{\frac{1}{2}}}{s\cdot(8w^2)^{\frac{1}{2}}}\right)+I_{\text{inc}}''(\theta), \quad (3)$$

where $I_{\text{inc}}''(\theta)$ represents the additional amount of incoherent scattering arising from the 4 extra oxygen atoms.

Table I contains a summary of the visual measurements. This interference pattern showed a rather sharp inner ring occurring at $(1/\lambda)\sin\frac{1}{2}\theta=0.16$ followed by a prominent minimum at 0.315. A very strong second maximum was observed which was followed by a strong second minimum. At approximately $(1/\lambda)\sin\frac{1}{2}\theta=0.66$ there occurred a diffuse band-like scattering with a sharp inner edge. It can be seen from the general characteristics of the interference pattern that considerable departure is shown from the P_4O_6 scattering.

Fig. 8 illustrates theoretical scattering curves using $\psi_i=Z_i$ for various models as listed in Table III. Positions of the experimental maxima obtained by visual measurement are indicated on this figure; none of the models considered gives good agreement. Considerable disagreement is noticed for the innermost ring which corresponds to a distance in the molecule of approximately 3.7A as would be given by a first interference maximum. Densitometer records were taken of the strong second maximum and a typical trace is shown in Fig. 9. It is noticed that a real maximum is obtained and its position comes at $(1/\lambda)\sin\frac{1}{2}\theta=0.379$ which is about 2 percent less than the value found by visual measurements. Intensity of electron scattering was calculated in the region of the second maximum according to Eq. (3) for model 5 using the exact values for ψ_i. Fig. 10 shows the curve obtained in this manner with a real maximum at $x_{p-p}=13.5$. Thus we obtained from

TABLE III. *Models used for calculating electron scattering curves for P_4O_{10}.*

Model No.	Type of Model	
1	P–O–P=109°30′	P–O=1.76A
	P–P=2.87A	P=O=1.60A
2	P–O–P=114°	P–O=1.68A
	P–P=2.82A	P=O=1.52A
3	P–O–P=120°	P–O=1.67A
	P–P=2.89A	P=O=1.60A
4	P–O–P=120°	P–O=1.67A
	P–P=2.89A	P=O=1.52A
5	P–O–P=130°	P–O=1.68A
	P–P=3.04A	P=O=1.60A
6	P–O–P=130°	P–O=1.68A
	P–P=3.04A	P=O=1.50A

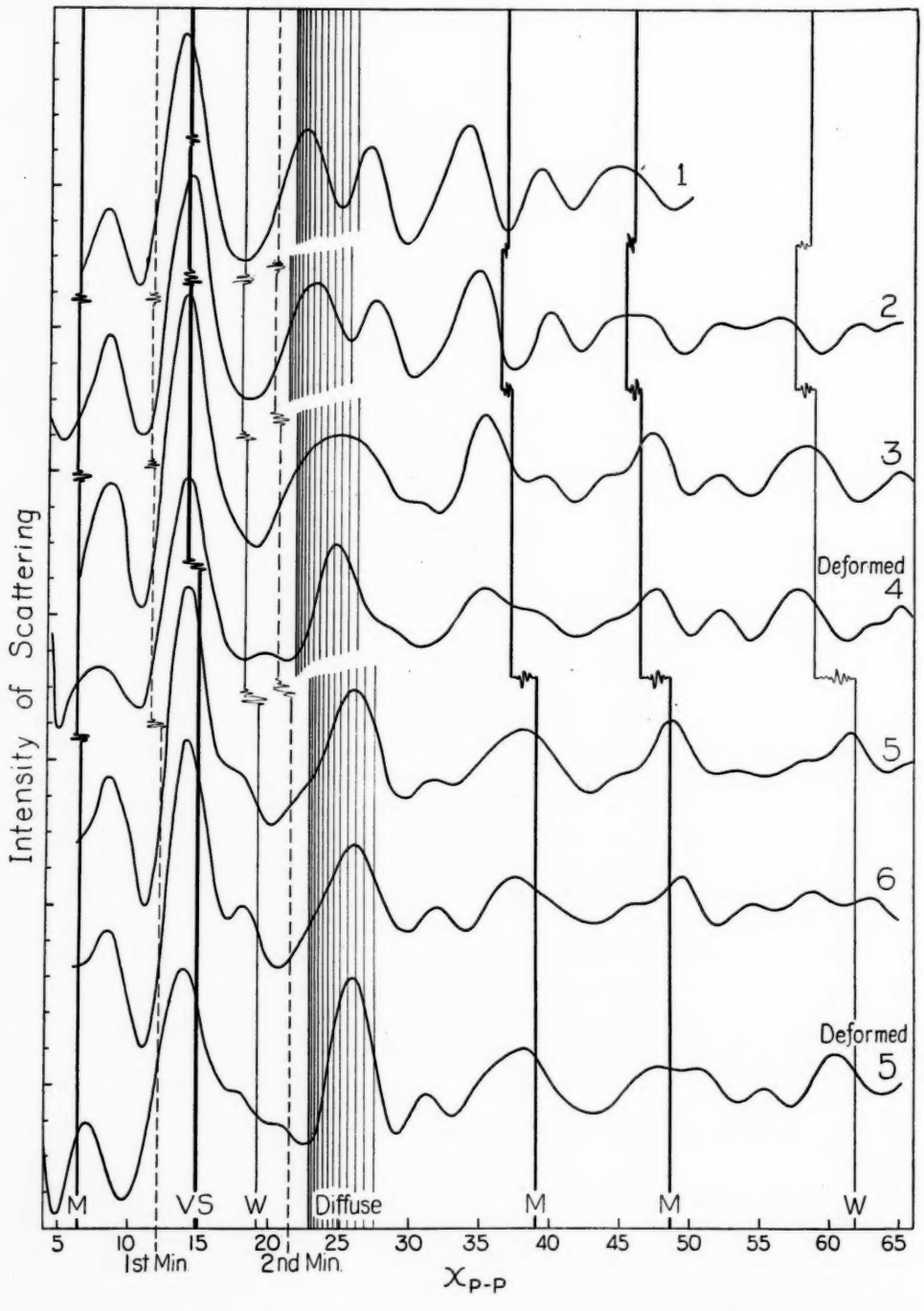

FIG. 8. Electron scattering curves for P_4O_{10} where ψ_i is replaced by Z_i calculated for various models listed in Table III. Vertical lines give the relative position of the experimental maxima and minima as governed by the models considered. The incoherent scattering has been omitted.

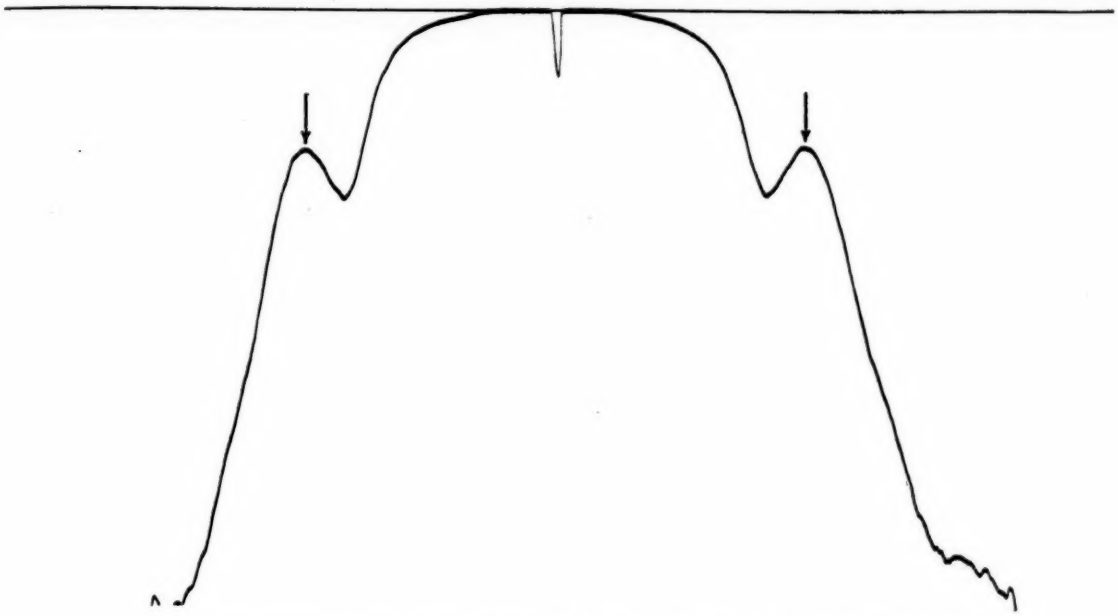

FIG. 9. Densitometer record taken of P_4O_{10} showing presence of a real second maximum.

Eq. (2) a $l_{p-p}=2.83$A which is in poor agreement with the actual assumed separation of 3.04A.

In the various models computed as shown in Fig. 8 it is noticed that the position of the second maximum does not greatly change as various alterations of the molecule are made so that one can estimate that the P−P separations must be near 2.9A as determined by the densitometer records.

From simply an inspection of the models calculated it is possible to exclude many other models for P_4O_{10}. For example, if model 5 were reduced in size to give a P−P=2.89A, P−O=1.60A, P=O=1.52A, maintaining the oxygen valence angle constant, the theoretical scattering curves expressed in terms of x_{p-p} would be identical with the curve given for model 5 in Fig. 8. The experimental maxima would all be proportionally decreased in position for comparison with the theoretical curve and hence give poor agreement especially for the outer maxima. This analysis can be applied to all the other models with subsequent disagreement as long as the oxygen valence angles are maintained unchanged. It is also possible to eliminate other models by a study of the theoretical curves shown for P_4O_6, for several of the prominent diffraction features of P_4O_6 are maintained in the P_4O_{10} scattering curves.

Calculations were also carried out for distorted models having the symmetry of the point group $V_d \equiv D_{2d}$. The constants were those given for

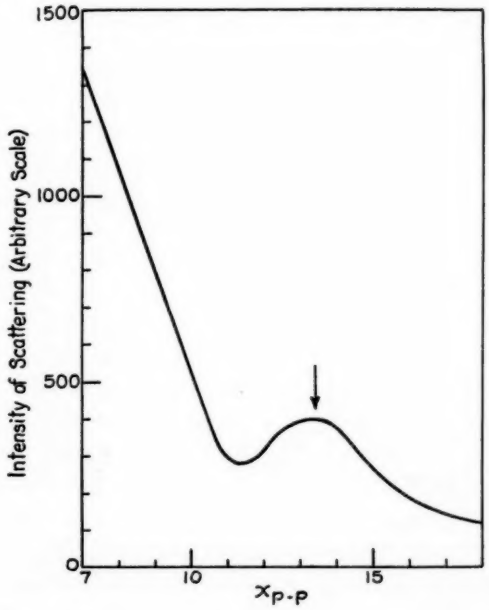

FIG. 10. Electron scattering curve for P_4O_{10} using the complete scattering formula for model 5.

models 4 and 5 of Table III with oxygen to oxygen distances (*www'* to *voo* and *ovo*) equal to 2.38A and 2.28A, respectively. Curves calculated for these models are also shown in Fig. 8. The agreement with the experimental data is not improved by these particular deformations which were used chiefly to facilitate calculations.

Discussion

There are essentially three determining factors that can be obtained from the structure found for P_4O_6, the valence angle of the oxygen and phosphorus atoms and the P to O single bond separation. The observed oxygen valence angle of 128.5° is greater than the angles of 100° to 118° as found for compounds not having a closed structure.[6] The P−O separation was found to be 1.67A which is less than the sum of the single bond radii 1.76A as given by Pauling and Huggins.[5] This departure is in the same direction as that observed for PCl_3, PF_3 and PF_5.[6] From the standpoint of the directed valence of the phosphorus atom the angle O−P−O comes out to be 98°±2° for P_4O_6 which does not differ greatly from values found for black phosphorus 102°,[7] PCl_3 101°[6] and $POCl_3$, 104°.[6] Thus it appears that the phosphorus oxygen distances and the phosphorus valence angles are preserved with resulting deformation of the oxygen valence angle.

For As_4O_6 several possible values were obtained for the oxygen valence angle. A final choice was not made although the model with a valence angle of 140° seemed to be slightly preferable. Crystal structure data from As_4O_6[8] give an As−O−As angle of 109° a value which is excluded by the electron diffraction results. The As−As distance in the crystal is 3.28A which is close to the electron diffraction value of 3.20±.05A.

Satisfactory explanation of the electron diffraction results from P_4O_{10} was not obtained for models having the symmetry of the point group T_d. Closest agreement for the outermost maxima was obtained for model 5 which has the same constants as the P_4O_6 structure with a P=O distance of 1.60A. In the case of P_4O_6 the character and calculated positions of the first three maxima were in good agreement with observation. However, this was not the case for P_4O_{10} and it is quite improbable that the additional oxygen atoms could produce the observed changes if the T_d symmetry were maintained. On the basis of the above considerations it seems logical to propose that the actual structure of P_4O_{10} is one of lower symmetry in which none of the atoms is in the position required by the symmetry T_d. However, there can be but little doubt that the phosphorus atoms have approximately the same arrangement as in P_4O_6.

No information is available on the crystal structure of the phosphorus oxides, however some prediction can be made in that regard. When yellow phosphorus changes to black phosphorus there is a transformation from a lattice consisting of small groups of atoms sharing covalent bonds to an extensive space network or homopolar lattice. This results in a change in valence angle of phosphorus from 60° to 102° or more nearly the valence angle found in PCl_3, $POCl_3$ and P_4O_6. Thus one expects that this larger angle would be preserved in a possible homopolar lattice of the pentoxide. Single bonds of the P_4O_{10} molecule could be rearranged in the transition for this compound and the resulting structure might be expected to be one with less distortion of the oxygen valence angle.

The authors wish to thank Mr. J. Floid Shultz for preparing the samples of P_2O_3 and P_2O_5 which were used in this work. P_2O_3 may have contained only a small amount of phosphorus as an impurity while the P_2O_5 was completely purified by distilling commercial P_2O_5 in O_2 in an iron furnace at 800°C.

We also wish to acknowledge the assistance of Mr. V. M. Mosley who operated the electron diffraction camera used.

Note on Phosphorus Tetroxide (P_4O_8) *Added in Proof July 9th, 1937:*

The above work was submitted for publication without information on phosphorus tetroxide because no suitable samples of the material were available. Dr. Emmett and Mr. Shultz of this laboratory have now prepared phosphorus tetroxide as a mixture with phosphorus pentoxide. Analysis by Mr. Shultz of the material condensed from

[5] L. Pauling and M. Huggins, Zeits. f. Krist. **87**, 205 (1934).
[6] L. O. Brockway, Rev. Mod. Phys. **8**, 231 (1936). Also H. Braune and P. Pinnow, Zeits. f. physik. Chemie **35**, 239 (1937).
[7] R. Hultgren, N. S. Gingrich and B. E. Warren, J. Chem. Phys. **3**, 351 (1935).
[8] R. M. Bozorth, J. Am. Chem. Soc. **45**, 1621 (1923).

the molecular beam in the electron diffraction camera showed approximately 50 percent phosphorus tetroxide and 50 percent phosphorus pentoxide. They will later describe the method of preparation used. Electron diffraction photographs obtained from this mixture gave an interference pattern almost identical to that found for P_4O_{10}. Values of $(1/\lambda)\sin\frac{1}{2}\theta$ for the interference maxima Nos. 2, 3, 5 and 6 agreed with the data given for P_4O_{10} in Table II above to within less than 1 percent. The first maximum appeared to be slightly weaker than the similar one found for P_4O_{10} but it had approximately the same position. Both first and second minima differed by less than 2 percent in position from the corresponding minima for P_4O_{10}. It was possible to see an additional weak maximum for the mixture at $(1/\lambda)\sin\frac{1}{2}\theta=0.87$ which was previously too weak for measurement in the case of P_4O_{10}.

Since the resultant diffraction pattern of this mixture is practically the same as for a pure sample of P_4O_{10} it is thus concluded that the true interference pattern of P_4O_8 must be approximately the same as found for P_4O_{10}.

AUGUST, 1937 JOURNAL OF CHEMICAL PHYSICS VOLUME 5

The Temperature Variation of Some Thermodynamic Quantities*

GEORGE M. MURPHY
Sterling Chemistry Laboratory, Yale University, New Haven, Connecticut

(Received June 15, 1937)

The quantity, $(F^0-E_0^0)/T$, calculated from spectroscopic data has been fitted to a five constant equation in T for 19 molecules. It may be differentiated and integrated to give values of S^0, E^0, H^0 and C_p^0 between 298.1 and 3000°K and is sufficiently exact for most purposes. The equilibrium constant for exchange reactions involving isotopes has been calculated and in each case, maxima exist and in one case a minimum also. This effect probably occurs at some temperature for all reactions involving isotopic molecules although not for other equilibria. An optimum temperature therefore exists for separation of isotopes by exchange reactions.

THE calculation of thermodynamic quantities from spectroscopic data has usually resulted in numerical values of these functions at a series of temperatures, 100° or so apart.[1] Since most experiments are performed at some odd temperature, interpolation in these tables is necessary in order to make comparison with the calculations. This may be done graphically from a large scale plot or by some method of numerical interpolation, either of which may be rather tedious. It is obvious that an analytical expression to represent these quantities as a function of the temperature would be useful. This has been done for the heat capacity of a number of molecules by Spencer and Justice[2] but a suitable expression for the variation of the free energy with temperature appears more satisfactory as this may be differentiated and integrated to give other thermodynamic quantities without the involved summation necessary to obtain them directly from the spectroscopic data.

The constants for a satisfactory analytical equation have been given recently[3] for H_2, D_2, HI and DI and it is the purpose of this paper to give the constants for other molecules and to apply the results in calculating the variation with temperature of the equilibrium constant of certain exchange reactions.

If we represent the free energy function by the equation[4]

$$-(F^{0*}-E_0^0)/T=a/T+b\log T+cT+dT^2+\cdots+i, \quad (1)$$

the well-known methods of thermodynamics[5] lead immediately to expressions for the additional quantities:

$$S^{0*}=-dF^0/dT=-b\{\log e+\log T\}+2cT+3dT^2+\cdots+i, \quad (2)$$

* Presented before the Division of Physical and Inorganic Chemistry of the American Chemical Society, Chapel Hill, N. C., April 14, 1937.

[1] For a review of the methods of calculation and references to molecules for which calculations have been made, see Kassel, Chem. Rev. **18**, 277 (1936).

[2] Spencer and Justice, J. Am. Chem. Soc. **56**, 2311 (1934).

[3] Murphy, J. Chem. Phys. **4**, 344 (1936); Blagg and Murphy, ibid. **4**, 631 (1936).

[4] For the meaning of the symbols used here, see Giauque, J. Am. Chem. Soc. **52**, 4808 (1930).

[5] See any text-book on thermodynamics, as Lewis and Randall, *Thermodynamics* (McGraw-Hill Book Co., New York, 1923).

TABLE I.

	a	b	$c\times10^4$	$d\times10^8$	i	REFERENCE
H_2	3.1414	15.5999	1.245	3.72	−14.2131	1
HD	− 12.5833	15.4831	2.200	3.04	−10.7961	2
D_2	− 46.0643	15.0859	4.972	25.70	− 9.5419	2
HCl	−153.6940	14.3834	7.836	− 3.73	2.4254	3
DCl	−120.3214	14.4026	10.286	− 6.13	3.5836	4
HBr	−122.2812	14.5503	7.748	− 2.72	4.7350	5
DBr	− 93.8502	14.4317	11.945	− 8.77	6.1790	6
HI	−108.6720	14.6592	7.649	− 4.00	6.2820	7
DI	−365.5120	11.1051	36.420	−67.80	16.5063	8
Cl_2	358.5050	19.2272	3.635	− 2.07	− 2.9302	3
Br_2	212.7441	19.1883	6.703	−10.76	2.4832	5
I_2	180.7780	19.8028	4.444	− 6.87	4.4605	7
N_2	−212.7056	13.9765	11.719	− 8.60	5.0589	9
O_2	− 25.0666	14.8456	12.108	− 9.47	5.0869	10
CO	−178.0274	13.9435	12.068	− 9.13	6.1073	11
H_2O	−218.0344	15.5972	16.472	− 4.64	− 1.1745	12
H_2S	−189.4691	15.1434	25.565	−15.22	3.5973	13
CO_2	727.1367	20.1610	25.200	−1.592	− 9.4306	14
SO_2	253.4268	18.8812	34.804	−36.78	1.9950	15

1. Giauque, J. Am. Chem. Soc. **52**, 4816 (1930); Davis and Johnston, ibid. **56**, 1045 (1934).
2. Johnston and Long, J. Chem. Phys. **2**, 389 (1934).
3. Giauque and Overstreet, J. Am. Chem. Soc. **54**, 1731 (1932).
4. Calculated for this paper. The spectroscopic constants for DCl were obtained from those of HCl (see reference 3) by well-known methods.
5. Gordon and Barnes, J. Chem. Phys. **1**, 692 (1933). Valid only to 1600°K.
6. Calculated for this paper by Mr. T. Ivan Taylor, Department of Chemistry, Columbia University. The spectroscopic constants for DBr were obtained from those of HBr (see reference 5) by well-known methods.
7. Murphy, J. Chem. Phys. **4**, 344 (1936). Valid only to 1500°K.
8. Blagg and Murphy, J. Chem. Phys. **4**, 631 (1936). Valid only to 1500°K.
9. Giauque and Clayton, J. Am. Chem. Soc. **55**, 4875 (1933); Johnston and Davis, ibid. **56**, 271 (1934).
10. Johnston and Walker, J. Am. Chem. Soc. **55**, 172 (1933); **57**, 682 (1935).
11. Clayton and Giauque, J. Am. Chem. Soc. **54**, 2610 (1932); **55**, 5071 (1933); Kassel, J. Chem. Phys. **1**, 576 (1933); Johnston and Davis (see reference 9).
12. Gordon, J. Chem. Phys. **2**, 65 (1934).
13. Cross, J. Chem. Phys. **3**, 168 (1935). Valid only to 1800°K.
14. Kassel, J. Am. Chem. Soc. **56**, 1838 (1934).
15. Gordon, J. Chem. Phys. **3**, 336 (1935). Valid only to 2800°K.

$$H^0=F^0+TS^0=(E_0{}^0-a)+bT\log e+cT^2+2dT^3+\cdots, \quad (3)$$

$$E^0=H^0-RT, \quad (4)$$

$$C_p{}^0=dH^0/dT=b\log e+2cT+6dT^2+\cdots. \quad (5)$$

In all of these equations and in Table I, the nuclear spin contributions have *not* been included. If absolute values of $(F^0-E_0{}^0)/T$ or S^0 are desired, it is necessary to add a constant term to the quantity i which appears in Eqs. (1) and (2). For details as to the magnitude of this constant, reference 1 may be consulted.

Consideration of Eqs. (1) to (5) shows that a knowledge of the five constants for Eq. (1) is sufficient to determine the other quantities as shown in Eqs. (2) to (5). The five constants have been determined for a number of diatomic and polyatomic molecules and appear in Table I. The data required have been taken from various places in the literature or computed by well-known methods,[1] the source of the data for each molecule being given in footnotes to Table I. The constants were determined in some cases by least squares, all of the temperatures for which $(F^0-E_0{}^0)/T$ had been summed, being used. However, it was found that sufficiently precise values could be obtained using the method of averages,[6] by which 15 or more equations of the form of (1) were reduced to five simultaneous equations which were then solved for the constants. In solving the five simultaneous equations, the constants involved must be eliminated in a particular order if any precision is obtained. Reference to Table I shows that the numerical value of the constants is approximately in the order $a>b>i>c>d$. They should thus be eliminated in the reverse order so that the final pair of equations should be solved for a. If this is not done, the cumulative errors involved give constants of an entirely different order of magnitude and will not reproduce the values of $(F^0-E_0{}^0)/T$.[7]

The minimum temperature for which the constants of Table I are valid is 298.1°K. The maximum temperature is in most cases 3000°K, the exceptions being given in Table I. Any extrapolation beyond these limits is not reliable. Extension beyond these temperatures in either direction, however, may easily be made by redetermining the constants with values of $(F^0-E_0{}^0)/T$ at higher and lower temperatures. If necessary, coefficients of higher powers of T may be added to Eq. (1).

The errors in reproducing the values of the thermodynamic functions as calculated from spectroscopic data with the constants of Table I and Eqs. (1) to (5) vary somewhat from one molecule to another. The average and maximum deviations for H_2 are shown in Table II. This

TABLE II. *Deviations from the thermodynamic functions of H_2 as calculated from Eqs. (1) to (5) and the constants of Table I and those calculated from the spectroscopic data.*

	$-(F^{0*}-E_0{}^0)/T$[a]	S^{0*}[a]	$C_p{}^0$[b]	$E^0-E_0{}^0$[b]
Average deviation	0.003 cal. 0.01%	0.014 cal. 0.04%	0.032 cal. 0.5%	8.25 cal. 1.2%
Maximum deviation	0.006 cal. 0.02%	0.085 cal. 0.2%	0.067 cal. 1%	36.6 cal. 5%

[a] Upper temperature limit of 3000°K.
[b] Upper temperature limit of 2000°K.

[6] Scarborough, *Numerical Mathematical Analysis* (The Johns Hopkins Press, Baltimore, 1930), p. 357.

[7] This is undoubtedly a general procedure in solving a set of simultaneous equations, although no statement of this fact could be found in books on numerical calculations.

may be considered as a good example as the deviations for other molecules are of about the same order of magnitude. The values of C_p^0 and E^0 begin to deviate rather badly toward the upper limit of the temperature range and for these functions, it is best to confine the calculations to something lower than 2000°K. Reference to Table II indicates that the precision of calculation with these empirical equations is probably as good as the experimental data in most cases. For molecules other than H_2, the errors will in general not exceed those in Table II and in some cases will be somewhat less. The ease in using these functions should make them useful in comparing experimental results with the corresponding quantities calculated from spectroscopic data.

Temperature Variation of the Equilibrium Constant

For a chemical equilibrium, the equilibrium constant is given by

$$\frac{-\Delta F^0}{T}=-\Delta\left\{\frac{F^0-E_0^0}{T}\right\}-\frac{\Delta E_0^0}{T}=R\ln K. \quad (6)$$

All molecules taking part in the equilibrium are assumed to be in their standard states and hence at unit activity and since gases are sufficiently ideal at moderate pressures to substitute partial pressure for activity, Eq. (6) refers to unit pressure of 1 atmosphere. By using the Gibbs-Helmholtz equation it is easy to show that

$$\frac{d\ln K}{dT}=\frac{\Delta H^0}{RT^2}, \quad (7)$$

and upon the assumption that ΔH^0 is independent of the temperature or that it varies only very slowly with the temperature, Eq. (7) may be integrated between two temperatures, this being valid if the temperature range is not large. The integrated form of Eq. (7) shows that a plot of $\log K$ against $1/T$ should give a straight line from the slope of which ΔH^0 may be determined. This procedure is very commonly followed but it will be shown below that this may lead to erroneous results in some cases. Eq. (3) shows how H^0 actually varies with the temperature and it is commonly supposed that the absolute value of ΔH^0 increases monotonically with the temperature. Under these conditions the equilibrium constant of a homogeneous gaseous reaction should increase (or decrease) monotonically with the temperature although the plot of $\log K$ against $1/T$ need not be a straight line. The possibility of a maximum or a minimum in the equilibrium constant should not be overlooked. As a matter of fact, a maximum in the ionization constant is actually observed in certain homogeneous liquid systems.[8] An indication of this effect is also noticeable in the calculations of Urey and Rittenberg[9] for the gaseous exchange reaction

$$H_2+2DI\rightleftharpoons 2HI+D_2. \quad (8)$$

Their equilibrium constants are 1.212, 1.234, 1.222 at 400°, 575° and 700°K, respectively, indicating a maximum at some temperature higher than 575°K. A more detailed calculation[3] of this equilibrium shows in fact a maximum near this temperature and a minimum near 1250°K. The exchange reaction[10]

$$2H_2O^{16}+O_2^{18}\rightleftharpoons 2H_2O^{18}+O_2^{16} \quad (9)$$

seems to have a minimum around 1500°K. Since this same effect would probably appear in other equilibria, a consideration of its cause seemed indicated. From Eq. (7) excluding the case where $T=0$ or ∞, it is obvious that the equilibrium constant will have a maximum, a minimum or a point of inflection if $\Delta H^0=0$. Correspondingly, if $\Delta C_p \gtreqless 0$ the equilibrium constant possesses a minimum, a maximum or a point of inflection, respectively. It may easily be shown that

$$H^0=E_0^0+\frac{5}{2}RT+RT^2\frac{d\ln Q}{dT}, \quad (10)$$

where the partition function, $Q=\sum pe^{-E/kT}$, summation is made over the required number of electronic, vibrational and rotational states and p is the statistical weight of the individual energy level. The partition function may be further written

$$Q=(\mu kT/hcB_0)(1-z)^{-1}f, \quad (11)$$

[8] See, for example, Harned and Embree, J. Am. Chem. Soc. **56**, 1050 (1934).
[9] Urey and Rittenberg, J. Chem. Phys. **1**, 137 (1933).
[10] Jones and Hall, J. Am. Chem. Soc. **59**, 259 (1937).

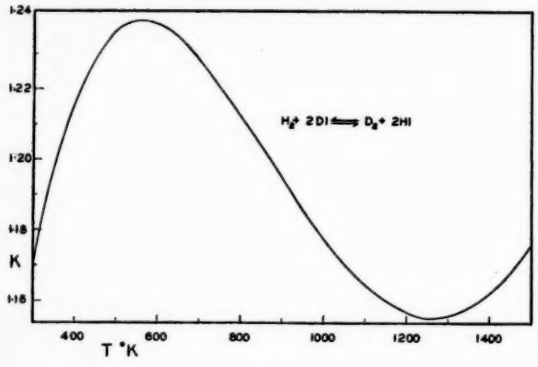

FIG. 1.

where $z=e^{-hc\omega_0/kT}$, the contribution from a linear harmonic oscillator of frequency, $c\omega_0$; the first term that from a rigid rotator with moment of inertia $h/8\pi^2cB_0$; the constant μ represents nuclear spin or symmetry contributions and the factor f which may be developed in a power series in T, all contributions from stretching, anharmonicity and other interaction terms. Substitution of Eq. (11) in Eq. (10) results in:

$$H^0=E_0{}^0+\frac{5}{2}RT+RT+\frac{zhc\omega_0R}{(1-z)k}+\{\alpha+\beta T+\gamma T^2+\delta T^3+\cdots\}, \quad (12)$$

where the first term is the zero-point energy and the next terms in order are translational, rotational, vibrational and anharmonic contributions to the heat content and may be indicated for convenience by H_t, H_r, H_v and H_a, respectively. For reactions of the type of (10) where there is no change in the number of moles, it is obvious that neither H_t nor H_r can cause a maximum or a minimum as these quantities will both cancel in forming ΔH^0. However, either H_v or H_a may vary with temperature in such a way that ΔH^0 may change sign from positive to negative and thus go through a maximum or minimum. A similar argument applies to ΔC_p, since

$$C_p{}^0=\frac{5R}{2}+R+\left\{R\left(\frac{hc\omega_0}{kT}\right)^2\left[\frac{z}{(1-z)^2}\right]\right\}+\{\alpha'+\beta'T+\gamma'T^2+\cdots\}, \quad (13)$$

where the terms are, respectively, C_t, C_r, C_v and C_a. If ΔH^0 were set equal to zero after substitution of equations of the form of (12) for the reactants and the reaction products and if this were solved for T, the results would be T_{max} or T_{min}. Unfortunately it is not an easy matter to solve these equations due to the presence of the exponential terms in T. Several attempts to solve them were made without success for even if the anharmonic terms are neglected, the resulting equation is rather difficult to handle and series approximations fail. A qualitative explanation, however, seems to be as follows. With increasing temperature H_t and H_r cause ΔH^0 to increase (or decrease) regularly. At a given temp. H_v for one molecule will begin to contribute to ΔH^0 and depending on whether one of the reactants or one of the reaction products begins to vibrate first, ΔH^0 will either decrease (or increase) giving a maximum or a minimum. At some higher temperature, a molecule on the other side of the equilibrium equation will begin to vibrate and ΔH^0 will again change sign.

It now remains to be seen whether this behavior is to be expected for every reaction. The condition given above may be written

$$\Delta H^0=(\Delta H^0-\Delta H_0{}^0)+\Delta H_0{}^0=0; \quad (14)$$

the quantity $\Delta H_0{}^0$ is, of course, independent of temperature and is of the order of 1000–10,000 calories for an ordinary chemical reaction. It does not seem likely that at any reasonable temperature, $\Delta(H^0-H_0{}^0)$ will vary enough to cause ΔH^0 to change sign. On the other hand, for exchange reactions, $\Delta H_0{}^0$ is of the order of only a few hundred calories and thus $\Delta(H^0-H_0{}^0)$ may easily cause ΔH^0 to change sign.

The exchange between the hydrogen halides and deuterium are convenient equilibria to apply to these calculations. The equilibrium constants may be obtained from Table I and by using Eqs. (8) and (1) are seen to be given by

$$-R\ln K=\Delta a/T+\Delta b\log T+\Delta cT+\Delta dT^2+\cdots+\Delta i+\Delta E_0{}^0/T. \quad (15)$$

TABLE III. *Zero-point energies in calories per mole.*

H_2	6180.46
HD	5364.85
D_2	4391.11
HCl	4222.96
DCl	3036.70
HBr	3730.92
DBr	2662.36
HI	3258.33
DI	2319.98

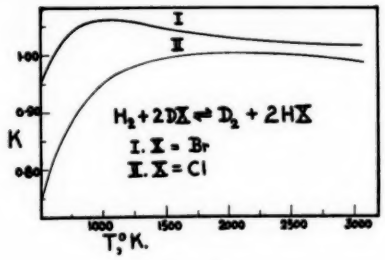

FIG. 2.

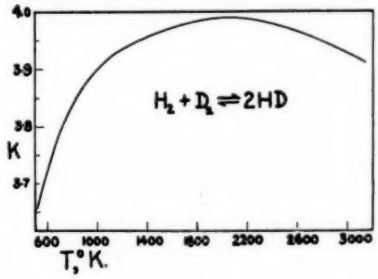

FIG. 3.

The quantity ΔE_0^0 in the case of these isotopic exchange reactions[11] is very simply obtained from the spectroscopic data, since

$$E_0^0 = hc\{\tfrac{1}{2}\omega_e - \tfrac{1}{4}x_e\omega_e + \cdots\}. \quad (16)$$

Values of E_0^0 are given in Table III for a few molecules. The corresponding variation of K with temperature for some exchange reactions is found in Figs. 1 and 2. Each is found to have a maximum and for the HI−DI reaction, a minimum as well. Presumably at higher temperatures, the others would also show a minimum. Unfortunately, none of these equilibria have yet been investigated experimentally over a wide enough temperature range to show the effect. The equilibria

$$H_2+DX \rightleftharpoons HD+HX, \quad (17)$$

where X = Cl, Br, I have been studied by Wirtz[12] but slightly higher temperatures are necessary to reach the maximum in K. Equilibria of the type shown in Figs. 1 and 2 could probably be studied most simply experimentally from the individual equilibria

$$2HX \rightleftharpoons H_2+X_2 \quad (18)$$

and the corresponding one

$$2DX \rightleftharpoons D_2+X_2, \quad (19)$$

and the constant for

$$H_2+2DX \rightleftharpoons 2HX+D_2 \quad (20)$$

would then be the ratio of the individual constants of (18) and (19).

A similiar maximum is found in the case

$$H_2+D_2 \rightleftharpoons 2HD \quad (21)$$

and shown in Fig. 3. A minimum may also be found at considerable higher temperature. An attempt to find a similar effect at very low temperatures due to changes in the rotational heat content were unsuccessful and probably do not exist for any reaction since H_r is too small compared with H_0^0, although there is a point of inflection in the curve below 100°K.[13]

No doubt other exchange reactions may be found showing maxima or minima and they may prove useful in the separation of isotopes since it is obvious that some one temperature offers the best opportunity of concentrating an isotope by exchange.

[11] In the case of reactions which do not involve isotopic exchanges, ΔE_0^0 must be obtained in other ways, see, for example, reference 4.

[12] Wirtz, Zeits. f. physik. Chemie, **B31**, 309 (1936).

[13] The values of $(F^0-E_0^0)/T$ and $(E^0-E_0^0)$ for D_2 and HD may be found in reference 2, but the values for HD at 150° are in error and should be 26.462 and 259.92, respectively.

The Infrared Absorption Spectrum of Carbon Suboxide

R. C. Lord, Jr.* and Norman Wright
Departments of Chemistry and Physics, University of Michigan, Ann Arbor, Michigan

(Received May 24, 1937)

The infrared absorption spectrum of carbon suboxide vapor has been studied under low dispersion in the region from 2μ to 25μ. The vibrational bands observed may be satisfactorily accounted for on the basis of a linear symmetric structure for the carbon suboxide molecule, in agreement with evidence obtained from Raman spectra and from electron diffraction investigations.

RECENT studies of the structure of the carbon suboxide molecule by electron diffraction[1,2] and by ultraviolet absorption and Raman spectra[3–5] have made desirable an investigation of the molecule's absorption spectrum in the infrared region. The information to be gained from such an investigation should be particularly helpful since the spectroscopic and electron diffraction evidence indicates that the most probable form of the carbon suboxide molecule is one possessing a symmetry center. For such a structure the Raman and infrared absorption spectra are complementary, the fundamental frequencies active in either type of spectrum being inactive in the other.

We have studied the absorption by carbon suboxide vapor under various pressures in the region between 2μ and 25μ. The absorption curves were made with the KBr prism, vacuum, recording spectrometer of Randall and Strong[6] operated in conjunction with the periodic amplifier described by Firestone.[7] The cell containing the absorbing gas was 12 cm in length, with plane polished KBr windows cemented to each end. The customary Nernst glower furnished the infrared radiation.

Professor J. O. Halford kindly supplied several samples of liquid carbon suboxide, of two or three cubic centimeters each, for our use. The material was prepared by the pyrolysis of diacetyl tartaric anhydride[8] and was purified by two distillations in an all-glass system. Measurements of the vapor pressure of the suboxide over a range of temperatures up to 0°C agreed satisfactorily with those in the literature.[9] The absorption cell was filled by distilling the *middle* fraction of the particular sample at hand into the evacuated cell, the desired pressure being obtained by surrounding the distilling vessel with a bath of acetone of the proper temperature.

While in every instance we were satisfied before making the absorption measurements that the carbon suboxide in the cell was of suitable purity, each absorption curve was examined for the presence of bands due to foreign

Table I. *Absorption bands of carbon suboxide.*

Wave-length in μ	Wave-number in cm^{-1}	Percent Absorption		
		$p = 14$ mm	67 mm	200 mm
2.18	4590		5	
2.64	3790		30	
2.96	3380		5	
3.17	3150	—	30	40
4.15	2410			
4.37	2290	80	90	95
4.57	2190			
5.05	1980	—	10	unresolved
5.41	1850	—	5	unresolved
5.68	1760	25*	40	80
5.98	1670		40	80
6.37	1570	25	75	95
6.80	1470	5	10	25
7.21	1387	20	30	70
8.16	1225	—	2	15
8.88	1126	—	10	35
9.76	1024	—	5	20
11.00	909	10	30	65
11.24	889	—	25	60
12.84	779	—	20	40
15.70	637	15	60	75
17.94	557		75	
18.18	550	50	65†	90
18.40	544		70	

Spectral range: 14 mm: 3μ–20μ; 67 mm: 2μ–25μ; 200 mm: 3μ–25μ.
* Water vapor band on a blank run with source intensity comparable to that used for the 14 mm run absorbs some 20 percent at this point. Most of this band in the 14 mm curve is doubtless due to water.
† Central minimum of this band resolved only in 67 mm curve.

* National Research Council Fellow.
[1] Brockway and Pauling, Proc. Nat. Acad. Sci. **19**, 860 (1933).
[2] Boersch, Naturwiss. **22**, 172 (1934); Wien Ber. **144** (IIb) 1 (1935).
[3] Badger and Barton, Proc. Nat. Acad. Sci. **20**, 166 (1934).
[4] Thompson and Healey, Proc. Roy. Soc. (London) **A157**, 331 (1936).
[5] Engler and Kohlrausch, Zeits. f. physik. Chemie **B34**, 214 (1936).
[6] H. M. Randall and J. Strong, Rev. Sci. Inst. **2**, 585 (1931).
[7] F. A. Firestone, Rev. Sci. Inst. **3**, 163 (1932).
[8] Hurd and Pilgrim, J. Am. Chem. Soc. **55**, 757 (1933).
[9] E.g., reference 4, p. 332.

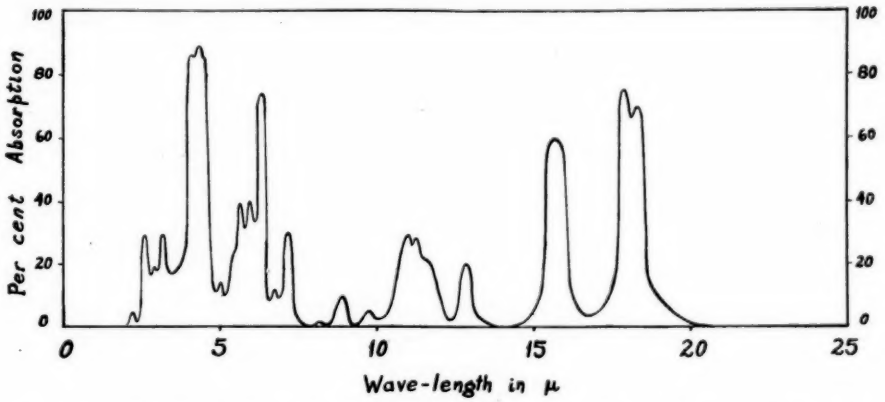

FIG. 1. Infrared absorption of carbon suboxide vapor. Cell length, 12 cm; pressure, 67 mm.

gases. Absorption bands in the region 3.2–3.5μ were either extremely weak or nonexistent. Since compounds with the C–H linkage exhibit rather powerful absorption in this region, the concentration of such possible impurities as ketene, acetic acid and other pyrolytic products with C–H groups must have been very small. The weak carbon dioxide bands present in the absorption curves were of the intensity to be expected from the amount of carbon dioxide in the air path of the incident radiation. The fundamental band of carbon monoxide, if present in the absorption curves, would have been masked by the strong and rather wide absorption band found at 4.4μ.

In the paper of Thompson and Healey,[4] attention is called to the possibility that carbon suboxide prepared by the pyrolytic method may be contaminated with a small amount of sulfur dioxide. There is no trace in our absorption curves of the strong sulfur dioxide fundamental at 8.67μ. The other strong fundamental, at 7.40μ, might be partially obscured by the 7.21μ band of the carbon suboxide spectrum, but the shape of the latter band gives no indication of a satellite on the long wave-length side. The remaining sulfur dioxide bands are of lower intensity, and of these, the ones which do not coincide with the bands of the suboxide make no appearance on the absorption records.

It might be of interest to remark that at no time did we experience difficulty due to polymerization of the carbon suboxide vapor in the absorption cell. Measurement of the pressure of the gas after it had remained in the cell for several days always led to the value, within a millimeter or two, of the initial pressure with which the cell had been filled. When the cell was filled for the first time (at about 700 mm pressure), a very faint fogging of the windows was observed after a few hours. This cloudiness did not increase with time, however. The windows were not visibly less transparent after the cell had been filled and emptied several times than at the time when the fogging was first observed. The absorption of the clouded windows was tested with the cell exhausted to an oil pump vacuum. Only those absorption bands due to the carbon dioxide and water vapor in the 50 cm airpath outside the spectrometer were observed. No trace of the strong bands of carbon suboxide appeared.

Absorption curves were made with the carbon suboxide under pressures of 14, 67, 200 and 700 mm. The absorption of the gas under 700 mm was not studied over the whole available range of the spectrograph because in the region first explored, from 10 to 20μ, it was found that absorption was too strong to allow satisfactory resolution of the individual bands. Table I lists the wave-lengths and wave numbers of the observed bands, together with the approximate percentages of absorption under the several pressures. Of these pressures, 67 mm was found to be the most favorable for resolution of the structures of the various bands. The curve for 67 mm is reproduced in Fig. 1. As the figure indicates, no absorption bands were found between 20 and 25μ.

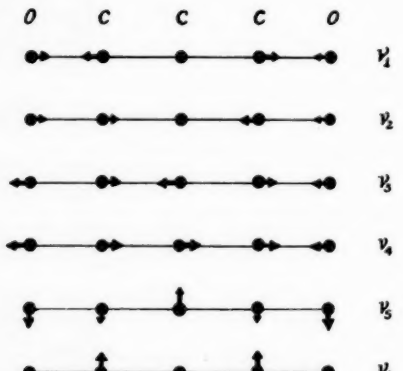

FIG. 2. Modes of vibration for linear carbon suboxide molecule.

DISCUSSION OF RESULTS

To interpret the infrared absorption data, one may make profitable use of some preconceptions about the structure of the carbon suboxide molecule. From the electron diffraction studies,[1,2] it appears very likely that all the atoms in carbon suboxide are on a line, and furthermore that the oxygen atoms and two of the carbon atoms are symmetrically disposed about the third carbon atom. Valence requirements dictate that the oxygen atoms occupy the two outermost positions.

The interatomic distances C−O and C−C as determined from the diffraction patterns lead to a calculated moment of inertia of 390×10^{-40} gram-cm^2 for the linear model. The spacing of the rotational lines for such a molecule will have the hopelessly small value of 0.14 cm^{-1}, and even the "spread" in the maxima of the P and R branch envelopes will amount to no more than 11 cm^{-1} at room temperature. Since the envelope maxima are not at all sharp, one would hardly expect the prism spectrometer to resolve the vibration bands into their rotational components, at least not those bands having wavelengths less than about 15μ. The rotational structure of the absorption bands will therefore not concern us, and we shall consider only their vibrational interpretation.

The essential elements of symmetry of the suggested structure are the figure axis and the symmetry center. A pentatomic molecule of this symmetry has seven vibration frequencies, three of which are doubly degenerate. The vibrational modes are shown in Fig. 2. Our frequency enumeration follows that of Engler and Kohlrausch.[5] These authors, as well as Thompson and Healey,[4] give both the vibration forms and also equations for the frequencies based on simple potential systems of the valence force type.

The four nondegenerate frequencies, which preserve the figure axis as an element of symmetry, may be classified as symmetrical (ν_1 and ν_2) and antisymmetrical (ν_3 and ν_4) to the symmetry center. The totally-symmetrical ν_1 and ν_2 may appear in the Raman effect, while ν_3 and ν_4, which produce temporary electric moments along the figure axis, should be active in infrared absorption. By estimating force constants from analogous frequencies in carbon dioxide and allene, Engler and Kohlrausch calculate that ν_1 and ν_2 should appear, respectively, at about 2200 cm^{-1} and 800 cm^{-1}. They are thus able to identify the Raman frequencies observed at 2200 cm^{-1} and 843 cm^{-1} with these vibrations. Having accomplished this assignment, they can then compute accurate values of the force constants and predict that ν_3 should lie at 2458 cm^{-1} and ν_4 at 1627 cm^{-1}. This prediction enables us to assign with some assurance the very strong infrared band at 2290 cm^{-1} to ν_3 and the strong band at 1570 cm^{-1} to ν_4.

The Engler-Kohlrausch frequency equations for the linear vibrations involve four constants, which measure the forces required to: (1) stretch the C−O bond; (2) stretch the C−C bond; (3) enlarge the distance between an oxygen atom and the central carbon; (4) enlarge the distance between the two noncentral carbons. It is of interest to calculate these constants with the help of the infrared data. If one makes the assumption that the constants (3) and (4) are negligibly small, calculation of (1) and (2) may be made independently from the Raman and from the infrared frequencies. In both instances one finds that the observed frequencies lead to imaginary values for (1) and (2), an indication that the simple valence force picture is an inadequate one. Straightforward solution of the four equations gives for the constants: (1) 13.7; (2) 9.1; (3) 1.2 and (4) 2.5, all in units of 10^5

dynes per cm. These may be compared with the values found from carbon dioxide: (1) 14.1; (3) 1.3 and from allene: (2) 9.5. No particular physical significance is to be attributed to the constants (3) and (4), save that their sizes indicate the extent to which the respective valence bond forces depart from quasi-elastic form.

Of the three degenerate frequencies, ν_7 alone is to be expected in the Raman effect. Since this vibration involves only the distortion of the C−C−O bond angle, its frequency may be estimated with the help of the constant for the distortion of the O−C−O angle in carbon dioxide. The calculated value lies very close to 586 cm^{-1}, the frequency of a line in the Raman spectrum. Engler and Kohlrausch have therefore assigned the latter to ν_7. These authors then proceed to compute the remaining degenerate frequencies by assuming that the constants for bending the C−C−C angle and the C−C−O angle are about equal. In this way they find $\nu_5=227$ cm^{-1} and $\nu_6=937$ cm^{-1}.

It should be noted here that the useful supposition of the equality of the two distortion constants, while necessary because further information is wanting, is a very rough assumption. One should therefore regard the calculated values of ν_5 and ν_6 simply as guides to the general spectral region in which these frequencies are likely to appear. In addition it is by no means safe to assume that the "constant" for the distortion of the C−C−O angle will have the same value in ν_5 and ν_6 as in ν_7. In closely analogous vibrations in acetylene and in benzene, it has been found that the corresponding bending "constants" are numerically quite different for frequencies of different symmetry types.[10]

Unless something is quite seriously wrong with the assumptions which have been made in order to calculate ν_5, that frequency should lie in the range 40–50μ, i.e., well beyond the limit of our spectrograph. Thus ν_5 will occur in our absorption curves only in combination tones. On the other hand ν_6 should appear at about 11μ, and there is actually observed at this point a rather wide band of medium intensity. One might attribute this band confidently to ν_6 if it were not for certain disquieting features of the absorption spectrum between 15 and 20μ. In this range are found two bands whose intensities are very large in comparison with the 11μ band. Assignment of either of these bands to ν_6 is not ruled out by calculations as rough as those which placed ν_6 at 11μ. If ν_6 be identified with either band, however, the other must still be interpreted and some alternative explanation worked out for the 11μ band. It is thus essential to consider the frequencies at which it is possible for overtones to appear.

Fortunately the appearance of overtones is considerably restricted by molecular symmetry. In the infrared absorption spectrum of a linear molecule with a symmetry center, all combinations tones must involve one or more fundamental frequencies antisymmetric to the symmetry center, and the changes in the quantum numbers of these antisymmetric frequencies must add up to an odd integer.[11] From this rule it follows readily that no observed band is the sum of or difference between other observed bands, and that the even overtones (e.g., $2\nu_5$, $4\nu_5$) of the active fundamentals never appear. The selection rule is a "strong" rule, for it follows from the symmetry properties of the molecular potential function and does not depend on assumptions of harmonic forces or on neglect of higher terms in the power series development for the vibrating electric moment.

The selection principle requires that binary combinations tones (i.e. tones in which the quantum numbers of only two frequencies change, each by one unit) be composed of one Raman active and one infrared active vibration. The binary combinations may be either summation or difference frequencies, but it must be kept in mind that the latter will have appreciable intensities only for combinations involving ν_5, since only for ν_5 should the Boltzmann factor have a value large enough to be comparable to unity. Binary tones involving ν_3 and ν_4 will therefore be observed below 5μ, and our interpretation of the region from 5 to 20μ must consider only combinations with ν_5 and ν_6.

[10] Compare the acetylene vibrations ν_4 and ν_5 (Colby, Phys. Rev. **47**, 388 (1935)) which are analogous to ν_5, $_6$ and ν_7 in carbon suboxide. Difficulties with the calculation of the corresponding frequencies in benzene, ν_{11} and ν_{10}, have been pointed out by Kohlrausch, Zeits. f. physik. Chemie **B30**, 313 (1935) and by Lord and Andrews, J. Phys. Chem. **41**, 151 (1937).

[11] See Dennison, Rev. Mod. Phys. **3**, 297 (1931).

TABLE II. *Allowed combination tones involving* ν_6.

COMBINATION	CALCULATED, $\nu_6=550$ cm^{-1}	OBSERVED BAND AT:	CALCULATED, $\nu_6=900$ cm^{-1}	OBSERVED BAND AT:
Binary:				
$\nu_1+\nu_6$	2750	—	3100	3150
$\nu_2+\nu_6$	1390	1387	1740	1760*
$\nu_7+\nu_6$	1130	1126	1480	1470
Ternary:				
$3\nu_6$	1650	1670*	2700	—
$2\nu_6+\nu_3$	3390	3380*	4100	—
$2\nu_6+\nu_4$	2670	—	3370	3380*
$2\nu_6+\nu_5$	1290	—	1990	1980
$2\nu_6-\nu_5$	910	909	1610	1670*
$\nu_6+2\nu_2$	2230	2290	2580	—
$\nu_6+2\nu_4$	3690	—	4040	—
$\nu_6+2\nu_5$	930	909	1280	—
$\nu_6-2\nu_5$	180	—	520	550
$\nu_6+2\nu_7$	1720	1760*	2070	1980
$\nu_1+\nu_2+\nu_6$	3590	—	3940	—
$\nu_1+\nu_6+\nu_7$	3340	3380*	3680	3790
$\nu_2+\nu_6+\nu_7$	1980	1980	2330	2290

All observed bands except those marked * may be satisfactorily interpreted independently of ν_6.

Assuming for the moment that the estimated value of ν_5 is correct, we should expect the band $\nu_7+\nu_5$ at about 800 cm^{-1}, $\nu_2+\nu_5$ at 1060, $\nu_1+\nu_5$ at 2420, $\nu_7-\nu_5$ at 360 cm^{-1}, $\nu_2-\nu_5$ at 620 and $\nu_1-\nu_5$ at 1970. Intensity maxima are actually observed at 779 cm^{-1}, 1024, 2410, 637 and 1980. (360 cm^{-1} is not within the range of the spectrometer.) The absorption spectrum thus indicates that the frequency calculated for ν_5 is probably roughly correct but somewhat large. The combination tones place ν_5 at 200 cm^{-1}.

If the wide band at 900 cm^{-1} be assigned to ν_6, the very strong absorption at 550 cm^{-1} must be given an interpretation involving ν_5. Since we have already seen that the binary tone $2\nu_5$ is forbidden, it is quite reasonable to interpret the band as the first allowed overtone to ν_5, namely $3\nu_5$. This interpretation implies a ν_5 of about 185 cm^{-1}, in fair agreement with the value suggested by the assignment of the binary tones. The intensity of this band is remarkably high for an overtone, and indicates that the fundamental should exhibit extremely strong absorption. The corresponding overtone in CO_2 was found by Barker and Wu by using a pressure of about an atmosphere and a cell seven feet long.[12]

If $3\nu_5$ shows such strong absorption, it is quite possible that $5\nu_5$ should appear with appreciable intensity. The roughly calculated frequency of $5\nu_5$ is 920 cm^{-1}, which lies just in the region of the absorption band we have ascribed to ν_6. This unfortunate coincidence is the source of considerable trouble, for it prevents a clear-cut decision on the origin of the 900 cm^{-1} band. Assuming provisionally that the band is due *only* to $5\nu_5$ we may use the observed frequency of the band in conjunction with that of the 550 cm^{-1} band to calculate the frequency of the fundamental. The two bands provide the data required to solve an anharmonic frequency formula[13] for the necessary constants. The frequency obtained is $\nu_5=190$ cm^{-1}.

The anharmonicity expression also helps to account for the doublet structure exhibited by the two bands. The doublets might be explained as rotational branches except that: (1) a Q branch ought also to be present; (2) the maxima of the P and R branches should be 11 cm^{-1} apart, while the observed spacing is 14 cm^{-1} in the 550 band and 20 cm^{-1} at 900 cm^{-1}. On the other hand if it be assumed that the low frequency maximum in each doublet is due to transition from the first excited vibrational level, the spacings calculated from the anharmonicity formula are 12 cm^{-1} and 19 cm^{-1}, respectively. The shoulder on the low frequency slope of the 900 cm^{-1} band and the broadness of the 550 cm^{-1} absorption may be contributed by transitions from the second excited level. The first and second excited levels have population factors of 0.80 and 0.46, referred to the ground state population.

An alternative explanation of these bands has been suggested to us by Professor Dennison. If the 550 band be assigned to ν_6, resonance degeneracy may occur between ν_6 and $3\nu_5$. Such an accidental degeneracy would lead to a small splitting of the 550 frequency and would account for the observed doublet structure of that band. In addition the doublet nature and the intensity (which is rather large for so high an overtone) of the band at 900 cm^{-1} are understandable on the basis of resonance degeneracy.[14] It is clear that a study of these bands under high

[12] Barker and Wu, Phys. Rev. **45**, 1 (1934).

[13] Cf. Dennison, reference 11, p. 296.

[14] Cf. the relatively high intensity of the overtones at 3610 and 3717 cm^{-1} in CO_2. This pair of bands constitutes a resonance doublet.

TABLE III. *Interpretation of observed bands.*

OBSERVED BAND:		CALCULATED FREQUENCY IN CM^{-1}	INTERPRETATION
λ in μ	$\tilde{\nu}$ in cm^{-1}		
18.12	550	[550]*	$[\nu_6](3\nu_5)$*
15.70	637	650	$\nu_2-\nu_5$
12.84	779	780	$\nu_5+\nu_7$
11.00	909	930 (900)	$\nu_6+2\nu_5(\nu_6)$
9.76	1024	1030; 980	$\nu_2+\nu_5$; $2\nu_7-\nu_5$
8.88	1126	1140 (1140)	$\nu_6+\nu_7(3\nu_5+\nu_7)$
8.16	1225	1190; 1240	$\nu_4-2\nu_5$; $\nu_2+\nu_7-\nu_5$
7.21	1387	1390 (1390); 1360	$\nu_2+\nu_6(\nu_2+3\nu_5)$; $\nu_5+2\nu_7$
6.80	1470	1500 (1490)	$2\nu_2-\nu_5(\nu_6+\nu_7)$
6.37	1570	[1570]	$[\nu_4]$
5.98	1670	1650; 1720 (1610; 1720)	$3\nu_6$; $2\nu_7+\nu_6(2\nu_6-\nu_5$; $2\nu_7+3\nu_5)$
5.68	1760	1720 (1740)	$2\nu_7+\nu_6(\nu_2+\nu_6)$
5.41	1850	1880; 1910	$2\nu_2+\nu_5$; $\nu_3-2\nu_5$
5.05	1980	1910; 2010 (1990)	$\nu_3-2\nu_5$; $\nu_1-\nu_5(\nu_5+2\nu_6)$
4.57	2190	2160 (2070)	$\nu_4+\nu_7(\nu_6+2\nu_7)$
4.37	2290	[2290]	$[\nu_3]$
4.15	2410	2390; 2410	$\nu_1+\nu_5$; $\nu_2+\nu_4$
3.17	3150	3130 (3100)	$\nu_2+\nu_5(\nu_1+\nu_6)$
2.96	3380	3340; 3390 (3370)	$\nu_1+\nu_6+\nu_7$; $2\nu_6+\nu_3(2\nu_6+\nu_4)$
2.64	3790	3770 (3690)	$\nu_1+\nu_4(\nu_1+\nu_6+\nu_7)$
2.18	4590	4490	$\nu_1+\nu_3$

* The interpretation enclosed in parentheses is that for $\nu_6=900$ cm^{-1}. Frequencies calculated on this interpretation are also put within parentheses. The square brackets enclose fundamental frequencies whose values were used in finding the calculated frequencies. We have used for the Raman active frequencies: $\nu_1=2200$ cm^{-1}; $\nu_2=843$ cm^{-1}; $\nu_7=586$ cm^{-1}.

resolution is prerequisite to a satisfactory interpretation of them.

Because the strong bands which might be attributed to ν_6 may also be accounted for in other ways, we must resort to combination tones to find a value for ν_6. Table II lists the allowed binary tones and such ternary tones involving ν_6 as should appear in the spectroscopic region we have studied. With two exceptions the difference tones have been excluded from the Table because their Boltzmann factors are too small (<0.1). The frequencies of the indicated combinations have been calculated for $\nu_6=550$ cm^{-1} and 900 cm^{-1}, and the frequencies of bands near the calculated values listed for comparison. It is apparent that neither assumed value of ν_6 is clearly superior to the other in interpreting those bands (marked with an asterisk) for which no alternative explanation is possible. The assignment $\nu_6=550$ is favored by the fact that the 1670 band, of fairly strong absorption, is attributed to the lowest allowed overtone of a strong fundamental. The interpretation of this band for $\nu_6=900$ is not particularly convincing because it involves a difference tone for which the corresponding summation frequency is quite weak. On the other hand, several frequencies predicted by the 550 interpretation are missing from the spectrum, in particular $\nu_1+\nu_6$ and $2\nu_6+\nu_5$. These bands should be expected to have appreciable intensity.

Under the 900 cm^{-1} assignment, absorption bands are observed for all the binary combinations. One of these bands can be interpreted only with the help of ν_6. The expected ternary combinations are found experimentally except for the important bands $3\nu_6$ and $2\nu_5+\nu_6$.

On the whole it does not seem possible to make a definite assignment for ν_6 on the basis of the data we have obtained. Further argument in favor of assignment to the 550 frequency is to be found in the remarkable intensity of this band, which seems surprisingly strong for a third overtone. In addition when $\nu_6=550$ cm^{-1}, all the interpretations involving $3\nu_5$ (see Table II) apply equally well if $3\nu_5$ be replaced by ν_6 so that none of these interpretations is invalidated by such an assignment.

If ν_6 be in truth at 900 cm^{-1} it must be weak enough so that it becomes confused with the other frequencies in the 11μ band. One should point out, however, that the low intensity of ν_6 is readily understandable from the form of the vibration. Suppose that in the distortion vibra-

tions the center of one electrical charge, either positive or negative, be at the central carbon atom and two centers of the other charge on the oxygen atoms. The vibrating electric moment in ν_6 should then be small because both the positive and negative charges move in the *same* direction and about the same amount. On the other hand ν_5 should have a large vibrating moment on this basis, and ν_5 should be quite intense. The latter fact is compatible with the assignment of $3\nu_5$ to the band at 550 cm^{-1}.

The presence of two apparent overtones at 1114 and 1174 cm^{-1} in the Raman spectrum of carbon suboxide might assist our assignment of ν_6. The latter line is very probably $2\nu_7$ and is of no help. $2\nu_6$ is also an allowed overtone in the Raman effect, and if this interpretation be placed on the 1114 cm^{-1} frequency, we obtain $\nu_6=557$, in excellent agreement with the absorption band at 550 cm^{-1}. Unhappily for this argument, however, the combination tone $\nu_5+\nu_6$ is also allowed in the Raman effect, and if ν_6 be given a value slightly larger than 900 cm^{-1}, we find $\nu_5+\nu_6=1114$ cm^{-1}. The Raman spectrum thus does not permit an unequivocal decision.

In passing it might be remarked that the suggestion of Engler and Kohlrausch[5] of resonance splitting to account for these weak lines is probably not acceptable. The proposed interaction of $\nu_5+\nu_6$ with $2\nu_7$ satisfies symmetry requirements, but such a perturbation is a second-order effect and should result in a splitting of a few wave-numbers at the most, rather than the observed 60 cm^{-1}. The large splitting of 103 cm^{-1} in the Raman spectrum of CO_2 is due to a first-order perturbation.

Patently further experimental study will be required to settle the assignment of ν_6. It would be of great assistance if the region from 2 to 7μ and the bands at 11μ and 18μ could be examined under considerably higher resolution. If a clearer notion of the individual components of these bands could be obtained, a definite decision about ν_6 might be possible. Direct experimental confirmation of the fundamental at 52μ would also be of interest.

We have assembled in Table III the complete interpretation of the observed bands. The interpretation is double for some bands because of our indecision with respect to ν_6. Since one or two quaternary bands may be found in the Table, we should state that we have examined systematically the three hundred or more possible quaternary tones. Nearly all of these may be rejected without further consideration because of one or more of these reasons: (1) wave-length outside the 2–25μ region; (2) Boltzmann factor too small (for difference bands); (3) very low predicted intensity, from consideration of observed intensities in analogous but simpler tones.

Despite our failure to assign definite values to all of the infrared active fundamentals, we have produced forceful evidence in favor of the symmetric linear structure for carbon suboxide. In the first place, there is no indication of the presence of Raman active frequencies in the absorption curve. Any sign of ν_1 would be obscured by the ν_3 band, but if there is absorption due to a frequency at 843 cm^{-1} (ν_2) it should certainly appear definitely close to 12μ. The long wave-length slope of the 11μ band shows no trace of an absorption band near 12μ. There is absolutely no indication of an absorption band at 586 cm^{-1} (ν_7). Similarly no sign of the strong infrared bands at 550, 635, 900, 1570 and 2290 cm^{-1} appears in the Raman spectrum. This is an excellent indication that the molecule in question contains a center of symmetry.

We have remarked previously that no band in the absorption spectrum of a symmetric linear molecule should be expressible, except by accident, as the sum of two other bands. Examination of the spectrum of carbon suboxide shows that this rule holds in the region of the spectrum where resolution is good enough to make the bands fairly narrow and the maxima sharp. For example, no absorption occurs at the sum of the two strong bands 550 and 635, at 550 plus 779, at twice 550 or at twice 635. This is further evidence for the postulated structure.

Finally the unmistakable appearance of the linear frequencies ν_3 and ν_4 close to the predicted points is an indication that the equations developed for a linear structure are valid for carbon suboxide. Agreement of the force constants with the analogous constants in the carbon dioxide molecule also supports the linear model.

In our opinion the preceding evidence is

sufficient to rule out any nonlinear or asymmetric structure for carbon suboxide. It is disappointing that we cannot make a complete vibrational analysis of the absorption spectrum, but it appears quite probable that absorption studies made under higher resolution will enable the analysis to be completed. We are grateful to Professor Halford for his kindness in furnishing us with the carbon suboxide, to Professor Randall for placing the spectrometer at our disposal and particularly to Professor Dennison for helpful discussions.

AUGUST, 1937 JOURNAL OF CHEMICAL PHYSICS VOLUME 5

Calculation of the Heat Capacity Curves of Crystalline Benzene and Benzene-d_6

R. C. LORD, JR.*
Department of Chemistry, University of Michigan, Ann Arbor, Michigan

J. E. AHLBERG AND D. H. ANDREWS
Department of Chemistry, Johns Hopkins University, Baltimore, Maryland

(Received March 27, 1937)

The heat capacity curve for solid benzene has been computed with the help of the set of internal frequencies previously proposed by Lord and Andrews. The agreement with experiment is satisfactory over the entire temperature range in which the internal frequencies contribute, indicating that the frequency values are essentially correct. A prediction of the heat capacity of benzene-d_6 has also been made.

THE existence of a complete set[1] of values for the internal frequencies of the benzene molecule makes it possible for the first time to calculate directly the contribution of these degrees of freedom to the heat capacity of crystalline benzene. Earlier attempts[2] to carry out computations of this sort involved empirical and rather rough estimates of these frequencies, and led only to qualitative information concerning the specific heat of the crystal. A precise calculation of the heat capacity of solid benzene is of interest, particularly in view of the experimental data obtained at "helium" temperatures recently by Ahlberg, Blanchard and Lundberg[3] and the other excellent values at higher temperatures which can be compared with calculated values. Our discussion will be concerned with this calculation and the conclusions to be drawn from such a comparison.

When thermal energy is absorbed at constant pressure by a crystalline solid such as benzene, this energy is distributed among: (1) the oscillations of the crystal lattice; (2) the internal vibrations of the molecules composing the lattice; and (3) the work of expanding the lattice. Before discussing these three components of the specific heat, we must emphasize that our ultimate interest lies in the contribution (2). Contributions (1) and (3) will be evaluated as accurately as possible by means of the traditional expressions for them, but it is not our purpose to improve these expressions or to criticize their theoretical origins.

Experience has shown that the share of the lattice vibrations in the specific heat of a crystal is ordinarily described rather accurately by the familiar Debye function $D(x)$:

$$C_v\,(\text{lattice}) = 3RD(x),$$

$$D(x) = \frac{12}{x^3}\int_0^x \frac{z^3 dz}{e^z - 1} - \frac{3x}{e^x - 1}, \qquad (2)$$

in which x is the parameter $(h\nu_D/kT)$. ν_D is the well-known Debye characteristic frequency which must be determined in some way if we are to utilize the function $D(x)$.

The physical significance of ν_D has been the subject of much discussion. In a recent critique

* National Research Council Fellow.
[1] Lord and Andrews, J. Phys. Chem. **41**, 149 (1937).
[2] D. H. Andrews, Proc. Roy. Soc. Amst. **29**, 744 (1926); Chem. Rev. **5**, 533 (1928); E. O. Salant, Proc. Nat. Acad. Sci. **12**, 334, 370 (1926).
[3] J. E. Ahlberg, E. R. Blanchard and W. O. Lundberg, J. Chem. Phys. **5**, 539 (1937).

of the Debye theory, Blackman[4] points out that there is no theoretical justification for identifying ν_D with any of the actual vibrations of the crystal lattice. The assumption that ν_D is a residual ray frequency, for example, appears to be unwarranted despite the closeness of agreement between ν_D and reststrahlen frequencies for a number of crystals. For our purposes, however, the physical meaning of ν_D is of secondary importance. If a value of ν_D can be found by means of which $D(x)$ reproduces the lattice C_v, our requirements will be satisfied.

Before considering the method of evaluating ν_D, it is necessary to take up a question arising from the fact that the lattice of solid benzene is not an atomic lattice. Functions of the Debye type apply to crystal lattices made up of mass points having no moment of inertia. Each mass point possesses only three degrees of freedom and the compressional waves in the three dimensions of the space lattice are the crystalline analog of the three degrees of translational freedom allowed to the particles of a monatomic gas. Doubtless the molecules in a benzene crystal may be fairly considered as mass points insofar as the propagation of compressional waves is concerned. These compressional vibrations should therefore take up thermal energy in the manner described by the Debye function. In addition, however, the benzene molecule possesses three moments of inertia and correspondingly three degrees of rotational freedom. If the component molecules of the benzene lattice were rotating freely and independently of one another, the contribution of these rotational degrees of freedom to the heat capacity would be the same as their contribution to C_v of gaseous benzene. The benzene molecules do not rotate freely, of course, and therefore we have to determine what the nature of the rotatory motion is and what its effect on the specific heat will be.

Each molecule in the benzene lattice is situated at an equilibrium position in the field of force resulting from the presence of the neighboring molecules. If one molecule be somewhat displaced from this position by a translation or by rotation through some small angle about its center of gravity, it will tend to return to the equilibrium position. The displacement will, however, affect the neighboring molecules, since the force field acting on each of them is partly due to the displaced molecule. This interaction of molecules undergoing translational displacement leads to the compressional waves mentioned above. Similarly *angular displacement* results in the production of *torsional waves*, in which the molecules in the crystal lattice execute rotatory oscillation through small angles. The oscillations of each molecule bear definite phase relationships to the oscillations of the others, and the oscillational waves are propagated in all three dimensions of the space lattice. It is our assumption that these torsional waves contribute to the specific heat in the same manner as the compressional waves, and that this contribution is accordingly described by a Debye function $D(x)$. The maximum frequency ν_D for the torsional waves will of course differ in general from ν_D for the compressional vibrations. The expression for the heat capacity of the benzene lattice will be therefore

$$C_v \text{ (lattice)} = 3R[D(x_1)+D(x_2)]. \qquad (3)$$

To evaluate the two ν_D's required by Eq. (3), we use the following procedure. At low temperatures, say below 50°K, the internal vibrations and work of expansion make only trifling contributions to the specific heat of benzene. Consequently, the experimentally observed heat capacity corresponds to that given by Eq. (3). Hence, if we select values for ν_{D_1} and ν_{D_2} which reproduce the heat capacity curve over the range 0°–50°K, we can feel confident that these values are the correct ones for use at higher temperatures.

When the two values of ν_D are not widely different, we may say

$$D(x_1)+D(x_2)=2D\left(\frac{x_1+x_2}{2}\right). \qquad (4)$$

Or, setting $h\nu_{D_1}/k=\theta$, $h\nu_{D_2}/k=\theta_2$ and $(\theta_1+\theta_2)/2=\theta$,

$$D(\theta_1/T)+D(\theta_2/T)=2D(\theta/T). \qquad (5)$$

From unpublished calculations by Dr. V. Deitz and Mr. C. F. Squire, extending the former's investigations of crystal lattices[5] it appears that θ_1 (for compressional oscillations) in benzene is about 25 percent smaller than θ_2 (for torsional

[4] Blackman, Proc. Roy. Soc. **A148**, 365, 384 (1935).

[5] V. Deitz, J. Frank. Inst. **219**, 459, 565, 703 (1935).

oscillations). When the θ's considered lie in the range 100–200 and differ by 25 percent, the approximation (5) holds to within experimental error at temperatures above 35°–40°K. Even at temperatures considerably lower the approximation is valid to better than 5 percent. Accordingly we may obtain from the heat capacity data at low temperature the value of a single θ and in terms of this θ express the heat capacity due to the lattice of crystalline benzene over the entire temperature range of the solid. The equation will be:

$$C_v \text{ (lattice)} = 6RD(\theta/T). \tag{6}$$

The question of the accuracy of Eq. (6) and of possible variatons in θ will be considered later.

The contribution made by the internal frequencies in the benzene molecule to the specific heat of the crystal is readily calculable. The heat capacity arising from one degree of internal freedom of frequency ν_i is

$$C_v = RE(x_i),$$

where $x_i = h\nu_i/kT$, and the Einstein function $E(x) = x^2e^x/(e^x-1)^2$. Hence the total internal heat capacity will be

$$C_v \text{ (internal)} = R \cdot \sum_{i=1}^{n} E(x_i). \tag{7}$$

The summation extends over the n internal degrees of freedom. n for benzene is thirty.

The addition of Eqs. (6) and (7) yields the heat capacity of the crystal at constant volume. To convert this into the experimentally measurable heat capacity at constant pressure, C_p, use is made of the standard thermodynamic formula

$$C_p - C_v = \alpha^2 VT/\beta, \tag{8}$$

where α is the crystal's coefficient of thermal expansion, β the coefficient of compressibility and V the molar volume of the crystal. Eq. (8) expresses the contribution made to C_p by the work required to expand the lattice.

The right-hand member of (8) can be changed to a more useful form by means of Mie's[6] relation:

$$\alpha V/\beta = \text{const.} \times C_v. \tag{9}$$

[6] Mie, Ann. d. Physik **11**, 657 (1903).

Grüneisen[7] has shown, by a combination of thermodynamic argument with the results of lattice theory, that such a relation should hold for atomic lattices whose C_v is given by Eq. (1). Extension of Grüneisen's reasoning to molecular lattices leads to the expression

$$\alpha V/\beta = \sum_i a_i (C_v)_i, \tag{10}$$

in which the a_i's are constants multiplying the several components of C_v, namely C_v due to compressional and to torsional lattice vibrations, and due to the various internal degrees of molecular freedom. Eq. (10) may be simplified by making two reasonable assumptions about the coefficients a_i. In the first place we assume, in keeping with our discussion of the relative magnitudes of the ν_D's of compression and of torsion, that the coefficient of C_v due to compressional oscillations is the same as that for C_v due to torsional oscillations. Secondly, we suppose that the coefficients for the various components of the internal C_v may be lumped together into one coefficient for the whole internal C_v. Thus we reduce (10) to

$$\alpha V/\beta = a' C_v \text{ (lattice)} + b' C_v \text{ (internal)}. \tag{11}$$

a' and b' are constants. If we make the empirically justifiable[8] assumption that the quotient V/β is temperature-independent, combination of (8) and (11) gives

$$C_p - C_v = [a \cdot C_v \text{ (lattice)} + b \cdot C_v \text{ (internal)}]^2 T. \tag{12}$$

The evaluation of the constants a and b is essential for our calculation of C_p, but unfortunately there is at present no independent way of determining them. We should expect the constant a to have a value of the order of magnitude of similar constants for atomic lattices, but no precedent exists for estimating b. We therefore resort to an empirical procedure for finding a and b.

The difference between observed C_p and calculated C_v above 50°K is ascribed to work of expansion. With the help of this difference at

[7] Grüneisen, *Handbuch der Physik*, Vol. X, p. 22 ff. See also Eucken, *Handbuch der Experimentalphysik*, Vol. VIII, part 1, p. 281.

[8] Cf. Eucken, reference 7, p. 282; cf. Grüneisen, Ann. d. Physik **26**, 211 (1908).

any two temperatures, we can calculate a and b from Eq. (12). When such a calculation is carried out,[9] a and b are found to have the same value within about 5 percent. We may therefore set $a=b$, and reduce Eq. (12) to:

$$C_p - C_v = kC_v^2 T. \qquad (13)$$

TABLE I. *Heat capacity of benzene and benzene-d_6.*

TEMPERATURE °K	LATTICE C_v	INTERNAL C_v	$C_p - C_v$	CALC. C_p	OBSERVED C_p	CALC. C_p ($\nu_{16}=160$ cm^{-1})	CALC. C_p C_6D_6
4	0.018			0.018	0.0195	.018	.024
6	.060			.060	.065	.060	.074
8	.144			.144	.147	.144	.173
10	.270			.270	.346	.270	.336
15	.908			.908	.920	.91	1.10
20	1.932			1.932	1.84	1.94	2.29
25	3.18		0.02	3.20	3.00	3.24	3.66
30	4.41		.04	4.45	4.24	4.57	4.94
40	6.45		.11	6.56	6.47	7.06	7.04
50	7.90		.20	8.10	8.14	9.20	8.56
60	8.90	0.02	.31	9.23	9.32	10.98	9.72
70	9.60	.07	.42	10.09	10.16	12.48	10.62
80	10.07	.17	.54	10.78	10.85	13.69	11.47
90	10.42	.31	.67	11.40	11.44	14.73	12.29
100	10.70	.51	.81	12.02	11.99	15.67	13.12
110	10.89	.79	.97	12.65	12.59	16.50	13.94
120	11.02	1.09	1.13	13.24	13.24	17.21	14.82
130	11.14	1.45	1.33	13.92	13.96	17.96	15.75
140	11.24	1.84	1.55	14.63	14.71	18.66	16.73
150	11.32	2.31	1.80	15.43	15.49	19.46	17.78
160	11.38	2.77	2.07	16.22	16.26	20.19	18.91
170	11.43	3.26	2.37	17.06	17.10	20.97	20.13
180	11.48	3.80	2.71	17.99	18.02	21.80	21.39
190	11.53	4.31	3.08	18.92	19.00	22.62	22.76
200	11.58	4.95	3.53	20.06	20.02	23.66	24.17
210	11.62	5.53	3.98	21.13	21.11	24.68	25.65
220	11.65	6.16	4.50	22.31	22.24	25.80	27.20
230	11.68	6.80	5.07	23.55	23.45	26.88	28.85
240	11.70	7.47	5.69	24.86	24.75	28.11	30.51
250	11.72	8.13	6.35	26.20	26.09	29.38	32.28
260	11.73	8.77	7.05	27.55	27.75	30.67	34.12
270	11.74	9.46	7.83	29.03	29.70	32.09	35.98

[9] The numerical determination of the two constants is made most reliably by utilizing the $C_p - C_v$ difference at two rather widely different temperatures, e.g. at 150° and 250°. The constants found at these two temperatures may be used in turn to calculate the expansion term for all other temperatures. The constants may also be evaluated separately. In the region 60°–100°, C_v (internal) makes no appreciable contribution to the $C_p - C_v$ difference. Hence the constant a may be determined independently of b at any temperature in this region. The evaluation of b is then possible at a single temperature above 100°, preferably at a temperature high enough so that the C_v (internal) term is relatively large. The a and b values found in this way agree well with those found by simultaneous solution of two numerical equations obtained from Eq. (12). It is of interest to note that the value of the constant a, 8.3×10^{-3} reciprocal calories, agrees reasonably well with the value one would compute from the formula proposed by Nernst and Lindemann (Zeits. f. Elektrochem. **17**, 817 (1911)) for this constant, namely $a^2=0.0214/T_m$, where T_m is the fusion temperature of the crystal. The value of a calculated from this expression is 8.77×10^{-3}.

The constant $k(k \leqq a^2 \leqq b^2)$ has the value of 6.45×10^{-5} reciprocal calories for crystalline benzene.

CALCULATION OF C_p FOR BENZENE

With the help of Eqs. (6), (7) and (13) we have calculated C_p for crystalline benzene over its entire temperature range. The value of θ used in (6), namely $\theta=150$, was obtained in the manner we have described. (See the discussion of Eqs. (3)–(6).) The internal frequencies for Eq. (7) have been taken from our previous paper.[1] The results of the calculation are listed in Table I together with values obtained by interpolating at a regular series of temperatures between the experimental results of Ahlberg, Blanchard and Lundberg[3] and Nernst[10] below 90°K, and of Huffman, Parks and Daniels[11] above 90°.

It will be seen from Table I that the agreement between calculation and experiment is remarkably good except for several points in the neighborhood of 25°K. These rather small discrepancies are probably to be ascribed to some fluctuation in the value of θ. Such fluctuations have been discussed by Blackman.[4] He points out that θ should fluctuate somewhat at low temperatures but should tend to remain constant at higher values of T. (For "higher values" one might say "values of T larger than $\theta/2$." Compare, for example, Blackman's Fig. 3, page 375, for one-dimensional lattices.)

For our purposes it is sufficient if θ remains reasonably near to 150 in the range above 80°K, for in that range the lattice C_v has very nearly attained its classical value and is not very sensitive to moderate changes in θ. The temperature region above 80° is of primary interest because in this region the internal vibrations make their contribution to C_p. It will be noticed that from 50° to 250° the agreement of theory with observation is quite satisfactory. This close check may be regarded as an excellent confirmation of the values of the internal frequencies used in Eq. (7). The slight divergence of theory and experiment close to the melting point may be due on the one hand to inaccuracy of Eq. (6)

[10] W. Nernst, Ann. d. Physik **36**, 395 (1911).

[11] Huffman, Parks and Daniels, J. Am. Chem. Soc. **52**, 1547 (1930).

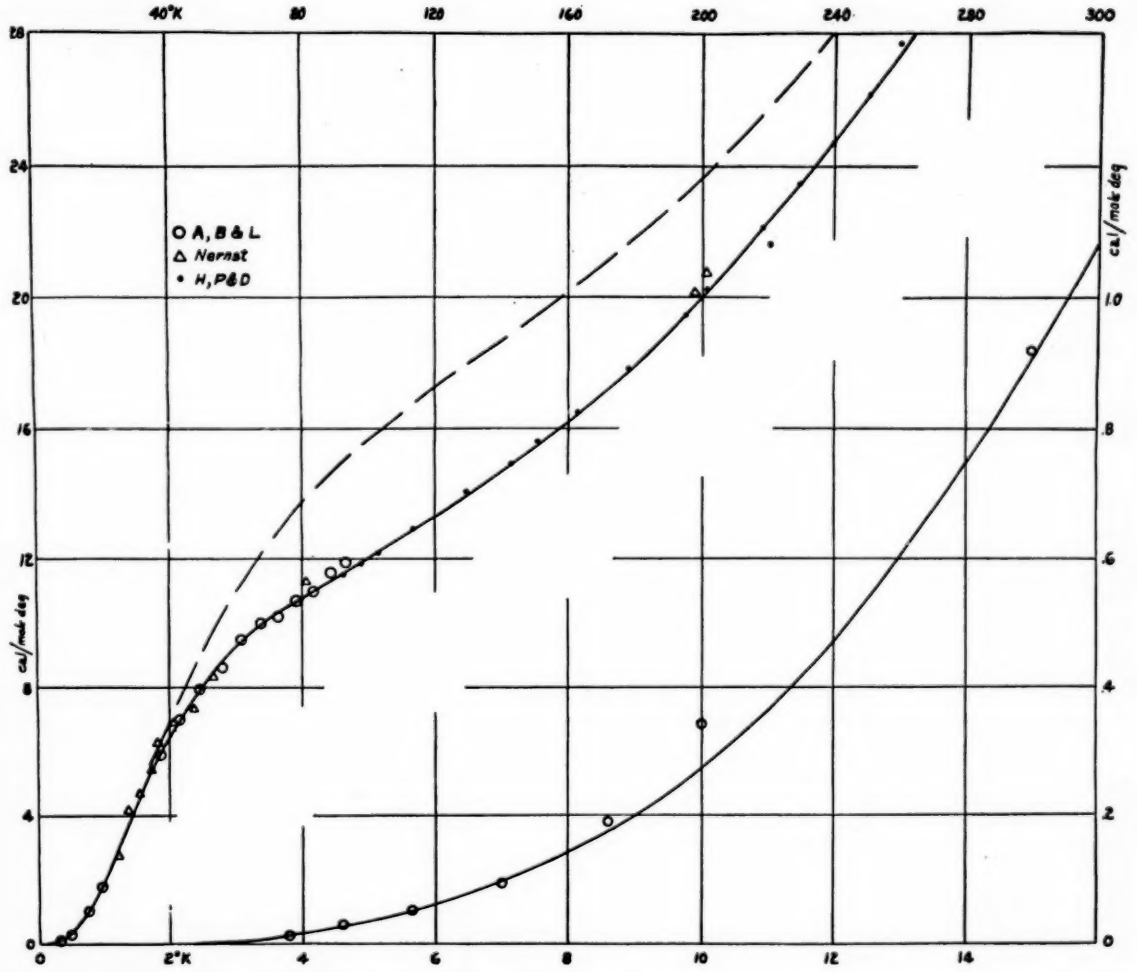

FIG. 1. The calculated values of the heat capacity of benzene with $\nu_{16}=406$ cm^{-1} and $\nu_4=538$ cm^{-1} (solid line); with $\nu_{16}=160$ cm^{-1} and $\nu_4=212$ cm^{-1} (dashed line). The experimental observations are taken from Ahlberg, Blanchard and Lundberg,[3] Nernst,[10] and Huffman, Parks and Daniels.[11]

or (13) when fusion is imminent, or on the other to slight increase in observed C_p near the melting point because of the presence of a trace of impurity in the sample under observation.

The exactness with which the theoretical and experimental C_p's coincide indicates that fundamental frequencies below 400 cm^{-1} can hardly be present in benzene. Evidence from the band spectra of benzene, however, has often been interpreted as demonstrating the presence of a fundamental frequency of 160 cm^{-1}. If such a fundamental were to exist in benzene, it would perforce belong to vibrational modes 4 or 16 (Wilson's notation[12]). The reasons for this assignment have been previously discussed.[1, 13] If we assume that ν_{16} has a value of 160 cm^{-1}, then ν_4 must lie somewhere in the neighborhood of 212 cm^{-1}. Column 7, Table I, gives C_p for benzene calculated on the assumption that ν_{16} and ν_4 have the respective values 160 cm^{-1} and 212 cm^{-1}, rather than 406 cm^{-1} and 538 cm^{-1}. The latter values (see reference 1) were used in obtaining the values of "calculated C_p" in the fifth column. The C_v portion of the values in column 7 has been obtained as before from Eqs. (6) and (7). To find the C_p-C_v term, we have used Eq. (13), in which the constant k has

[12] Wilson, Phys. Rev. **45**, 706 (1934).

[13] Angus, Bailey, Hale, Ingold, Leckie, Raisin, Thompson and Wilson, J. Chem. Soc. (London) 984 (1936).

been assigned the empirically determined value 6.45×10^{-5} cal^{-1}.[14] For comparative purposes these results have been plotted in Fig. 1. It will be seen from this plot that a fundamental frequency of 160 cm^{-1} is incompatible with the heat capacity curve over the whole range 50°–250°K.

Prediction of C_p for Benzene-d_6

A calculation of the heat capacity of benzene-d_6 seemed desirable because comparison of theoretical and experimental C_p's should indicate just how accurate are the low internal frequencies which have been worked out for that molecule.

The lattice C_v for benzene-d_6 is assumed to be given by Eq. (6). The shift in θ was estimated by presuming that

$$\theta_1' = \theta_1(M/M')^{\frac{1}{2}}, \qquad \theta_2' = \theta_2(I/I')^{\frac{1}{2}}, \tag{14}$$

where θ_1 and θ_2 are the compressional and torsional θ's, respectively (see Eq. (5)). M is the molecular weight and I *any* moment of inertia of benzene. The primes refer to the corresponding quantities in benzene-d_6. (There is no ambiguity in regard to the moments of inertia, for the ratio I/I' is the same for all three moments in benzene.) From (14) and the assumption that $\theta_1 \leqq \theta_2$, we find that

$$\theta' = (\theta/2)[(M/M')^{\frac{1}{2}} + (I/I')^{\frac{1}{2}}]. \tag{15}$$

(15) yields the value $\theta' = 140$.

The vibrational frequencies of benzene-d_6 as given in reference 1 were used in Eq. (7) to compute the internal C_v. The constant k in Eq. (13) was taken as 6.45×10^{-5} reciprocal calories. Column 8, Table I, gives C_p for benzene-d_6.

Despite the rough nature of the method of finding θ', it is likely that our estimate of the $\theta-\theta'$ shift is fairly good, so that the contribution of the lattice C_v to the net specific heat has been pretty closely estimated. Presumably the expansion formula is as valid as it proved to be for benzene. The accuracy of our prediction, then, depends upon the accuracy with which the internal frequencies are known. Excepting ν_4 and ν_{16}, the important (i.e., low) frequencies in benzene-d_6 have been observed spectroscopically and are known with a precision adequate for our purposes. The calculation of C_p therefore hinges to a large extent on the correctness of our estimate of ν_4 and ν_{16}.

The assignment of ν_{16} in benzene to the faint Raman frequency at 406 cm^{-1} is apparently substantiated by the excellence of agreement between theoretical and observed C_p's. It is to be remarked, however, the doubt here lies not in the value of the Raman line in question but in the assignment of ν_{16} to it. If the assignment is correct, we know the value of ν_{16} to within two or three cm^{-1}. Unfortunately, the corresponding line has not been observed for benzene-d_6, so that it is necessary to calculate the frequency at ν_{16} in the latter. There is some considerable degree of doubt about the accuracy of such a calculation and therefore we can scarcely expect to find the same excellence of agreement between theoretical and experimental C_p's for benzene-d_6 as was obtained for benzene. The measurement of C_p for crystalline benzene-d_6, which will be undertaken in the immediate future, is awaited therefore with considerable interest, for if such measurement agrees closely with our calculation, the frequencies of the distortion vibrations 4 and 16 have been correctly estimated. The extent of any discrepancy between theory and observation, on the other hand, will indicate the size and direction of the error in our estimate of ν_4 and ν_{16}.

[14] One might object, with considerable reason, that it is hardly legitimate to use here a constant found empirically under the assumption of different values for certain of the internal frequencies. This objection may be answered in part by remarking that the value of the constant used is close to that given by the independent formula of Nernst and Lindemann (reference 9). In addition it should be remembered that we are attaching no particular theoretical significance to the hypothetical C_p curve other than its utility in demonstrating the improbability of the presence of the very low frequencies in benzene. Even if the expansion term is disregarded entirely, the low frequencies still cause some contradiction with experiment, for in the region 80°–140°K the calculated C_v is *larger* than observed C_p by 1–2 percent.

Molecular Rotation in Crystalline Disubstituted Ethanes

ADDISON H. WHITE AND S. O. MORGAN
Bell Telephone Laboratories, New York, N. Y.

(Received May 5, 1937)

The dielectric constants and conductivities of ethylene chloride, ethylene bromide, ethylene cyanide, ethylene diamine and ethylene thiocyanate have been measured over a wide temperature range in the solid and liquid states and in the frequency band 1–100 kc. Thermal measurements have revealed hitherto unreported transitions in ethylene cyanide at −38° to −46° and in ethylene bromide at −23° to −25°. The ethylene cyanide molecule rotates about all three axes in the crystal between the transition and melting temperatures. The internal rotational motion of atomic groups about the central C−C bond, which is believed to characterize this molecule in the liquid state, is not observably restricted by solidification. This internal motion is believed to facilitate molecular rotation in the crystal by increasing the time-average symmetry of the molecule. An atomic polarization of about 17 cc below the transition is ascribed to the persistence of some degree of torsional vibration within the molecule even in the low temperature phase of the crystal. In none of the other crystals does the polar form of the molecule rotate below the freezing point nor is there evidence of unusual intramolecular motion except possibly in ethylene thiocyanate. It is probable, however, that the *trans* form of the ethylene bromide molecule rotates about its long axis between the transition and melting points.

THE existence of internal rotation about the C−C bond in the ethane molecule[1] has led to a number of measurements of the dipole moments of its symmetrically disubstituted derivatives. This work has all been done in either dilute solution or the gaseous state. If such an internal motion persists in the solid phase, the resulting dielectric properties should be unusual. Relative mobility of the parts of the molecule might be expected to facilitate rotation of the whole molecule in the lattice in a manner similar to that suggested for the pliable cyclohexane derivatives.[2] This paper presents the results of dielectric measurements of a series of such compounds in the crystalline and incidentally the liquid states.

The consensus of the theoretical and experimental work on ethylene chloride (1,2-dichloroethane) and ethylene bromide (1,2-dibromoethane) is that at room temperature and in dilute solution or the vapor phase most of the molecules are in states which involve internal rotational oscillation of considerable amplitude.[3] Experimentally the dipole moments of these molecules increase with temperature, so it is quite clear that their configuration of minimum potential energy is the *trans* form, whose moment is zero. This is due to the predominance of the electrostatic repulsion which tends to force the two internal dipoles as far apart as possible.

Williams'[4] measurements of the dipole moments of three ethylene halides and ethylene cyanide (succinonitrile), all in dilute benzene solution at 25°C, are summarized in the fourth column of Table I. Using the observed moments of the corresponding ethyl derivatives of the type C_2H_5X for the two component dipoles within each of these molecules, the resultant effective molecular moments, calculated for perfectly free internal rotation[4] with no distortion of carbon valence angles, are listed in the third

TABLE I.

	$\mu_{C_2H_5X}$	μ_{calc}	μ_{obs}	$\frac{\mu_{obs}}{\mu_{calc}}$
$C_2H_4Cl_2$	2.0*D*	2.7*D*	1.75*D*	0.65
$C_2H_4Br_2$	1.9	2.5	1.4	.56
$C_2H_4I_2$	1.7	2.3	1.3	.57
$C_2H_4(CN)_2$	3.45	4.6	3.8	.83

[1] Ebert, Leipziger Vortrage (1929), p. 44; Wagner, Zeits. f. physik. Chemie **14B**, 166 (1931); Eyring, J. Am. Chem. Soc. **54**, 3191 (1932); Eucken and Weigert, Zeits. f. physik. Chemie **23B**, 265 (1933); Bartholomé and Karweil, Naturwiss. **25**, 172 (1937); however, cf. Kemp and Pitzer, J. Chem. Phys. **4**, 749 (1936) and Howard, Phys. Rev. **51**, 53 (1937).

[2] White and Morgan, J. Am. Chem. Soc. **57**, 2078 (1935).

[3] Smyth, J. Am. Chem. Soc. **46**, 2151 (1924); L. Meyer, Zeits. f. physik. Chemie **8B**, 27 (1930); Smyth, Dornte and Wilson, J. Am. Chem. Soc. **53**, 4242 (1931); Zahn, Phys. Rev. **38**, 521 (1931); Phys. Rev. **40**, 291 (1932); Greene and Williams, Phys. Rev. **42**, 119 (1932); Smyth and Kamerling, J. Am. Chem. Soc. **53**, 2988 (1932); Lennard-Jones and Pike, Trans. Faraday Soc. **30**, 830 (1934).

[4] Williams, Zeits. f. physik. Chemie **138A**, 75 (1928).

column of the table. Such values should be valid for purposes of comparison. It is obvious that the agreement between observation and calculation is best in ethylene cyanide (succinonitrile), and that it would only be improved by allowing in the calculation for distortion of the carbon valence angles due to dipole repulsion. It may fairly be concluded that of these molecules ethylene cyanide possesses much the greatest freedom of internal rotational motion. This conclusion is not significantly affected by the fact that the absence of measurements of the effect of temperature on this dipole leaves doubt as to whether the *trans* or the *cis* configuration of the molecule is the more stable. Weissberger[5] has suggested that if the quantum-mechanical exchange interaction were sufficiently large in such a compound, the potential energy of the *cis* form would be less than that of the *trans*.

The situation is more complicated in ethylene diamine because the molecule has three possible degrees of internal rotational freedom. Zahn's[6] measurement of the dipole moment yielded him no definite information as to the degree of internal motion about the C−C bond, although he believed the polar NH_2 groups to be freely rotating.

Regarding the persistence of intramolecular rotation in the crystal, Mizushima[7] and his collaborators interpret their Raman spectra data for ethylene chloride and bromide to mean that these molecules are almost all in the *trans* configuration in the solid, although both the *cis* and the *trans* states are found in the liquid. X-ray measurements made by Klug[8] have definitely located the iodine atoms in the crystal of ethylene iodide, showing that there is little internal motion of this molecule in the crystal at room temperature. According to the hypothesis, then, none of these halides should be unusually likely to show end-over-end rotation of the unit molecule in the solid state.

No evidence has been found, as far as we know, regarding the internal motion of the ethylene cyanide, ethylene diamine, or ethylene thiocyanate molecules when they are in the crystal. The dielectric properties of these crystals were measured with the hope that they might supply information on this point. Measurement of the halides was expected to confirm the results of the Raman measurements.

Purification of Materials

Ethylene chloride

Material from Eastman Kodak Company was dried for several days over anhydrous calcium sulfate and twice fractionally distilled; b. p. 83.8±0.05°.

Ethylene bromide

Eastman's product was dried over anhydrous calcium sulfate for several weeks and fractionally distilled; b. p. 131.6±0.05°.

Ethylene cyanide

Two samples were obtained from Eastman Kodak Company. That used in the dielectric measurements was twice fractionally crystallized from acetone, employing a narrow temperature range. After removing the acetone by evacuation the m. p. was 54.2°. The material used for the thermal measurement was found to melt at 54.2 as received, and was not further purified.

Ethylene diamine

Material from Eastman was thrice distilled from sodium. The second and third middle fractions boiled at the same temperature, 116.7°, after correction of the thermometer used by comparison with one calibrated by the National Bureau of Standards. The density of the best fraction was found to be 0.8970 g/cm at 19.9°. Although the above b. p. is 0.5° higher than the latest reported in the literature, this density agrees well with that reported by the same author,[9] 0.8978 g/cm at 20.0°. Since density is much more sensitive than b. p. to the presence of the hydrated compound, it is concluded that the latter was absent in the material as purified.

Ethylene thiocyanate

The Eastman product was twice fractionally crystallized from absolute alcohol; m. p. 89.8°.

[5] Weissberger, Trans. Faraday Soc. **30**, 852 (1934).
[6] Zahn, Physik. Zeits. **33**, 525 (1932).
[7] Mizushima, Morino and Noziri, Nature **137**, 945 (1936).
[8] Klug, Zeits. f. Krist. **90**, 495 (1935).
[9] Wilson, Ind. and Eng. Chem. **27**, 867 (1935).

Experimental Method and Results

Cooling and heating curves were run on the ethylene chloride, bromide, and cyanide by well-known methods. The calibration of Southard and Andrews[10] was used for converting the observed potential E_o of the copper-constantan thermocouples to temperature, after correcting with the equation

$$E = 1.0056E_o + 0.005 \text{ millivolts.}$$

The condensers used for dielectric measurement are illustrated in Fig. 1 and Fig. 2. They are designed for use in glass containers so that phase changes in the dielectric may be visually observed. The design of Fig. 1 is for grounded capacity measurements, and was used for all liquids and those solids which melt below room temperature. The outside plates are grounded, and are separated from the central electrode by clear fused quartz washers and bushings. The error due to edge effect was minimized by calibration of the condenser with benzene. In solids a more important source of error is the formation of voids upon solidifying or cooling. With ethylene cyanide and thiocyanate it was possible to reduce this error by using the condenser of Fig. 2

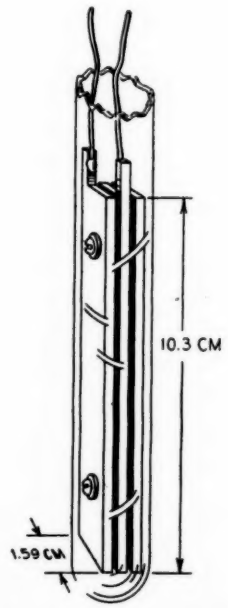

Fig. 1. Condenser for measurement of liquids.

[10] Southard and Andrews, J. Frank. Inst. **207**, 323 (1929).

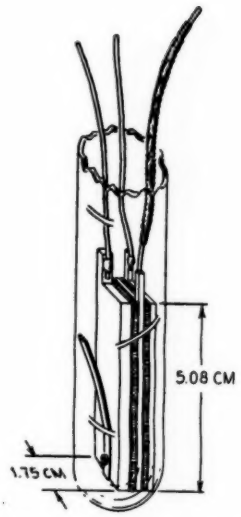

Fig. 2. Condenser for measurement of solid sheets.

for measurement of pressed sheets of the material. The capacity of the leads was eliminated by making direct capacity measurements and using a shielded lead to the high potential electrode. The correction for the edge effect was calculated. Homogeneous sheets of ethylene cyanide about 1.0 mm thick were obtained by pressing the waxy material under 2500 pounds ram pressure in a 5.08×1.75 cm mold. Gold plated brass electrodes 0.8 mm thick were pressed on each side of the sheet to facilitate its separation from the plungers of the press and to insure good electrical contact upon measurement. These added electrodes are not shown in Fig. 2, which illustrates the manner in which a steel spring holds the condenser together. Some air was entrapped in the sheets of ethylene thiocyanate, which was much harder than the cyanide and not so readily formed even at 20,000 pounds ram pressure. The low temperature form of the cyanide could also be seen to be inhomogeneous, due probably to the development of cracks associated with a sharp density change at the transition. In such cases the error in the measurement of dielectric constant is difficult to estimate, but the observed values may be safely said to be too low. Even in the most favorable circumstances the observed results are probably low, and no accuracy greater than 5 percent can be claimed for the measurement of solids. The values of conductivity, recorded in

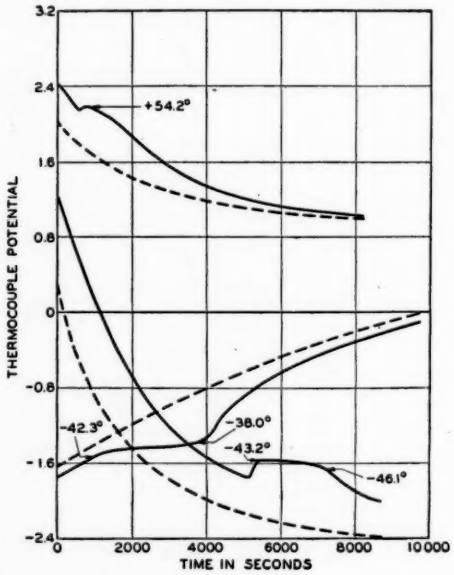

FIG. 3. Cooling and heating curves for ethylene cyanide; broken lines represent bath temperatures.

ohm^{-1} cm^{-1}, are of assistance in interpreting the behavior of dielectric constant, but are not to be taken as physical constants of the compounds in question.

The equipment used for measurement of the capacity, conductance and temperature and for control of the temperature was essentially that previously described.[11]

Figures 3 and 4 show the cooling and heating curves for ethylene cyanide and bromide; bath temperatures are represented by broken lines. Both heating and cooling curves display well-defined arrests in the solid state below the m. p., indicative of thermal transitions which have not previously been reported. The data do not supply quantitative heats of fusion and transition, but they clearly indicate that in the ethylene cyanide the heat of transition is very much larger than the heat of fusion, while the converse is true in ethylene bromide. The same sample of ethylene cyanide was used for the two cooling curves; the experiment was divided into two parts because of the wide temperature range involved.

The upper curve of Fig. 3 shows a very short arrest at 54.2° for the freezing of the cyanide, with a freezing range extending at least to 52.0°. According to the van't Hoff law, however, a relatively small amount of impurity is capable of producing this effect where the heat of fusion is so low. The cooling curve shows supercooling of about 6° before the transition at −43.2° sets in. Even after starting, the transition is not very sharp in this sample; its range extends to about −46.1°. Upon heating, the same transition begins at −42.3° and appears to progress most rapidly at about −40°. On the whole, the evidence favors the existence of a temperature hysteresis at the transition, although the absence of stirring makes this conclusion uncertain.

Figure 4 shows that freezing in ethylene bromide continues for about two degrees below the initial freezing point. The transition is found at about −24°. Here again there is some evidence of temperature hysteresis of the transition, which is observed at −24.6° with cooling and −23.0° with heating.

The heating curve for ethylene chloride, which is not shown, reveals no transition between −95° and its m. p.

The dielectric properties of ethylene cyanide are recorded in Fig. 5 and Table II. Above room temperature the specific conductivity Γ is high because of ionization.[12] Electrode polarization capacity therefore increases the apparent value of dielectric constant at low frequencies. This effect was eliminated by extrapolating the dielectric constant ϵ to high frequencies.[13] The resulting values of the true dielectric constant are given in Table II in the column headed ϵ_t and in Fig. 5 by filled circles. The only other value of the

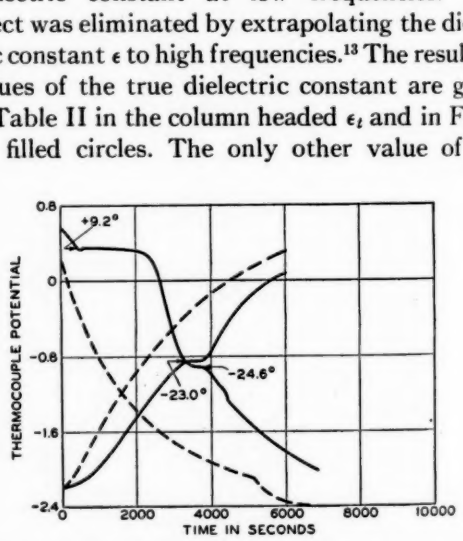

FIG. 4. Cooling and heating curves for ethylene bromide; broken lines represent bath temperatures.

[11] Morgan and Lowry, J. Phys. Chem. **34**, 2385 (1930).

[12] Walden, Zeits. f. physik. Chemie **54**, 128 (1906).

[13] Vd., e.g., Yager and Morgan, J. Phys. Chem. **35**, 2039 (1931).

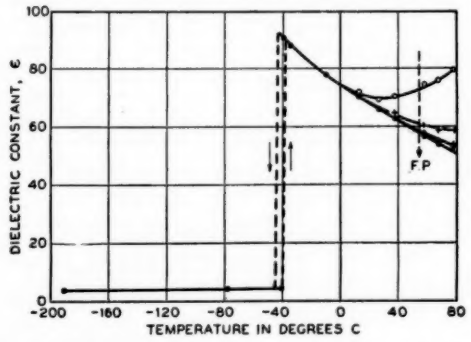

FIG. 5. Dielectric constant of ethylene cyanide; circles, 10 kc; crosses, 30 kc; triangles, 100 kc; dots, corrected for electrode polarization capacity.

dielectric constant of the solid recorded in the literature, 66.6 at 23°,[14] falls almost exactly on the curve of Fig. 5. The two values reported for the liquid, 61.2 at 60° [14] and 57.3 at 58° [15] are both higher than our value of 56.5 at 57.4°.

Figure 5 shows no significant discontinuity of dielectric constant at the freezing point. In the crystal ϵ rises rapidly with declining temperature, in a manner characteristic of polar liquids, down to the transition temperature, where its value drops abruptly to about 4.4. This figure is likely to be too low, as indicated by the less homogeneous appearance of the dielectric below the transition, which is taken to be evidence of the appearance of voids.

The temperature of the dielectric transition was determined by using a condenser of the type of Fig. 1, in which good thermal contact is obtained. The actual values of dielectric constant thus observed are not recorded, being too low,

[14] Schlundt, J. Phys. Chem. **5**, 503 (1901).
[15] Walden, Zeits. f. physik. Chemie **46**, 103 (1903).

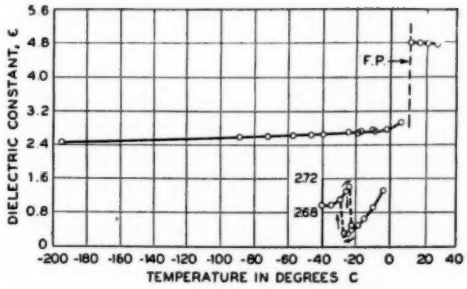

FIG. 6. Dielectric constant of ethylene bromide at 100 kc; large scale inset shows behavior at transition temperature.

but the break in the curve was found to occur between −42.6° and −44.9°, as determined through a declining sequence of constant temperatures. Reversing the temperature sequence, the rise of dielectric constant had just started at −40.4° and was complete at −38.0°. These temperature ranges agree well with those observed thermally, and tend to confirm the reality of the temperature hysteresis of the transition, since a different sample was used and much better thermal equilibrium was possible than in the thermal measurements.

The dielectric constant of ethylene bromide breaks sharply at the freezing point, as may be seen in Fig. 6 and Table III. Some premelting probably affects the values observed at about 5°. When the first two runs were made on this material, no evidence of a transition was noticed. After the thermal transition was observed, more careful measurements (run No. 3) in the indicated temperature range revealed an extremely small but quite definite break in the curve, as shown in the large-scale inset of Fig. 6. The only

TABLE II. *Dielectric properties of ethylene cyanide.*

	1 KC		3 KC		10 KC		30 KC		100 KC		
t°C	ϵ	Γ	ϵ	Γ	ϵ	Γ	ϵ	Γ	ϵ	Γ	ϵ_i
78.2 Liquid	600	1.7×10^{-5}	170	1.7×10^{-5}	79.2	1.7×10^{-5}	58.4	1.7×10^{-5}	53.5	1.7×10^{-5}	52.3
67.7	521	1.4	157	1.4	75.5	1.4	58.2	1.4	54.5	1.4	53.6
57.4	440	1.2	143	1.2	74.5	1.2	59.9	1.2	57.4	1.2	56.5
36.7 Solid	113.5	1.3×10^{-6}	73.1	1.3×10^{-6}	69.1	1.3×10^{-6}	64.4	1.3×10^{-6}	63.2	1.4×10^{-6}	62.6
25.7	101.3	1.0	74.3	1.0	69.0	1.0	66.9	1.0	65.9	1.1	65.5
12.8	88.3	6.9×10^{-7}	74.9	6.9×10^{-7}	71.8	6.9×10^{-7}	70.4	7.0×10^{-7}	69.8	7.0×10^{-7}	69.6
−10.0							77.4	2.1	77.3	2.2	77.3
−34.7							87.7	2.2×10^{-8}	87.7	3.2×10^{-8}	87.7
−40.7	$4.41<3.4\times10^{-11}$								4.41	$<3.4\times10^{-11}$	4.41
−76.8	$4.24<3.4$								4.24	<3.4	4.24
−190	$3.90<3.4$								3.90	1.6×10^{-10}	3.90

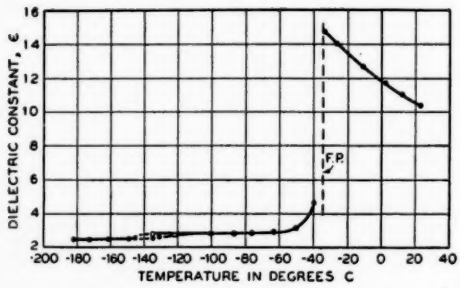

FIG. 7. Dielectric constant of ethylene chloride; circles, 10 kc; dots, 100 kc.

accuracy claimed for the fourth significant figure in these results is that relative to temperature variation in this particular sample. Virtual dielectric constant rises below this transition. With heating, the break occurs between $-24.0°$ and $-22.0°$, in agreement with the thermal results; with cooling, it falls between $-26.6°$ and $-29.0°$, fully two degrees below the thermal arrest. The dielectric data confirm the existence but not the magnitude of the temperature hysteresis. A plot of the data of runs No. 1 and No. 2 on a very large scale gives results consistent with the existence of the transition between $-20°$ and $-30°$, but in both cases shows a drop of about 0.04 units in dielectric constant in place of the rise of similar magnitude observed in run No. 3. The results are those to be expected at a transition involving a small change of density and homogeneity of the sample but no change of molar polarization.

TABLE III. *Dielectric properties of ethylene bromide.*

		1 KC		10 KC		100 KC	
$t°C$		ϵ	Γ	ϵ	Γ	ϵ	Γ
Run No. 1:							
25.9	Liquid	4.79	1.7×10^{-9}			4.74	2.0×10^{-9}
20.5		4.80	1.5	4.77	1.6×10^{-9}	4.77	1.7
15.3		4.82	7.9×10^{-10}	4.80	1.4	4.79	1.5
10.5		4.84	11	4.82	1.2	4.81	1.3
5.9	Solid	3.03	1.9	2.95	2.5×10^{-10}	2.94	5.4×10^{-10}
−0.2		2.85	1.1	2.80	1.6	2.78	
−9.3		2.79	6.7×10^{-11}	2.75	1.2	2.74	4.3
−19.3		2.76	5.1	2.73	1.0	2.72	3.8
−31.6		2.69	3.1	2.68	7.0×10^{-11}	2.67	4.3
−195.8		2.46	1.9			2.45	$<3.\times10^{-11}$
Run No. 2:							
5.0		3.07	1.4×10^{-10}	3.02	2.0×10^{-10}	3.01	6.5×10^{-10}
−2.6		2.86	7.2×10^{-11}	2.82	1.4	2.80	6.0
−10.7		2.81	5.3	2.78	1.1	2.76	5.1
−25.0		2.76	3.4	2.73	8.7×10^{-11}	2.73	4.3
−32.4		2.71	2.5	2.69	6.5	2.68	4.3
−39.5		2.70	1.9	2.68	6.5	2.67	4.6
−46.6		2.69	1.5	2.67	5.4	2.67	4.6
−57.6		2.66	1.1	2.64	5.4	2.64	3.2
−72.6		2.63	7.3×10^{-12}	2.62	4.6	2.62	2.7
−94.4		2.62	5.4	2.60	3.8	2.59	2.7
Run No. 3:							
Falling temperature:							
−4.0		2.850	1.02×10^{-10}	2.745	2.9×10^{-10}	2.710	6.4
−10.0		2.808	8.7×10^{-11}	2.712	2.4	2.688	6.6
−15.0		2.778	7.6	2.694	2.0	2.674	4.4
−22.7		2.727	5.7	2.670	1.3	2.661	2.0
−24.1		2.718	5.2	2.667	1.1	2.656	2.6
−26.6		2.712	4.7	2.664	1.0	2.656	2.3
−29.0		2.736	4.0	2.703	7.7×10^{-11}	2.697	2.1
−34.3		2.718	2.8	2.694	4.8	2.691	1.3
−39.8		2.706	2.0	2.697	3.5	2.691	1.2
Rising temperature:							
−26.0		2.736	3.7	2.712	6.7	2.706	1.1
−24.0		2.742	4.2	2.715	6.9	2.712	1.9
−22.0		2.709	3.9	2.685	8.0	2.670	1.1
−18.4		2.703	5.4	2.682	10.	2.670	2.1

TABLE IV. *Dielectric properties of ethylene chloride.*

		1 KC		10 KC		100 KC	
t°C		ϵ	Γ	ϵ	Γ	ϵ	Γ
22.2	Liquid	10.45	1.5×10^{-9}	10.43	1.5×10^{-9}	10.39	1.6×10^{-9}
11.4		11.07	2.0			11.02	2.0
+1.3		11.73	2.0			11.69	2.0
−12.0		12.71	1.7			12.67	1.7
−27.2		14.01	1.4			13.98	1.4
−34.7		14.72	1.3			14.68	1.3
−40.0	Solid	4.82	1.0	4.66	1.1	4.65	1.1
−50.1		3.48	1.1	3.14	1.3	3.13	1.3
−63.1		3.29	1.1	2.94	1.3	2.93	1.4
−76.1		3.12	7.5×10^{-10}	2.87	9.2×10^{-10}	2.86	9.2×10^{-10}
−86.6		3.01	5.5	2.84	6.4	2.84	6.6
−100		2.80	1.2	2.77	1.5	2.75	5.2
−109		2.77	4.0×10^{-11}	2.76	6.9×10^{-11}	2.75	4.6
−119						2.74	7.5
−122		2.75	6.3×10^{-12}	2.75	3.5×10^{-10}	2.70	8.9
−131						2.66	4.9×10^{-9}
−135		2.75	7.8	2.75	3.2	2.54	3.4
−149		2.50	1.1	2.48	5.8×10^{-11}	2.46	4.0×10^{-10}
−161		2.48	3.5	2.47	2.6	2.47	2.3
−172		2.47	2	2.47	1.7	2.46	2.3
−182		2.45	4			2.45	3.5

TABLE V. *Dielectric properties of ethylene diamine.*

	1 KC		3 KC		10 KC		30 KC		100 KC	
t°C	ϵ	Γ	ϵ	Γ	ϵ	Γ	ϵ	Γ	ϵ	Γ
26.5 Liquid	146	1.12×10^{-5}			18.8	1.12×10^{-5}	13.6	1.12×10^{-5}	13.5	1.12×10^{-5}
17.4	117	1.00			16.3	1.00	14.5	1.00	14.5	1.00
9.7	81.9	7.4×10^{-6}			16.3	7.4×10^{-6}	15.4	7.4×10^{-6}	15.2	7.4×10^{-6}
6.7 Solid	16.9	5.5×10^{-7}	9.57	5.6×10^{-7}	7.93	5.6×10^{-7}	7.05	5.8×10^{-7}	5.88	6.4×10^{-7}
1.7	9.83	1.5	7.90	1.5	6.77	1.6	5.93	2.1	5.13	3.3
−8.1	8.03	5×10^{-8}	6.75	5.5×10^{-8}	5.64	6.0×10^{-8}	4.76	6.9×10^{-8}	3.98	9.8×10^{-8}
−26.4	5.46	2.9×10^{-9}	4.61	4.1×10^{-9}	3.92	6.9×10^{-9}	3.45	1.2	3.11	2.4×10^{-8}
−46.0	3.53	4.4×10^{-10}	3.17	8.1×10^{-10}	2.93	1.6	2.81	2.7×10^{-9}	2.73	4.9×10^{-9}
−78.5	2.63	2.1×10^{-11}	2.60	3.7×10^{-11}	2.60	7.2×10^{-11}	2.60	1.4×10^{-10}	2.60	3.2×10^{-10}

TABLE VI. *Dielectric properties of ethylene thiocyanate.*

	1 KC		10 KC		100 KC	
t°C	ϵ	Γ	ϵ	Γ	ϵ	Γ
84.6	21.8	6.6×10^{-8}	8.61	8.8×10^{-8}	5.05	1.4×10^{-7}
68.9	3.73	3.5×10^{-10}	3.41	8.7	3.32	2.3
47.9	3.36	2.7×10^{-11}	3.31	1.3	3.29	1.1
24.8	3.41	9.3	3.38	1.4	3.33	1.7
0	3.36	9.0×10^{-12}	3.34	1.3	3.30	1.2×10^{-9}
−78.5	3.23	1.7×10^{-11}	3.18	1.2×10^{-10}	3.17	5.6×10^{-10}
−195.8	3.10	7×10^{-13}	3.09	$<3\times10^{-12}$	3.10	7×10^{-11}

The observed dielectric constant of the liquid at 18° is 1.6 percent lower than that recorded in the I. C. T. Near −30° our values are about 10 percent below those obtained at low frequency by Fleming and Dewar,[16] who have not recorded the m. p. or b. p. of their material.

[16] Fleming and Dewar, Proc. Roy. Soc. (London) **61**, 316 (1897).

The behavior of ethylene chloride at the freezing point is similar to that of the bromide, as shown in Fig. 7 and Table IV. Below −86.6° the data were obtained by embedding the tube containing the condenser in aluminum granules in a Dewar flask, cooling with liquid nitrogen, and afterwards making measurements as the system drifted to higher temperatures. There is

a region of anomalous dispersion between −150° and −120° in the 1–100 kc band, as shown by the maxima of conductivity in this temperature range and the successive increases of dielectric constant for the various frequencies from about 2.47 to about 2.75. There is no dielectric evidence of a transition of any magnitude in the solid state.

In the liquid state the observed values of dielectric constant differ from those of Smyth, Dornte and Wilson[3] by an average of less than 1 percent. No data for the solid have been found in the literature.

The real dielectric constant of ethylene diamine drops sharply at the freezing point. In Table V the variation of ϵ and Γ with temperature and frequency above −60° is characteristic of electrolytic polarization capacity, as might be expected from the electrolytic action of the compound in solution.[17] This behavior may mask any small discontinuity of true dielectric constant, but the results are essentially normal for an organic crystal of high ionic conductivity. Measurement below −80° was abandoned when the sample exploded upon being cooled to liquid nitrogen temperature.[18]

The observed dielectric constant of the liquid is about 10 percent lower than that reported by Mathews, whose sample boiled in the range 118–121°.[19] In this case, where great care is required to prevent contamination of the sample with water, it is likely that the lower value is the better.

In Table VI the dielectric constant of ethylene thiocyanate is shown to be almost independent of temperature between −195.8° and +68.9°, indicating that there are no dielectrically observable transitions in this region. At 84.6° visually evident decomposition and the tremendous increase of conductivity indicate that even at 100 kc the observed value of dielectric constant includes the spurious effects of electrolytic polarization capacity.

Discussion of Results

The continuity of dielectric constant through the freezing point of ethylene cyanide is evidence that: (1) its polar molecules rotate in the solid state to much the same extent as in the liquid; (2) the dipole moment of the molecule is unchanged upon solidification; and (3) the dielectric constant of the single crystal is isotropic. Conclusion (3) may indeed be inferred from (1), since it is very likely that rotation of the individual molecule in the liquid and hence in the solid occurs about the three Cartesian axes. Directly, however, anisotropy of dielectric constant in the single crystal would be almost certain to produce a discontinuity of measured dielectric constant of the mass of randomly oriented crystals at the melting point.

The thermal data show the heat of fusion of ethylene cyanide to be less than its heat of transition. The value of the former found in the *International Critical Tables*, 940 calories per mole, is also much less than that of similar compounds in whose crystals there is no evidence of molecular rotation, as for example ethylene diamine, whose heat of fusion at 0°C is 4600 cal./mole.[9] Such thermal behavior is to be expected of crystals whose molecules are rotating, according to Clusius,[20] who suggested that when this rotation sets in at a transition, the entropy of melting is less than would otherwise be expected by approximately the amount of the entropy of transition. Similarly low heats of fusion[21] have been observed in those cyclohexane and camphor derivatives which have been found by dielectric measurement[2, 22] to rotate below the melting point. Thus the thermal evidence is consistent with the view that ethylene cyanide molecules rotate in the crystal above the transition temperature.

Smyth, Dornte and Wilson[3] have found that when the polarization of ethylene chloride in heptane solution is measured through the concentration range, it fails to decline with increasing concentration as would be expected in view of the usual effects of molecular association and of the limitations of the Clausius-Mosotti equation.[23] They regard this as evidence of increased

[17] Bredig, Zeits. f. physik. Chemie **13**, 289 (1894).

[18] It has been suggested that this was due to the liquefaction of oxygen from the air in the tube on cooling to −195°.

[19] Mathews, J. Phys. Chem. **9**, 641 (1905).

[20] Clusius, Zeits. f. Elektrochem. **39**, 598 (1933).

[21] Kelley, J. Am. Chem. Soc. **51**, 1400 (1929); Parks and Huffman, ibid. **52**, 4381 (1930); Pirsch, Ber. **68**, 67 (1935).

[22] Yager and Morgan, J. Am. Chem. Soc. **57**, 2071 (1935).

[23] Wyman, J. Am. Chem. Soc. **56**, 536 (1934); v. Arkel and Snoek, Trans. Faraday Soc. **160**, 707 (1934); Kumler, J. Am. Chem. Soc. **57**, 100 (1935).

molecular dipole moment due to reduced interaction of the two internal dipoles of the molecule in the more concentrated solutions. Any factor which directly reduces the electrostatic interaction between the charges within such a molecule should similarly reduce the energy of quantum-mechanical exchange interaction, since the former is the perturbation in the wave equation out of which the latter arises. Hence it may be inferred that the freedom of internal rotational motion of the molecule of ethylene cyanide should similarly increase in concentrated solution, regardless of the relative importance of repulsive and attractive forces in determining its configuration. In the absence of evidence to the contrary, these cyanide molecules may therefore be expected to have more internal freedom of motion in the pure liquid than in benzene solution.

Any significant change in the freedom of internal motion about the central C−C bond in the ethylene cyanide molecule at the freezing point would be reflected by a change in its effective dipole moment. The evidence practically excludes this possibility. Hence it is fully as probable in the crystal as in the liquid that the rotating ethylene cyanide molecules are characterized by a very considerable internal rotational motion.

The dielectric constant of 4.4 or more which is found immediatey below the transition in ethylene cyanide is in itself an unusually high value for an organic solid. Assuming that at −40.7° the density is no more than 1.15, about 12 percent greater than that at +45°,[24] the molar polarization at the former temperature is found to be at least 37 cc. The molar refraction or electronic polarization found by extrapolating the refraction values of Landolt-Bornstein to low frequencies is only 20.0 cc, equivalent to a dielectric constant of 2.22. It is almost impossible to account for the remaining polarization of 17 cc on the basis of a residual molecular rotation below the transition temperature, for this quantity is still quite large at liquid air temperature, where the dielectric constant is at least 3.9. The conductivity at this temperature and 100 kc is so low as to indicate that the natural frequency of any remaining rotational polarization is greater than 10^7 c.p.s.; otherwise the dielectric loss always observed when the measuring frequency is within two decades of the natural frequency of rotation would appear. At −190° it is very unlikely that any untransformed fraction of the ethylene cyanide crystal would contain molecules rotating 10^7 c.p.s., when it is remembered that in organic crystals such as cyclohexanol, for example, the natural frequency of rotational motion may be inferred from the anomalous dispersion to be about 10^5 c.p.s. at −50°C.[2] Since accepted methods of accounting for this polarization in terms of molecular or electronic motion fail, it is reasonable to conclude that it is associated with the motions of the atomic nuclei within the molecule. It may then be said that the atomic polarization of ethylene cyanide at −40.7° is at least 17 cc, an unusually high value.

Accepting Mizushima's conclusion[7] that ethylene bromide is in a nearly pure *trans* state below the freezing point, the sharp drop of dielectric constant at that point does not exclude the possibility of rotation of the nonpolar form of the molecule in the crystal. It seems likely that the thermal transition at −24° marks the rise of molecular rotation of a nonpolar kind, since the absence of dielectric effects excludes the alternate possibility that rotation of the polar $-CH_2Br$ groups within the molecule sets in at this temperature. The Raman data also show that regardless of the rotational motion of the unit molecule within the crystal, the internal motion of one end with respect to the other is greatly restricted upon solidification. This must be explained in terms of crystal forces. Such a specific effect of these forces in fixing the shape of the molecule would not be expected if it were rotating about three axes, particularly when the *trans* configuration thus fixed is the longest and hence the least favorable, geometrically, for end-over-end rotation. Experimental evidence against the onset of three-dimensional molecular rotation at −24° is furnished by the small value of the heat of transition, which may be roughly estimated from Fig. 4 to be only about one-fourth as large as the heat of fusion. The entropies of transition and fusion must be in substantially the same ratio. Table VII compares the corre-

[24] *Handbook of Chemistry and Physics* (Chemical Rubber Publishing Co., 1936), p. 750.

sponding ratio for a number of organic compounds for which the dielectric or structural evidence supplies definite information as to the number of degrees of rotational freedom above the transition temperature. The magnitude of the ethylene bromide transition favors its classification with those of the paraffin derivatives, which rotate about only one axis. It is therefore believed that if the transition in ethylene bromide at $-24°$ is due to molecular rotation, that rotation must be about only one axis. Obviously, the most likely axis for such a rotation of the *trans* form of this molecule is that of the zigzag Br−C−C−Br chain. Rotation about this long axis is consistent with the sudden restriction of intramolecular motion in favor of the *trans* form at the freezing point, since this form requires a much smaller volume for such a rotation than does the *cis*.

The dielectric constant of solid ethylene bromide is 2.80 at $-2.6°$, a value sufficiently low to indicate that the atomic polarization is not unusually large. Assuming a reasonable minimum of 2.3 for the density at this temperature, the corresponding maximum for the total polarization is 30.6 cc. Extrapolation of the molar refraction as recorded in Landolt-Börnstein yields an electronic polarization of 26.3 cc. Hence the atomic polarization is probably less than 4 cc.

In ethylene chloride the absence of any thermal transition above $-95°$ indicates that there is no significant molecular rotation about any axis in the crystal, except for the rather remote possibility that a transition occurs below $-95°$. The sharp drop of dielectric constant at the freezing point to a relatively low value tends to confirm Mizushima's conclusion that there is little rotational vibration within the molecule in the crystal. However, a small polarization remains even at $-100°$, and disappears with anomalous dispersion below this temperature. The source of this effect is not known. Below $-150°$ the dielectric constant of 2.46 shows at most only a small atomic polarization.

There is then strong evidence that in the ethylene cyanide crystal above $-40°$ a remarkably free molecular rotation is associated with relatively free rotational motion of atomic groups within the molecule, while in the crystalline ethylene chloride the absence of molecular rotation is associated with a corresponding lack of group rotation. If there is any molecular rotation in the ethylene bromide crystal above $-24°$, it is probably restricted to that about the long axis of the *trans* form of the molecule; here again, the absence of extensive group rotation within the molecule below the freezing point is quite definite. Now such factors as strength of dipole moment and length of the carbon chain would ordinarily be expected to make the ethylene chloride and bromide molecules more likely than ethylene cyanide to rotate end for end in the crystal. It is therefore believed that the greater freedom of internal motion in the latter molecule is the factor which makes possible a molecular rotation which would not otherwise occur below the freezing point. The presumed effect of the internal motion may be described by saying that it increases the time-average symmetry of the molecule, thus reducing the variability of its interaction with its neighbors as a function of the angle of molecular orientation. This reduces the magnitude of the potential energy hump which according to Pauling's theory[25] restrains the rotation of a molecule in the crystal.

In view of the irregular behavior of the atomic polarization of cyanides,[26] the large value of P_A observed below the transition in ethylene cyanide seems most easily accounted for on the assumption that the unusually free rotational vibration

TABLE VII.

	Entropy of Transition	Entropy of Fusion	S_T/S_F
Rotation about three axes:			
Methane[a]	0.95	2.47	0.39
Carbon tetrachloride[b]	4.80	2.30	2.09
Cyclohexanol[c]	7.44	1.37	5.43
d-Camphor	7.65[2]	3.61[d]	2.12
Rotation about one axis:			
n-$C_8H_{17}COOH$[e]	5.0	17.0	0.29
n-$C_{10}H_{21}COOH$[e]	6.4	19.8	0.32
n-$C_{22}H_{46}$[f]	22.0	37.0	0.59
n-$C_{26}H_{54}$[f]	25.9	42.7	0.61
n-$C_{30}H_{62}$[f]	26.2	48.7	0.54
n-$C_{34}H_{70}$[f]	33.7	55.4	0.61

[a] Clusius, Zeits. f. physik. Chemie **B3**, 41 (1929).
[b] Johnston and Long, J. Am. Chem. Soc. **56**, 31 (1934).
[c] Kelley, J. Am. Chem. Soc. **51**, 1400 (1929).
[d] Framdsen, Nat. Bur. Stand. J. Research **7**, 477 (1931). This figure was obtained for dl-camphor, but probably represents d-camphor with sufficient accuracy for the purpose.
[e] Garner and Randall, J. Chem. Soc. **125**, 881 (1924).
[f] Garner, Van Ribber and King, J. Chem. Soc. 1533 (1931).

[25] Pauling, Phys. Rev. **36**, 430 (1930).
[26] Sugden, Trans. Faraday Soc. **30**, 734 (1934).

of the polar $-CH_2CN$ groups within the molecule persists to a certain degree below the transition temperature. The natural frequency of such a polarization should be high and relatively unaffected by temperature. It is not certain that the decline of dielectric constant from 4.4 at $-40.7°$ to 3.9 at $-190°$ is real, because of the possibility of increased void formation. If it is real, the objection might be raised that an atomic polarization should not vary with temperature. However, there is in the classical theory no reason for expecting a polarization due to vibration to be independent of temperature unless the oscillation in question is simple harmonic. Hooke's law is usually assumed to apply only to small displacements in molecular systems. By hypothesis the vibration in question involves unusually large displacements. It is pertinent that there is no indication of a large atomic polarization in the ethylene chloride and bromide, in which molecules there is independent evidence that the torsional vibration is more restricted in both the solid and liquid states.

The proposed explanation of the dielectric properties of these disubstituted ethanes could be checked by a number of experiments. Raman spectra should reveal any internal rotational motion within the ethylene cyanide molecule in the liquid and the two solid phases. Measurement of the variation of dipole moment with temperature should show whether the *cis* or the *trans* configuration is the more stable. The symmetry of the ethylene cyanide crystal should be greater above the transition, with cubic or hexagonal structures most probable.[27] If the ethylene bromide molecule is rotating about one axis above the transition, X-ray measurements should show anisotropic thermal expansion similar to that found in the paraffins.[28]

[27] Vd., e.g., Smyth, Proc. Am. Phil. Soc. **76**, 485 (1936).
[28] A. Müller, Proc. Roy. Soc. **127A**, 417 (1930).

There is little independent evidence regarding the internal motion of the ethylene diamine and thiocyanate molecules. It is certain from the dielectric data that neither case resembles ethylene cyanide. There is no great amount of atomic polarization at or below $-46°$ in the ethylene diamine, nor does the polar form of the molecule rotate end-over-end below the melting point. Ethylene thiocyanate also shows no evidence of molecular rotation in the crystal. The observed dielectric constant, 3.33 at room temperature, is somewhat high for an organic solid and may indicate that the atomic polarization is large for the same reason as in the ethylene cyanide. The inability of so long a molecule to rotate end-over-end in the crystal is not surprising, even granting a considerable increase in symmetry due to inner rotation about the central C–C bond.

If the proposed explanation of molecular rotation in ethylene cyanide is correct, it would be expected that this rotation should be found in other ethane derivatives. A transition has been found at 71.1° in hexachloroethane which we believe marks the rise of molecular rotation in that crystal, although dielectric measurement should yield no information, because the molecule is nonpolar. Parijs[29] found the entropy of this transition, 7.26 E.U., to be greater than the entropy of fusion at the same temperature, 5.84 E.U. Wiebenga[30] found the crystal to change from the triclinic to the cubic form at this temperature. In both cases the behavior is typical of a rotational transition.[31]

[29] Parijs, Zeits. f. anorg. allgem. Chemie **226**, 425 (1936).
[30] Wiebenga, Zeits. f. anorg. allgem. Chemie **225**, 38 (1935).
[31] While this paper was in press, it was found that the dielectric constant of solid *sym*-tetramethyl ethylene dichloride (m.p. 159–160°) rises from 2.5 at $-80°C$ to 4.5 at $+5°C$, then falls gradually to 4.3 at $+60°C$. This behavior suggests molecular rotation at the higher temperatures.

LETTERS TO THE EDITOR

This section will accept reports of new work, provided these are terse and contain few figures, and especially few halftone cuts. The Editorial Board will not hold itself responsible for opinions expressed by the correspondents. Contributions to this section must reach the office of the Managing Editor not later than the 15th of the month preceding that of the issue in which the letter is to appear. No proof will be sent to the authors. The usual publication charge ($3.00 per page) will not be made and no reprints will be furnished free.

The Rotation of Some Long Molecules in the Solid State

In order to investigate the possible rotation of long molecules in crystals dielectric constant measurements have been made upon carefully purified substances with long-chain molecules in the solid and liquid states, the apparatus used being that employed in previous work.[1]

The dielectric constant of ethyl undecylate drops sharply on solidification, after which it decreases slowly and uniformly with falling temperature in the manner commonly shown by polar substances in which some of the molecules may have some slight freedom of bending or rotation without the existence of any general rotational freedom.

Ethyl palmitate, which undergoes a monotropic transition from an α- to a β-form immediately upon solidification at 19.6°, shows a sharp rise in dielectric constant as solidification occurs followed within 0.5° of the freezing point by a drop twice as great. The further slow but uniform decrease of dielectric constant with falling temperature is interrupted by a slight but reproducible hump in the curve at 14.6°. The dielectric constant of the β-form, which melts at 22°, rises to that of the liquid without the sharp peak shown by the cooling curve. As no anomalous dispersion or apparently high conductance is found in the region of the $\alpha \rightarrow \beta$ transition, it is suggested that the sharp peak is due to the development of molecular freedom caused by a molecular disorder greater during the process of transition than that existing in the liquid state, where the molecules must be more or less oriented. In other words, the potential hump to be crossed by a molecule in order to rotate is lower on the average during the transition than it is in the liquid state. In the β-form, as in ethyl undecylate, it is too high to permit rotation except in rare instances, the rarity increasing with falling temperature.

The sharp drop in the dielectric constant and the molar polarization of ethyl stearate on solidification shows a reduction in the freedom of molecular rotation. However, the rise in the dielectric constant of the solid with further temperature decrease at a rate only slightly less than that in the liquid shows that a limited freedom of rotation persists down to the enantiotropic transition, which is accompanied by a small drop in dielectric constant and followed by a gradual decrease corresponding to an absence of rotational freedom like that in the solid undecylate and the β-form of the palmitate.

Cetyl alcohol resembles ethyl palmitate in that its dielectric constant rises sharply on solidification, but differs in that the height of the rise depends upon the frequency used in the measurement, strong anomalous dispersion occurring throughout the region between the freezing point and a transition at 32.3°, below which the dielectric constant behaves like those of the undecylate and the β-forms of the palmitate and stearate. The form existing between 47.8° and 32.3° shows the dielectric behavior of a viscous liquid. That this is not the effect of impurities giving rise to a Maxwell-Wagner effect is shown by the length of the temperature region over which the phenomenon exists, by the sharpness of the boundaries of this region and by the absence of appreciable conductance in the liquid and in the solid below the transition.

CHARLES P. SMYTH
WILLIAM O. BAKER

Frick Chemical Laboratory,
Princeton University,
Princeton, New Jersey,
July 12, 1937.

[1] Smyth and Hitchcock, J. Am. Chem. Soc. **54**, 4631 (1932); ibid. **55**, 1296, 1830 (1933); ibid. **56**, 1084 (1934); Kamerling and Smyth, ibid. **55**, 462 (1934); Smyth and McNeight, ibid. **58**, 1597, 1718, 1723 (1936).

Raman Frequencies of Dioxane

As there are some discrepancies in the various published Raman frequencies of dioxane (Villars,[1] Wolkenstein and Syrkin,[2] Simon and Feher,[3] Venkateswaran[4]) it seems desirable to submit the following values which were determined in the course of another investigation. An iron spark was used for interpolation, and an Eastman 2A filter was employed in some runs to reduce the mercury 4047A group of lines.

The values are as follows, with estimated relative intensities and mercury line sources according to the Kohlrausch designations: 433 (1-ek), 486 (2-cek), 834 (4-ceik), 852 (0-ek), 1014 (3-ek), 1107 (2-ek), 1126 (1-ek), 1216 (2-ceik), 1304 (2-cek), 1334 (0-ek), 1443 (2-cek), 1459 (1-cek), 2660 (0-ek), 2718 (1-ek), 2748 (00-ek), 2852 (4-eik), 2885 (1-e), 2966 (4-eik). With the exception of 1334 and 2748, these results check well with those of Simon and Feher. Venkateswaran's values were not at hand.

R. C. WILLIAMSON

Department of Physics,
University of Florida,
Gainesville, Florida,
June 19, 1937.

[1] Villars, Kohlrausch, *Raman Effect*.
[2] Wolkenstein and Syrkin, J. Chem. Phys. **3**, 594 (1935).
[3] Simon and Feher, Chem. Abs. **30**, 2492 (1936).
[4] Venkateswaran, Proc. In. Ac. Sci. **2A**, 279 (1935).

Raman Spectra of Gaseous, Liquid and Solid Hydrogen Sulfide

Measurements of the infrared spectra,[1] as well as chemical and other evidence, indicate that the hydrogen sulfide molecule is of the symmetrical bent type, such as water, and belongs to the symmetry group, C_{2v}. Three vibrational frequencies are to be expected, all of which are permitted in both the infrared and Raman spectra. The only previous measurements resulted in the observation of one Raman line for the gas and the liquid.[2] Four Raman frequencies have been reported for the solid.[3]

We have photographed the Raman spectra of hydrogen sulfide in all three states, using the unfiltered radiation from a helical Pyrex arc such as described by Glockler and Davis.[4] The gas was at a pressure of about two atmospheres. Scattered lines were observed from both the 4358 and the 4047 mercury lines. The average of the results from four plates gives the frequency of the only line observed as 2615 cm^{-1} in agreement with the previous work on the Raman and infrared spectra. This line appeared on our plates within fifteen minutes, and exposures one thousand times as long failed to show any further scattered lines.

With the liquid kept at $-80°$ by means of a dry ice-alcohol bath, four spectra were obtained showing a single frequency of 2577 cm^{-1}, again in agreement with earlier work.

Photographs of the Raman spectra of the solid were obtained with the latter kept at liquid air temperatures. Two frequencies were observed of 2550 and 2523 cm^{-1}. The two frequencies of 80 and 2558 cm^{-1}, previously reported[3] were not present on our plates although an anti-Stokes line appeared (2523 cm^{-1}) in a one-hour exposure. An exposure of five hours failed to show anything different.

The precision in each case is about 5 cm^{-1}.

A preliminary experiment on D_2S gas shows one frequency of 1885 cm^{-1}, in fair agreement with infrared spectra.[1] The complete results will be reported later and will include measurements of liquid and solid D_2S as well as of HDS.

GEORGE M. MURPHY
JOHN E. VANCE

Sterling Chemistry Laboratory,
Yale University,
New Haven, Connecticut,
July 13, 1937.

[1] Bailey, Thompson and Hale, J. Chem. Phys. **4**, 625 (1936); Sprague and Nielsen, ibid. **5**, 85 (1937); Nielsen and Nielsen, ibid. **5**, 277 (1937).
[2] Bhagvantam, Nature **126**, 502 (1930).
[3] Sirkar and Gupta, Ind. J. Phys. **10**, 189 (1936).
[4] Glockler and Davis, J. Chem. Phys. **2**, 881 (1934).

Low and High Raman Frequencies for Water

During the course of the last five years, many workers reported having observed a number of high and low frequency bands other than the 3200–3600 band for water. A systematic and thorough examination of these frequencies was recently made by Magat[1] and Hibben.[2]

As workers in this line ever since the discovery of the Raman effect, we were following with interest the results of different experimenters on this problem of water. The new frequencies reported by others were not unnoticed by us, but were rejected as either spurious mercury lines making their appearance during long exposures of the photographic plate, or genuine Raman bands of frequency 3200–3600, excited, not by the mercury line assigned by these authors, but out of other comparatively feeble lines of the mercury arc. Finding that even systematic investigations of the type of those of Magat and Hibben reveal these new lines, a critical study of the Raman spectrum of water was made by us which confirmed our previous interpretation.

Table I gives the results of our analysis, as compared with that of others.

TABLE I.

Assignment of Other Workers			Our Assignment		
$\Delta\nu$	ν_{Hg}	ν_R	λ_{Hg}	ν_{Hg}	$\Delta\nu$
175(32)	39412	39237	2345(4)	42622	3385
740(24)	"	38672	2378(6)	42032	3360
1145*	"	38267	2399(8)	41633	3396
2150(14)	"	37262	2464(4)	40570	3308
—	—	—	2482(6)	40276	—
3200 3400 (80) 3600	"	36012	2537(10R)	39412	3400
4023(47)	"	35389	2576(6)	38803	3414
5100(45)	"	34312	2652(8)	37695	3383
500(40)	"	38912	2464(4)	40571	1659
1659(?)	"	37753	2537(10R)	39412	1659

The Raman band noted with an asterisk was not pointed out by other workers. It is noted for the first time by us, but represents only the 3200–3600 band excited by the strong 2399 line of mercury.

The table clearly shows that the bands reported by other workers correspond not to different frequencies of water excited by the same 2537 line of the mercury arc, but to the same 3200–3600 band excited by lines other than the 2537 line. The excitation by these lines appears to have been entirely ignored by all these workers. We have systematically investigated excitation by all the other strong lines of the mercury arc both in the visible and ultraviolet regions and find not even a trace of these frequencies, though these exciting lines are nearly as intense as the 2537 line.

The only other frequency which we find to be genuine is of $\Delta\nu = 1659$ as is evident from the table.

I. RAMAKRISHNA RAO
P. KOTESWARAM

Andhra University,
Waltair, India,
June 3, 1937.

[1] M. Magat, Ann. d. physique **6**, 108 (1936).
[2] J. H. Hibben, J. Chem. Phys. **5**, 166 (1937).

The Crystal Structure of Alloys of Zinc with the Alkali and Alkaline Earth Metals and of Cadmium with Potassium

The binary system of sodium and zinc is remarkable for the fact, that these metals form a compound notwithstanding the very low mutual solubility in the liquid state. Moreover the only compound contains about 3 percent Na, corresponding to $NaZn_{11-12}$. Compounds of about the same composition are reported for some of the other systems mentioned in the title.

The x-ray investigation by the powder method with Cu $K\alpha$ and Cr $K\alpha$ radiation revealed the same cubic structure for the alloys of zinc with Na, K, Ca, Sr and Ba and of cadmium only with K. No phase corresponding to the compounds with zinc was found in the other systems of cadmium.[1] Large crystals were obtained by slowly cooling down a large amount of molten KCd_{13}. Single crystal diagrams were made by oscillation round the cube edge and round the diagonal of the cube face. The dimensions of the elementary cell are:

$NaZn_{13}$	$a=12.25_5\pm0.005$A	$CaZn_{13}$	$a=12.13\ \pm0.005$A
KZn_{13}	$a=12.33_5\pm0.005$A	$SrZn_{13}$	$a=12.21_5\pm0.005$A
KCd_{13}	$a=13.78_5\pm0.005$A	$BaZn_{13}$	$a=12.33\ \pm0.005$A.

The number of atoms in the elementary cell was calculated from the density as 111, 113 and 111, respectively, for KCd_{13}, $NaZn_{13}$ and $CaZn_{13}$.

The structure is based on the face-centered lattice, as follows from the period observed in the direction of the diagonal of the cube face. As all reflections hhl with l uneven are absent the space group will be either O_h^6 or T_d^5.[2] Only the general positions of T_d^5 or 96 (i) in O_h^6 are possible for the cadmium atoms since many reflections with odd indices are strong. The position 96 (i) of O_h^6 is a special case having $x=0$ of the general positions of T_d^5.

T_d^5 96(h): xyz $x\bar{y}\bar{z}$ $\frac{1}{2}+x\,z\,y$ $\frac{1}{2}+x\,\bar{z}\,\bar{y}$ (+000, $0\frac{1}{2}\frac{1}{2}$, $\frac{1}{2}0\frac{1}{2}$, $\frac{1}{2}\frac{1}{2}0$)
$\bar{x}yz$ $\bar{x}\bar{y}z$ $\frac{1}{2}-x\,\bar{z}\,y$ $\frac{1}{2}-x\,z\,\bar{y}$.

The position 96 (i) in O_h^6 is a special case of this with $x=0$.

A discussion of the possible values of the three parameters x, y, z with regard especially to the intensities of the reflections $h00$ leads strictly to only one possible set: $x=0$, $y=2/16$, $z=3/16$. The value found for x indicates that the true space group will be O_h^6. As O_h^6 (and also T_d^5) contains no 4- but only two 8-equivalent positions the constitution can only be: 8 potassium and 8+96 cadmium atoms, corresponding to the formula KCd_{13}. A decision between both 8-equivalent positions can also be made from the observed intensities. So the structure is:

O_h^6 K 8(a): $\frac{1}{4}\frac{1}{4}\frac{1}{4}$, $\frac{3}{4}\frac{3}{4}\frac{3}{4}$ (+000, $0\frac{1}{2}\frac{1}{2}$, $\frac{1}{2}0\frac{1}{2}$, $\frac{1}{2}\frac{1}{2}0$)
Cd 8(b): 000, $\frac{1}{2}\frac{1}{2}\frac{1}{2}$ (+000, $0\frac{1}{2}\frac{1}{2}$, $\frac{1}{2}0\frac{1}{2}$, $\frac{1}{2}\frac{1}{2}0$)
Cd 6(i): $0yz$ etc. (see above).

The best accordance between observed and calculated intensities is obtained with the parameter values ($x=0$) $y=0.117\pm0.003$, $z=0.183\pm0.003$.

The spatial arrangement is thus, that each Cd atom on the 96-equivalent position is surrounded by ten other Cd atoms and one K atom. There are five Cd at distances of 2.90–2.99A and five Cd at 3.12–3.22A, in accordance with the values found in pure cadmium: six at 2.97A and six at 3.29A. A Cd atom in the 8-equivalent place is surrounded by 12 Cd atoms at 2.99A. Each K atom has 24 neighboring Cd atoms at 3.98A as compared with 3.90A for the sum of the radii.

The number of electrons contained in the inscribed sphere of the first Brillouin zone (531) was calculated, following the theory of Jones,[3] to be 216.8; that is 1.94 electron pro atom. This ratio calculated directly from the composition has the value 1.93 for $NaZn_{13}$ etc., resp. 2.00 for $CaZn_{13}$ etc. It seems that the compounds $NaZn_{13}$ etc. may be designed as a Hume-Rothery compound with the typical ratio 27/14. The isomorphism between the alkali and the alkaline earth compounds of zinc seems quite remarkable.

J. A. A. Ketelaar
Laboratory for Inorganic and Physical Chemistry,
University, Leyden,
The Netherlands,
May 24, 1937.

[1] The compound KHg_{11} is also cubic, but with a different structure; the cell containing 36 atoms.
[2] *International Tables for the Determination of Crystal Structures.* (Chemical Catalog Co., New York.)
[3] H. Jones, Proc. Roy. Soc. **144A**, 225 (1934).